

EFFICIENT AND SECURE NETWORK SERVICES IN WIRELESS SENSOR NETWORKS

by

Min-gyu Cho

A dissertation submitted in partial fulfillment
of the requirements for the degree of
Doctor of Philosophy
(Computer Science and Engineering)
in The University of Michigan
2009

Doctoral Committee:

Professor Kang G. Shin, Chair
Professor Atul Prakash
Associate Professor Sugih Jamin
Associate Professor Mingyan Liu

© Min-gyu Cho 2009
All Rights Reserved

ACKNOWLEDGEMENTS

First of all, I would like to express my gratitude to my advisor, Professor Kang G. Shin. Without his continuous guidance and encouragement, I could never have completed my dissertation. I would also like to thank my other committee members, Professors Atul Prakash, Sugih Jamin, and Mingyan Liu. Thanks to their invaluable comments, I could significantly improve the quality of my dissertation.

I thank great colleagues at the Real-Time Computing Laboratory including Songkuk Kim, Jai-jin Lim, Taejoon Park, Kyu-Han Kim, Jisoo Yang, Hyoil Kim, Zhigang Chen, Alex Min, Antino Kim, Sangsoo Park, Youngjune Choi, Katharine Chang, and Buyoung Yun. I am grateful for what they shared with me professionally and personally over the years of my graduate study.

I have been very fortunate to share life-enriching friendship with special people. With wonderful memories with them, my long journey during my graduate study has been much more enjoyable and enduring. My special thanks go to Sang-hyun Kim, Kijung Kim, Kyunghoon Min, Hongseok Kim, Joongho Won, Kyung-Joon Park, Jiyoung Kim, Minjoong Kim, Jungkeun Yoon, Hyunmin Kang, Goo Jun, Yang-won Jung, Eunjin Jung, Jooyong Jun, Sangwoo Lee, Wook Chang, Daeho Lee, Yoonna Oh, Taemin Earmme, and Jiwon Kim.

Last but not least, I would like to express my deepest love to my parents for their endless love and support for my whole life.

TABLE OF CONTENTS

ACKNOWLEDGEMENTS	ii
LIST OF FIGURES	vi
LIST OF TABLES	x
ABSTRACT	xi
CHAPTER	
I. INTRODUCTION	1
1.1 Overview of Wireless Sensor Networks	1
1.2 Existing Network Services	2
1.2.1 Localization	2
1.2.2 Geographic forward routing	4
1.2.3 Data-Centric Storage	5
1.2.4 Time Synchronization	6
1.3 Motivation and Contributions	6
1.3.1 Distributed Location Service Protocol	6
1.3.2 Distributed Hole Detection	7
1.3.3 Attack-Resilient Collaborative Message Authentication	8
1.4 Architecture of Sensor Network Applications	8
1.5 Outline	9
II. DISTRIBUTED LOCATION SERVICE PROTOCOL	11
2.1 Introduction	11
2.1.1 Background	12
2.1.2 Proposed Approach	15
2.2 Distributed Location Service Protocol	17
2.2.1 Selection and Update of Location Servers	17
2.2.2 Processing of Location Queries	19
2.3 Conditions for High Packet-Delivery Ratio	20

2.3.1	Conditions for High Packet-Delivery Ratio under DLSP	21
2.3.2	Configuration of Protocol Parameters for DLSP	24
2.3.3	Choice of Design Paradigm	25
2.4	Analysis of Location-Service Overhead	26
2.4.1	Analysis of Location-Update Overhead	26
2.4.2	Optimization of DLSP	27
2.5	Adaptation of Location Service	28
2.5.1	Adaptive Location Updates	29
2.5.2	Condition for High Query-Delivery Ratio	30
2.5.3	Analysis of Overall Energy-Efficiency	32
2.5.4	Comparison of Hierarchical Location Services	32
2.6	Evaluation	32
2.6.1	The Simulation Setup	33
2.6.2	Simulation Results Using 802.11 MAC	35
2.6.3	Simulation Results Using S-MAC	41
2.6.4	Results with Additional Mobility Models	43
2.6.5	Results on Robustness Against Node Failures	45
2.6.6	Results on Robustness with Low Densities	47
2.7	Conclusion	48
 III. DISTRIBUTED HOLE DETECTION		50
3.1	Introduction	50
3.2	Related Work	52
3.3	System Assumptions	54
3.3.1	Radio Model	54
3.3.2	Localization Service Model	56
3.4	Distributed Hole Detection	57
3.4.1	Overview	57
3.4.2	Definition of a Hole	57
3.4.3	Identification of Candidate Nodes	60
3.4.4	Handling Special Cases	62
3.4.5	Identification of hole boundary	63
3.4.6	Detection of Topology Changes	67
3.5	Geographic Forward Routing with Hole Avoidance	67
3.5.1	Overview	67
3.5.2	Detouring Messages Using Hole Information	68
3.6	Evaluation	71
3.6.1	Distributed Hole Detection	71
3.6.2	Geographic Forward Routing with Hole Avoidance	77
3.7	Conclusion	80
 IV. ATTACK-RESILIENT COLLABORATIVE MESSAGE AUTHENTI-		
CATION		83

4.1	Introduction	83
4.2	Related Work	86
4.3	System Model	89
4.3.1	Sensor Network Model	89
4.3.2	Attack Models	90
4.4	Key Management	92
4.4.1	Polynomial-based Key Pre-distribution	92
4.4.2	Key Distribution	93
4.4.3	Key Assignment	94
4.5	Attack-Resilient Collaborative Message Authentication (ARCMA)	96
4.5.1	Overview	96
4.5.2	Collaborative Message Authentication	97
4.5.3	Securing DCS Operations Using ARCMA	100
4.6	Authentication Tree Construction	104
4.7	Group Assignment Protocol	107
4.8	Evaluation	107
4.8.1	Security Analysis	107
4.8.2	Performance Evaluation	112
4.9	Conclusion	117

V. CONCLUSION	119
--------------------------------	------------

BIBLIOGRAPHY	122
-------------------------------	------------

LIST OF FIGURES

<u>Figure</u>		
1.1	The architecture of sensor network applications with our contributions . . .	9
2.1	The location servers selected at three levels of the grid	18
2.2	Round 1 of location query processing	19
2.3	In round 2, only the location server in the shaded level-1 neighbor square is visited	19
2.4	The timeline of events for location query processing at level-0.	21
2.5	<i>R</i> sends updates to two level-1 location servers at $P(R, T_2)$, because $P(R, T_3)$ is in the selected neighbor square of $P(R, T_2)$	27
2.6	Location queries (or data packets) from S_1 and S_2 travel less hops during <i>round</i> 1 with adaptive location updates.	29
2.7	The query-delivery ratio of DLSP is higher than 96% for all network sizes if the mobile's speed $\leq 15m/s$. The speed limit from our analysis is 14m/s. 35	35
2.8	The query-delivery ratio of DLSP-SN is close to that of DLSP below the speed limit, and noticeably better in case of high speeds.	35
2.9	There is no single speed limit for different network sizes in GHLS be- cause it does not scale.	36
2.10	The delivery ratio of GLS degrades because many forward pointer mes- sages are lost.	36
2.11	DLSP incurs a very high update overhead because there may be as many as 8 location servers at each level.	37

2.12	DLSP-SN reduces the update overhead by 70% or more. Its overhead is comparable to that of GHLS in a network of 900 nodes or more.	37
2.13	GLS incurs a very high update overhead because each level has 3 location servers, and boundary-crossing incurs additional overhead.	38
2.14	DLSP-SN has longer query paths due to gridding effect.	38
2.15	The delivery ratios of DLSP and GHLS match the results in previous figures.	40
2.16	The energy cost of DLSP-ASN is even less than GHLS when the speed is below 15m/s, when both provide high packet-delivery ratios.	40
2.17	The query-delivery ratio of DLSP with S-MAC in a 1600m×1600m network. DLSP with S-MAC scales well if the mobile's speed is below the threshold shown in Table 2.3.	43
2.18	The query-delivery ratio of DLSP-SN with S-MAC in a 1600m×1600m network. DLSP-SN with S-MAC also scales well if the mobile's speed is below the movement threshold.	43
2.19	GHLS with S-MAC shows a similar trend as GHLS with 802.11 MAC. Since there is no single speed limit for different network sizes in GHLS, the performance degrades even at a lower speed for large networks.	44
2.20	The random way-point model (RWP), the random walk model (RWP) with the duration of 20s (RW20) and 40s (RW40), and the Gauss-Markov model with the duration of 10s (GM10) and 20s (GM20) are simulated with DLSP in an 800m×800m network.	45
2.21	The random way-point model (RWP), the random walk model (RWP) with the duration of 20s (RW20) and 40s (RW40), and the Gauss-Markov model with the duration of 10s (GM10) and 20s (GM20) are simulated with DLSP in an 1600m×1600m network.	45
2.22	The delivery ratios with void areas are normalized to that of the scenario without any void area. These plots show that the delivery ratio of DLSP degrades slightly when a void area is introduced. The delivery ratio degrades more as the void area gets relatively larger, i.e., the network becomes smaller or the void area becomes bigger or both.	46
2.23	The delivery ratio of DLSP degrades as the density of the deployed network decreases, and the speed of the mobile increases.	47

3.1	This figure shows examples of holes.	59
3.2	This figure shows examples of candidate nodes.	61
3.3	The special cases handled by the TRAVERSE algorithm.	62
3.4	Examples of cases to consider two-hop neighbor lookups when TRAVERSE selects the next node to follow.	66
3.5	This figure shows examples of holes.	69
3.6	The result of TRAVERSE for the networks with holes of various shapes.	72
3.7	The result of TRAVERSE for the networks with varying average degree when an artificial circular hole exists in the center of the deployment area. The small squares represent the node in the deployed area, and the thick lines represent the boundaries identified by the proposed algorithm. As the average degree increases, the boundaries found by TRAVERSE get tighter since more nodes exist close to the boundaries of the central hole and the network boundary.	73
3.8	The result of TRAVERSE for the networks with varying parameters for the log-normal shadowing radio propagation model. As the value of σ is increased, the average node degree is decreased, resulting in looser boundaries and more small holes in the deployment area.	75
3.9	The result of TRAVERSE for the networks with varying parameters for the location errors. As the value of σ is increased, the average node degree is decreased, resulting in looser boundaries and more small holes in the deployment area.	76
3.10	An example of routing with hole-avoidance. In each figure, the boundaries of holes are drawn along with the summary of a hole by red line. Also the paths taken by GPSR and GFRHA are represented by a thin black line and a thick magenta line. The sources of left, middle, and right figure are middle-bottom, left-middle, and left-bottom, respectively. The destination of left, middle, and right figure are middle-top, right-middle, and right-top, respectively.	78

3.11	An example of routing with hole-avoidance. In each figure, the boundaries of holes are drawn along with the summary of a hole by red line. Also the paths taken by GPSR and GFRHA are represented by a thin black line and a thick magenta line. The sources of left, middle, and right figure are middle-bottom, left-middle, and left-bottom, respectively. The destination of left, middle, and right figure are middle-top, right-middle, and right-top, respectively.	79
3.12	The average path length for the random source-destination pairs with different shapes of holes.	81
4.1	Example of authentication trees: This figure shows ATs in a given topology when $k = 5$	97
4.2	The average number of transmissions per group increases as k increases in MIN.	114
4.3	The average number of transmissions per group increases at a much slower pace as k increases in OPT.	114
4.4	These graphs show the cost of constructing ATs with MIN and OPT heuristics while varying k and node density.	115
4.5	When removing a faulty node, the average number of affected nodes per AT increases as k increases for both heuristics.	116
4.6	When reconstructing ATs, the number of iterations remain at a small number in MIN, while it increases as k increases in OPT.	116

LIST OF TABLES

Table

2.1	List of symbols	17
2.2	Comparison of hierarchical location services	31
2.3	Average per-hop latency of DLSP using S-MAC. The average per-hop latency and its standard deviation vary with the network size. The movement thresholds can thus be derived from our analysis using Eq. 2.13 for different network sizes.	42
2.4	Average per-hop progress with varying numbers of nodes in 1600m×1600m networks.	48
3.1	The size of the area confined by the outer boundaries identified by TRAVERSE when the standard deviation of the normal distribution for the location estimation errors vary. As the location estimation error increases, the size of the hole area is slightly decreased.	77
3.2	The path lengths taken by GPSR and GFRHA, and their differences (%). Depending on the shape of the hole and the locations of sources and destinations, the performance gain (or loss) by GFRHA over GPSR significantly differs.	81
4.1	Notations used for ARCMA	95

ABSTRACT

EFFICIENT AND SECURE NETWORK SERVICES IN WIRELESS SENSOR NETWORKS

by

Min-gyu Cho

Chair: Kang G. Shin

Wireless sensor networks (WSNs) have been deployed for environment monitoring and surveillance. A message delivery service is one of the most fundamental services for WSNs, thus making its efficiency and effectiveness important. A widely-adopted protocol for message delivery in WSNs is a geographic forward routing (GFR), in which messages are greedily forwarded to their destinations. In this thesis, we develop network services complementary to the existing GFR for *efficient* and *secure* message delivery in WSNs.

We first develop a *distributed location service protocol* (DLSP) for message delivery to mobile nodes. Since GFR represents destinations of messages with destinations' geographic locations, the knowledge of location of mobile nodes is necessary to ensure correct message delivery. In DLSP, mobile nodes select some sensor nodes as their location servers, and publish the mobiles' location information to the location servers. Sensor nodes contact those location servers to retrieve the current location of mobile nodes when needed.

DLSP provides systematic methods for mobile nodes to select location servers and publish their location to those servers, and for sensor nodes to query mobiles' location.

We then design an algorithm called TRAVERSE for hole boundary detection and *geographic forward routing with hole avoidance* (GFRHA) for efficient message routing. TRAVERSE identifies boundaries of holes, i.e., areas without any functioning sensor node. GFRHA then utilizes the identified hole information to route messages around holes while being forwarded before they encounter holes. This way, the message path lengths, and subsequently the message delay and energy consumption, can be significantly reduced, depending on hole shapes and source and destination locations.

We also develop *attack-resilient collaborative message authentication* (ARCMA) for message delivery. ARCMA is designed to tolerate node-capture attacks, in which attackers obtain valid keys by compromising physically-exposed sensor nodes, and use the keys to generate forged messages. To defend against such attacks, in ARCMA, messages are *collaboratively* authenticated by a set of sensor nodes rather than by one node. The security of ARCMA does not degrade unless attackers simultaneously compromise more than a certain number of sensor nodes.

CHAPTER I

INTRODUCTION

1.1 Overview of Wireless Sensor Networks

Wireless sensor networks (WSNs) have gained popularity since they are suitable for numerous new applications. They are being adopted by various commercial, academic, and military applications, such as healthcare systems, smart buildings, habitat monitoring, fire detection and military surveillance.

WSNs are composed of a large number of *sensor nodes* and a relatively small number of *mobile nodes*. Sensor nodes are used to monitor surrounding physical environments. They are equipped with various sensors depending on the underlying application, such as photometer, temperature sensor, and magnetometer. They also have a radio communication module so that they can communicate with each other. However, to reduce the deployment cost, they are typically stationary and resource-limited; they have limited memory and processor capability, and they are battery-powered.

On the other hand, mobile nodes are carried by humans, or attached to manual or automated vehicles. They are used by human or automated users to interact with sensor nodes. They usually have relatively abundant resources; they have more memory, more CPU power, and faster and more stable wireless communication hardware. Also, they are usually equipped with GPS-like devices to obtain their own geographic location.

In the typical application scenarios, sensor nodes are used to detect events of interest,

and mobile nodes are used to interact with sensor nodes to retrieve the information acquired by sensor nodes. To detect the events of interest, sensor nodes are equipped with adequate sensors. For example, temperature sensors and magnetometers are equipped for fire detection and military surveillance applications, respectively. Sensor nodes often collaborate with other sensor nodes to improve the accuracy of detection. Mobile users such as humans or automated vehicles use mobile nodes to query the events detected by sensor nodes. These queries should be properly handled by sensor nodes.

To support these application scenarios, we need several network services. When an event is identified by sensor nodes, we typically need to know the location and time of the event. Thus, we need localization and synchronization services, which provide the location estimation of sensor nodes and time synchronization among sensor nodes, respectively. As in other networks, we also need a service to route messages to their destinations. We also need a mechanism to process queries issued by mobile nodes.

In the rest of this chapter, we first describe existing network services in Section 1.2. Then, we summarize our contributions with their motivations in Section 1.3, followed by the overall architecture of sensor network applications with our contributions in Section 1.4. Finally, this thesis is outlined in Section 1.5.

1.2 Existing Network Services

1.2.1 Localization

Although the knowledge of a geographic location, i.e., a coordinate in 2-D space, is required for various sensor network applications, sensor nodes cannot determine their geographic location before their deployment. Adopting GPS-like devices to provide their geographic location is often too expensive due to their manufacturing cost, and, more importantly, their energy consumption. Therefore, localization services [47, 48, 59] are provided for sensor nodes to estimate their geographic location.

Most localization services estimate the geographic location of sensor nodes using two phases: distance (or angle) estimation, and distance (or angle) combination. In the estimation phase, sensor nodes estimate the distance to (or angle with) other nodes in the neighborhood, and in the combination phase, local estimations are combined to give the global geographic location for every node in the WSN.

For the estimation phase, several techniques can be used to estimate the distance (or angle) between a pair of nodes. The most popular techniques are received signal strength indicator (RSSI), time of arrival (ToA), time difference of arrival (TDoA), and angle of arrival (AoA). RSSI is measured by the communication circuit, and the measurement of received signal strength is transformed into the distance between a pair of nodes. ToA and TDoA are time-based measurement techniques, and they use the propagation delay as an estimation of the distance between two nodes. TDoA uses two signals with different propagation delays such as ultrasound or RF signals. AoA is measured by the directional antennas, and such a measurement gives the relative direction (or angle) between two nodes.

In the combination phase, the global location of each sensor node is estimated by triangulating the local estimations based on the aforementioned techniques. Several techniques, such as convex optimization, multidimensional scaling (MDS), and quadrilaterals [48] have been proposed to improve the efficiency or the accuracy of estimation.

Anchor nodes (or beacon nodes), which have exact geographic locations, are often used for the combination phase to reduce the overhead or increase the accuracy of estimation. A small portion of sensor nodes can be used as anchor nodes; they obtain their geographic locations through GPS-like devices or by manual measurement of their locations.

Even though some localization services [47, 48] do not require anchor nodes, the anchor nodes may be necessary to transform the coordinates used by localization services to common reference coordinates. When no anchor node is used, the estimation results of localization services can be realized in a Euclidean space only up to isometry (in the case of distance estimation) or conformal transformation (in the case of angle estimation). Thus, a

small number of anchor nodes are necessary if we want to transform the coordinate system used by the localization service to the reference coordinate system.

After completing the two processes of localization services, each sensor node knows its geographic location. We can also broadcast the coordinates of nodes that have the minimum and the maximum value for x- or y-coordinates to inform sensor nodes the deployment area boundary.

In this thesis, we adopt localization services [47, 48] which do not require any special hardware such as GPS-like devices or directional antennas. Without any GPS-like devices, sensor nodes can use any of the aforementioned localization services to estimate their geographic location. We may need to load geographic location information to a small number of sensor nodes that are used as anchor nodes. Alternatively, we may use a small number of mobile nodes equipped with GPS-like devices to emulate anchor nodes. Throughout this thesis, we assume that sensor nodes know their geographic location and the size of deployment area from a localization service.

1.2.2 Geographic forward routing

Geographic forward routing (GFR) protocols [7, 33, 39] have been widely adopted by various sensor network applications because of their low resource requirements. In GFR, sensor nodes are assumed to know their geographic location, and the destination of a message is specified with a geographic “*location*” instead of another network identifier such as an IP address or a node ID. As most sensor network applications require sensor nodes to know their geographic location through a localization service, GFR adds little communication and memory overhead to maintain routing information; GFR only requires sensor nodes to have their own and their immediate neighbors’ geographic location.

GFR greedily forwards messages using only locations of immediate neighbors. In GFR, a forwarding node selects the next hop closer to the destination than itself. Typically, the node closest to the destination would be selected as the next hop. Then, the message will

be forwarded towards the destination at each hop, and eventually it will be delivered to the destination location. When the message is delivered to the destination location, a node closest to the destination location will process it.

However, a forwarding node may not have any neighbor node closer to the destination than itself if there is a hole (or a void area) on the network. A hole can be viewed as an area without any functioning sensor node. When a hole is encountered, GFR should invoke a mechanism to route the message around the hole. For example, GPSR [33], a well-known GFR protocol, starts *perimeter* forwarding, in which a message is forwarded around the perimeter of the hole using the right-hand rule. This forwarding mode is expensive because a path taken by this mode can be much longer than the shortest path to the destination.

1.2.3 Data-Centric Storage

Data-centric storage (DCS) [24,27,42,56] provides in-network storage and query mechanisms for sensor networks. In DCS, events identified by sensor nodes are stored at the sensor nodes, called *storage nodes*, at the predestined locations by their event types. The information about identified events is forwarded to the storage nodes, and queries issued by (typically, mobile) users are forwarded to, and processed at, the storage nodes. Different types of events will be stored at different storage nodes for load-balancing and reliability.

DCS was initially proposed in [56], where a geographic hash table (GHT) is used to determine the location of storage nodes. In a GHT, sensor nodes are required to know their geographic locations and route messages using GFR. In a GHT, the locations of storage nodes are determined by common hash functions shared by all nodes. The hash function takes the event type as an input, and generates geographic locations to determine location of storage nodes for the given type of events. Several improvements for DCS have been proposed to enhance the performance of GHT [24, 27, 42].

1.2.4 Time Synchronization

Time synchronization among sensor nodes is required for numerous sensor network applications and security protocols. Sensor network applications require knowledge of the time of the event identification. Also, many security protocols require (loose) time synchronization to prevent replay, or other attacks.

Synchronization services continuously adjust the clocks of sensor nodes to achieve global synchronization by compensating for the time differences caused by different clock drift rates of sensor nodes. Synchronization services typically adjust the clocks of nodes in the neighborhood and propagate the adjustment as necessary to achieve global synchronization.

Several time-synchronization protocols [16, 22, 63, 64] have been proposed for WSNs. These services can be categorized by the type of messages exchanged for local clock adjustments, and the existence/absence of master nodes whose clocks are used as reference clocks [77].

1.3 Motivation and Contributions

1.3.1 Distributed Location Service Protocol

Geographic forward routing (GFR) protocols are widely used for WSNs since they are well-suited for the requirements of WSN applications. Since a geographic location is specified as a destination in GFR, delivering messages to mobile nodes is difficult since their locations are not fixed. When sensor nodes need to send messages to a certain mobile node, they may not have the mobile's current location. Therefore, we need a network service to provide the geographic location of mobile nodes to enable message delivery using GFR.

In this thesis, we develop a *distributed location service protocol* (DLSP) to provide the current location of the mobile users. Using DLSP, sensor nodes can retrieve the current

location of mobile nodes, so as to send messages to mobile nodes using GFRs. We assume that mobile nodes obtain their geographic location by GPS-like devices, while sensor nodes do so by a localization service.

In DLSP, each mobile node publishes its location information to some sensor nodes, called *location servers*, and sensor nodes access those location servers to retrieve the mobiles' location information when necessary. DLSP provides systematic methods to select location servers, publish mobile nodes' location, and query location information based on a hierarchical grid structure. Specifically, we design DLSP and propose the optimizations of DLSP, and evaluate them with mathematical analysis and extensive simulation.

1.3.2 Distributed Hole Detection

The deployment areas of WSNs may contain holes, which are the areas without any functioning sensor node. Holes are formed by obstacles in the battery-deployment areas, the depleted or faulty nodes, or active attacks of malicious users.

Detecting holes in WSNs is important for network management. With the hole information, one can determine the terrain of the deployment area or the active events, such as an attack. We can also use the hole information to improve the performance of network protocols on WSNs. For example, we can use the information to route messages around holes to avoid the use of expensive detouring mechanisms in GFR.

We develop an algorithm, called TRAVERSE, to detect hole boundaries. After deploying a sensor network, TRAVERSE is invoked to locate holes on the WSN. TRAVERSE is a distributed algorithm, and has only nodes around the possible holes participate in the hole detection process. The algorithm is also invoked upon detection of a topology change.

We also propose *geographic forward routing with hole avoidance* (GFRHA) to route messages around the detected holes. In GFRHA, the identified hole information is disseminated to sensor nodes near the detected holes. GFRHA utilizes this information to route messages around the holes without invoking any expensive detouring mechanism. By de-

touring messages around holes, the path length is shortened, reducing the delay and the energy consumption for message delivery.

1.3.3 Attack-Resilient Collaborative Message Authentication

Sensor networks are often used for collecting critical information. However, securing sensor networks is very difficult, especially because sensor nodes are often physically exposed to attackers. In WSNs, attackers can launch node-capture attacks in which the attackers *physically* access and compromise sensor nodes. After compromising sensor nodes, the attackers may retrieve all the information stored in the sensor nodes including keying materials. We cannot afford expensive hardware-based solutions for sensor nodes since we usually need to deploy a large number of sensor nodes.

We design a security mechanism by focusing on authenticated message delivery for DCS under node-capture attacks. In DCS, as in other sensor network applications, authenticated message delivery is very important to prevent attackers from inserting, modifying, and accessing information. We achieve authenticated message delivery by proposing *attack-resilient collaborative message authentication* (ARCMA).

In ARCMA, a message is *collaboratively* authenticated by a set of sensor nodes. More specifically, a message is authenticated by k nodes instead of a single sensor node, where k is a user-defined parameter. For this, we require dense deployment of sensor nodes such that any event can be detected by k or more nodes. With ARCMA, we can prevent the insertion or modification of fakes messages. Thus, we can prevent attackers from reporting false data to storage nodes, issuing queries, and responding to queries with false data. The security of ARCMA is not degraded if less than k nodes are compromised.

1.4 Architecture of Sensor Network Applications

Figure 1.1 shows the overall sensor network application architecture with our contributions. In this thesis, we develop three protocols for better message delivery. DLSP

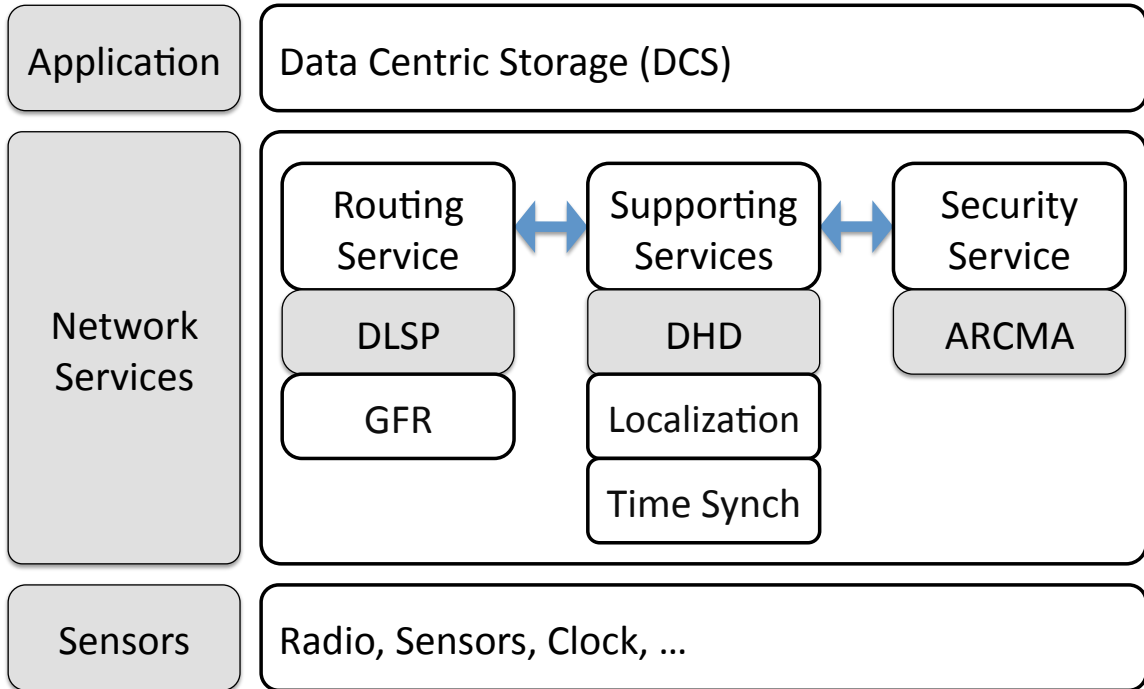


Figure 1.1: The architecture of sensor network applications with our contributions

enables message delivery to mobile nodes using GFR, DHD provides the hole information and improves the performance of GFR in the presence of holes, and ARCMA provides the authenticated message delivery in WSN.

1.5 Outline

The rest of this thesis is organized as follows. Chapter II presents the distributed location service protocol (DLSP) to provide the location of mobile nodes for message delivery to mobile nodes with geographic forward routing. Chapter III presents a distributed hole detection algorithm, called TRAVERSE, which identifies the boundaries of holes in a WSN, and geographic forward routing with hole avoidance (GFRHA), which uses the identified hole information to route messages around holes. Chapter IV describes attack-resilient collaborative message authentication (ACRMA), which supports authenticated message delivery in WSNs. ARCMA can tolerate node-capture attacks. Chapter V concludes this

thesis.

CHAPTER II

DISTRIBUTED LOCATION SERVICE PROTOCOL

2.1 Introduction

Many sensor network applications, such as habitat monitoring [45], emergency rescue, battlefield surveillance, and border monitoring [51, 77] require interaction between stationary sensor nodes and mobile nodes. That is, a large number of resource-limited sensor nodes are deployed in a certain geographical area for physical-environment monitoring, and some mobile nodes may move around the area and receive event notifications from the stationary sensors. For example, in the emergency-rescue or military applications, emergency rescuers/vehicles or soldiers/military vehicles, as mobile nodes, need to rescue missing people or track enemies. In these applications, mobile nodes interact with sensor nodes to retrieve mission-related information such as the location of missing people or enemies.

To support the aforementioned applications, we need to provide a routing mechanism to forward information about the events detected by sensor nodes to mobile nodes. This information routing/forwarding should be done by sensor nodes since mobiles may not always form a connected network depending on their density and movement, although mobiles often have a longer radio communication range than sensor nodes. To meet the application requirements, the routing mechanism should perform well for a wide range of the mobiles' speed and movement pattern. Depending on their mission and resources,

mobile nodes may travel with varying speeds to arbitrary locations in the network. For example, foot soldiers or emergency-rescuers may move at a low speed while ambulances, fire trucks, or military vehicles may move at a high speed to reach the missing people, or detect enemies.

2.1.1 Background

There are two types of approaches to routing sensed data to a mobile node: (1) TTDD [72], Bread Crumb Routing [69], and Last Encounter Routing (LER) [28] that do not require knowledge of the mobile's whereabouts, and (2) Geographic Forward Routing (GFR) [33, 39], Landmark Routing [65], and Beacon Vector Routing (BVR) [20] that require knowledge of the mobile's location.

In (1), TTDD allows data sources (i.e., sensors) to proactively build grid structures over the entire network to disseminate the sensed data, so the overhead of publishing data may be amortized when there are many mobile nodes. Bread Crumb Routing assumes a mobility model under the constraint that the sensors marked by the mobile node must form a connected path. However, in the above-mentioned scenarios, this path may be disconnected because (i) the mobile fails to leave marks on sensors as a result of message loss; (ii) the path may run through a deployment *hole*, and thus, the sensor marked by the mobile cannot communicate directly with any of previously-marked sensors; (iii) a sensor node on the path may fail or be destroyed. In LER, each node keeps the database of the location and time of other nodes it has directly communicated with, and uses the database to route packets using the updated location information as packets are being routed to the destination. This routing scheme becomes very similar to Bread Crumb Routing in our application scenario, where sensor nodes are stationary. Thus, LER shares the same problems with Bread Crumb Routing.

In (2), the mobile needs to periodically report its geographic location or virtual address to selected nodes, called *location servers*, in order to use GFR, Landmark Routing, or

BVR. Other nodes can acquire the mobile's location from one of its location servers and then deliver data to the mobile node using one of these routing protocols.

A number of location-service protocols have been proposed for mobile ad hoc networks (MANETs) to be used with GFR. GHLS [12], Twins [66], and Home-Zone-Based Location Service all use hash functions to select a centralized location server. That is, they select only one location server for a given mobile node. Particularly, GHLS hashes the mobile node's ID into a geographic location, and the node closest to that location serves as the central location server for the mobile. In these protocols, location queries are forwarded to and processed by the centralized location server.

XYLS [62] lets the mobile node select a *thick column* of nodes as its location servers. In XYLS, a mobile node updates nodes in the same column, i.e., nodes whose x-coordinate is within a certain range of the mobile node. Queries are forwarded in the same row, i.e., in the parallel direction of the x-axis until they reach location servers.

GLS [40], DLM [70], HLS [34], and MLS [19] are hierarchical location service protocols, i.e., the mobile node constructs a hierarchy of location servers over a grid structure. In these protocols, mobile nodes send their location to location servers, and location queries are forwarded to and processed by those location servers. Beacon Location Service (BLS) [52] is developed for the location service for BVR, in which routing is based on a beacon-vector, i.e., a vector of hop-distance to beacon nodes, instead of geographic location as in GFR. Also, Landmark Routing [65] provides a hierarchical lookup service to provide a mapping between the node ID and the landmark address. The hierarchical lookup mechanisms provided by these protocols are similar, but they are tailored differently by different designs of location update and query mechanisms. Note that BVR and landmark routing need a separate service to map a specific location to beacon-vector or landmark address if we want to send a packet to the location, which is often required in a WSN. Also, landmark routing is not scalable since the discovery of landmarks are based on the distance-vector routing; additional route-discovery packets should be exchanged. In GFR-based location

services, such landmark discovery is not necessary since location servers are selected at the pre-defined geographic locations.

These location service protocols, however, are not applicable to sensor networks due to the usually high per-hop latency in a sensor network which ranges from a few hundred milliseconds to a few seconds [43, 75], while that of a MANET is an order-of-magnitude lower (tens of *ms*) [26, 35]. The high per-hop latency in a sensor network can be attributed to scheduling delay and transmission time. First, wireless communication consumes much more energy than other operations for (severely energy-constrained) sensor nodes. Hence, energy-efficient MAC protocols avoid idle listening and overhearing by scheduling transmission and listening periods (e.g., S-MAC [76] and T-MAC [11]), or low-power channel polling (e.g., WiseMAC [15] and BMAC [54]), or both (e.g., SCP [75]). As a result, the radio's duty cycle can be limited to a few percentages. Thus, a packet has to be held for a certain period of time before taking its next hop. Second, a sensor node's radio usually has a lower bandwidth, incurring a longer transmission time. For example, Mica2 (MicaZ) has a bandwidth of 19.5 kbps (250 kbps), while MANETs typically use wireless LAN cards of 11 Mbps or 54 Mbps.

This high per-hop latency makes packet transmission in a sensor network much slower than in a MANET. Moreover, a sensor network is usually of much larger scale than a MANET. Therefore, the location-service protocols intended for MANETs are unlikely to perform well in sensor networks, because, while a message is being delivered from its source to a location server, then to the mobile receiver's location obtained from the location server, the mobile could have moved too far away to receive the message directly as in GHLS or even by using forward pointers as in GLS. This problem becomes more evident as the mobile moves faster.

2.1.2 Proposed Approach

In this chapter we present a *distributed location service protocol* (DLSP) for a hybrid wireless network of stationary sensors and mobile nodes. DLSP is built on a hierarchical grid structure. A mobile selects multiple location servers at each level of the hierarchy, and sends location updates more frequently to the lower-level location servers than to the higher-level ones. A location query (that also contains a data packet to be delivered) may take multiple rounds of “lookup-and-chase” to reach the mobile receiver.

Through a rigorous analysis, we derive the condition under which a high query-delivery ratio (i.e., the data-delivery success rate in DLSP) is achieved, and show how to configure the protocol parameters to ensure the scalability of the location service. Here ‘scalability’ means that, as the network size increases, the location service protocol preserves the high query-delivery ratio and the protocol overhead is proportional to $O(\log(N))$, where N is the network size. We find that, in order to preserve a high query-delivery ratio, the mobile’s speed should be below a certain fraction of the packet-transmission speed, which depends on the underlying movement threshold. For example, if the movement threshold for the lowest-level location servers is the same as the node’s radio range, the mobile’s speed limit is one-tenth of the packet-transmission speed. The theoretical speed limit is a one-fifth of the packet-transmission speed beyond which DLSP does not scale regardless of the movement threshold.

DLSP incurs a high location-update overhead because a mobile needs to update multiple location servers at each level with its location information. To alleviate this problem, we propose an optimization, called *DLSP with a Selected Neighbor* (DLSP-SN), in which the mobile updates the location server in at most one neighbor square at each level. A neighbor square is selected based on the mobile’s trajectory. DLSP-SN achieves a significant reduction of update overhead. However, due to the gridding effect,¹ DLSP-SN may

¹‘Gridding effect’ means that the source and destination nodes across but close to the boundary of a high-level square may require the query to travel many hops upward (in the hierarchy) to the common (parent) square containing both nodes. Both GLS and DLSP-SN suffer from the gridding effect, but DLSP does not.

incur more rounds of lookup-and-chase than DLSP, thus making the average path length of location queries greater than that of DLSP and increasing data-delivery cost. In order to make a tradeoff between location-update and data-delivery costs, we present a greedy adaptation mechanism, called DLSP-ASN, to improve the overall energy-efficiency.

The contributions of this work are summarized as follows.

- **Design of DLSP:** We design a novel hierarchical location service. In DLSP, location-updates are published to hierarchical location servers, and location-queries are processed recursively using these hierarchical location servers. DLSP can efficiently provide mobiles' location information with a wide range of mobiles' speeds even in the presence of sensor node failures.
- **Optimization of DLSP:** We provide two optimized algorithms for DLSP, DLSP-SN and DLSP-ASN. The former focuses on reducing the location-update overhead, while the latter makes a good balance between the location-update overhead and the data-delivery ratio.
- **Evaluation of DLSP:** We rigorously and thoroughly evaluate DLSP and its optimizations. First, we derive the condition under which DLSP guarantees a high data-delivery ratio using a mathematical analysis. Second, we extensively simulate DLSP with various scenarios and parameters to show its performance in diverse environments.

The rest of this chapter is organized as follows. Section 2.2 describes the details of DLSP. Section 2.3 derives the condition for DLSP to achieve a high packet-delivery ratio, while Section 2.4 analyzes the overhead of DLSP, and presents an enhanced version of DLSP, called DLSP-SN. Section 2.5 proposes a greedy adaptation mechanism, DLSP-ASN. In Section 2.6 we use simulation to evaluate the performance of location services. We conclude the chapter and discuss future directions in Section 2.7.

$P(S),$ $P(R, T)$	Location of a stationary sensor node S , or of a mobile node R at time T
$S_{k,j}(S),$ $S_{k,j}(R, T)$	$S_{k,0}(S)$ is the level- k square the sensor S resides, and $S_{k,j}(S)$ ($j = 1, \dots, 8$) are the eight level- k neighbor squares adjacent to $S_{k,0}(S)$. $S_{k,j}(R, T)$ is the level- k square the mobile R resides at time T , and $S_{k,j}(R, T)$ ($j = 1, \dots, 8$) are the level- k neighbor squares
$LS_{k,j}^R(S),$ $LS_{k,j}^R(R, T)$	R 's level- k location server in the square $S_{k,j}(S)$, or $S_{k,j}(R, T)$
$ALS_k^R(S)$	R 's adaptive location server for a data source S in the square $S_{k,0}(S)$
L	Edge length of the square field of interest
h	Level of the largest square, i.e., the entire deployment field
ℓ	Edge length of a level-0 square
m	Movement threshold for level-0 location servers $2^{-m}\ell$
τ	Time threshold for location updates at level-0 location servers
t_h	Average per-hop latency, including transmission/retransmission time, and scheduling delay
p	Average per-hop progress, or decrease of Euclidean distance to the destination for each hop taken
r	Radio range
\bar{v}	Mobiles' average speed
$dist(P_1, P_2)$	Distance between two locations, P_1 and P_2

Table 2.1: List of symbols

2.2 Distributed Location Service Protocol

We now present the details of DLSP. We assume that a large number of stationary sensors have been placed randomly and uniformly in a field of interest and a relatively smaller number of mobile nodes move around within the field. Geographic routing (e.g., GPSR [33]) is used for multi-hop routing. Each sensor node can determine its location by using a localization service [31, 59]. Likewise, each mobile either is equipped with a GPS receiver or can estimate its location using the neighbor sensors' location information.

Table 2.1 lists the notation used in this chapter.

2.2.1 Selection and Update of Location Servers

A sensor network is assumed to have been deployed in a square field as in GHT [56]. Similar to GLS [40], the entire square field is partitioned into a grid as shown in Figure 2.1.

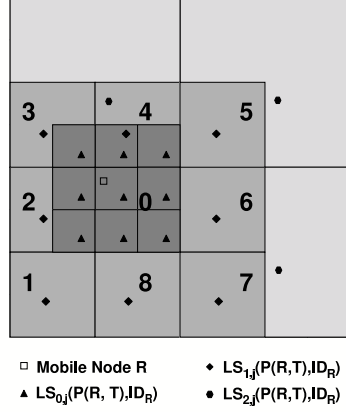


Figure 2.1: The location servers selected at three levels of the grid

Four level-0 squares make up one level-1 square, four level-1 squares make up one level-2 square, and so on. To avoid overlap between two squares of the same size, a particular level- k square is part of one and only one level- $(k + 1)$ square. For simplicity, we assume that the field is perfectly gridded, i.e., the field is a square of edge length $L = 2^h \ell$. We will discuss how this restriction can be relaxed in Section 2.6. Each node is pre-loaded with h , ℓ , and the location of the lower-left corner of the field, and it can calculate the entire grid structure using this information.

Suppose a mobile R needs to send its location updates at time T (we will later elaborate on when to send location updates). It selects a location server in its level-0 square and also the neighbor squares, denoted as $LS_{0,j}^R(R, T)$ ($j = 0, \dots, 8$). To randomize the selection, R uses a common hash function² to compute a location in a square, and the sensor node closest to that location is chosen as the R 's location server. A neighbor square is omitted if it is outside of the field boundary. At level-1, R picks a location server from each of the neighbor squares, $S_{1,j}(R, T)$. There is no location server in $S_{1,0}(R, T)$, as it is fully covered by the level-0 location servers, and so on.

Location servers at *different* levels are updated at *different* rates. Suppose at time T , R

²The hash function can be defined in many different forms. For example, $H(R, Sq) = (f_x(R) \cdot 2^k \ell, f_y(R) \cdot 2^k \ell)$, where f_x and f_y are uniform distribution functions within the interval $(0, 1)$, and Sq is a level- k square. Note that the hash function computes a relative location inside Sq .

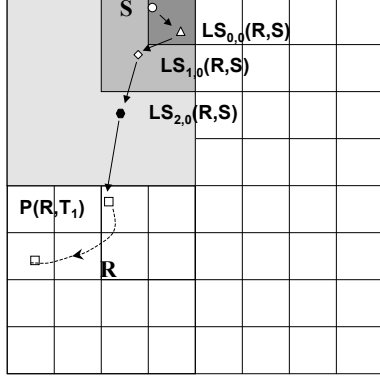


Figure 2.2: Round 1 of location query processing

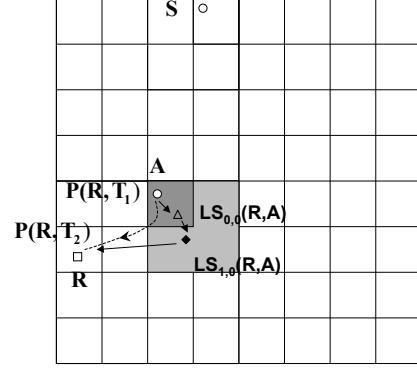


Figure 2.3: In round 2, only the location server in the shaded level-1 neighbor square is visited

has sent a location update (i.e., $P(R, T)$) to level- k location servers. It will then send the next update to the level- k servers at $T + \Delta T$ if and only if $dist(P(R, T), P(R, T + \Delta T)) \geq 2^{k-m}\ell$ (i.e., the movement threshold) or $\Delta T \geq 2^k\tau$ (i.e., the timeout). R sets the *lifetime* of its location servers to be slightly larger than $2 \cdot \Delta T$, where $\Delta T = \min(2^k\tau, \frac{2^{k-m}\ell}{v})$, to tolerate a loss of location update or jitter. If a location server does not receive a new update from the mobile R before this lifetime expires, it is no longer a location server for R .

Selection of location servers in all neighbor squares ensures the availability of a level- k location server if the distance to the mobile node is within $2^k\ell$, and thus, prevents a gridding effect. Also, the hash function lets different mobile actors choose different sensor nodes as their location servers. As a result, the protocol evenly distributes the workload and energy consumption among the sensor nodes.

2.2.2 Processing of Location Queries

When a sensor node S sends a data message to R , it only knows R 's ID. First, it tries to find R 's location from its neighbor's table and local location cache (i.e., it is a location server for R). If R 's location is not found, S encapsulates the data into a location query, and sends it to a location server. Once R 's location is found, the data message is sent to

that location using geographic-location-based-routing. This *lookup-and-chase* process is illustrated by an example in Figures 2.2 and 2.3.

In Figure 2.2, S first assumes that R has visited somewhere nearby — R and S are in the same level-0 square or two adjacent level-0 squares. Formally, S assumes $LS_{0,j}^R(R, T)$ to be $LS_{0,0}^R(S)$. So, the location query is sent to $LS_{0,0}^R(S)$. However, $LS_{0,0}^R(S)$ does not have R 's location information, so it tries to find R 's location in a larger square by sending the query to $LS_{1,0}^R(S)$, and so on. Eventually, $LS_{2,0}^R(S)$ has R 's location information at time T_1 (i.e. $LS_{2,0}^R(S)$ is also $LS_{2,4}^R(R, T_1)$), denoted as $P(R, T_1)$, so it sends the query to $P(R, T_1)$. This process of looking for the location of, and chasing, the mobile is called a *round*.

If R moves fast and if S and R are far apart, by the time the location query reaches the location $P(R, T_1)$, R could have moved too far away from $P(R, T_1)$ to receive the location query. In such a case, the query will be received by the node A closest to $P(R, T_1)$. Unlike GLS, A does not maintain any forwarding pointer³ under DLSP. Instead, it starts a new *round*. As shown in Figure 2.3, the query first goes to $LS_{0,0}^R(R, A)$, then to $LS_{1,0}^R(R, A)$ (i.e., $LS_{1,6}^R(R, T_2)$), which has more recent R 's location information, $P(R, T_2)$. Finally, the query catches up with R near $P(R, T_2)$.

After receiving the query, R may decide whether or not to send its location information to S , which caches the location for later queries. Such a decision should depend on the sender's transmission rate, as discussed in Section 2.5.

2.3 Conditions for High Packet-Delivery Ratio

In this section, we first derive the condition for achieving a high packet-delivery ratio under DLSP. Then, we discuss how to configure the parameters of DLSP to make it scalable. DLSP is found to be scalable if the mobile's speed is lower than a certain fraction of

³In GLS, a mobile leaves a *forwarding pointer* in the lowest-level grid from which it moves out, so that a query may follow the mobile using the forwarding pointers.

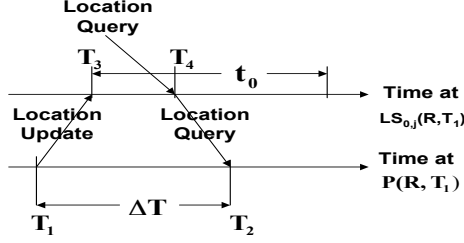


Figure 2.4: The timeline of events for location query processing at level-0.

the packet-transmission speed, which depends on the movement threshold used. Finally, we present the condition for achieving a high packet-delivery ratio in GHLS, and also show that GHLS is not scalable.

2.3.1 Conditions for High Packet-Delivery Ratio under DLSP

Our analysis of DLSP consists of the *base* case and the *inductive* step. The base case analyzes how a location query can catch up with the mobile receiver after obtaining its location information from a level-0 location server. The inductive step analyzes how the location query can get closer to the mobile by completing each round.⁴

2.3.1.1 The Base Case

Suppose, at time T_1 , R sends its location, $P(R, T_1)$, to a level-0 location server, $LS_{0,j}^R(R, T_1)$, $j \in \{0, 1, \dots, 8\}$. The location server receives the location update at time T_3 . At time T_4 , it receives a location query and forwards the query to $P(R, T_1)$. The location query reaches location $P(R, T_1)$ at time T_2 . The timeline of these events are shown in Figure 2.4.

In order to have R receive the query at T_2 , the following condition must be satisfied:

$$\text{dist}(P(R, T_1), P(R, T_2)) \leq r. \quad (2.1)$$

Suppose $\Delta T = T_2 - T_1$, then $\text{dist}(P(R, T_1), P(R, T_2))$ is bounded by $\Delta T \bar{v}$, because

⁴The analysis of DLSP was coworked with Zhigang Chen and published in [10]. For the completeness of the thesis, the analysis is presented here.

the distance is maximized when R moves on a straight line between T_1 and T_2 . The average speed is computed as the length of the trajectory curve between T_1 and T_2 over ΔT . ΔT can be broken into three components, $T_3 - T_1$, $T_4 - T_3$, and $T_2 - T_4$. $T_3 - T_1$ denotes the average latency of the location update from $P(R, T_1)$ to $LS_{0,j}^R(R, T_1)$; $T_4 - T_3$ represents the average obsolescence of the location information at the location server; $T_2 - T_4$ denotes the average latency of the location query from $LS_{0,j}^R(R, T_1)$ to $P(R, T_1)$.

Let d_0 be $\text{dist}(P(R, T_1), L_{0,j}(R, T_1))$, the average distance between R and a level-0 location. Then, considering R as a random point in an $\ell \times \ell$ square, and the location server as a random point in the same square or one of the eight adjacent squares, we get $d_0 \approx 1.27\ell$ according to a numerical analysis. Also, we let t_0 be the update interval for level-0 location servers. We have $T_3 - T_1 = T_2 - T_4 = \frac{d_0}{p}t_h$, and $T_4 - T_3 = \frac{1}{2}t_0$ because T_4 ranges from T_3 to $T_3 + t_0$. So,

$$\Delta T = \frac{1}{2}t_0 + 2\frac{d_0}{p}t_h. \quad (2.2)$$

Also, from Section 2.2, we have

$$t_0 = \begin{cases} \tau & \text{if } \bar{v} < \frac{2^{-m}\ell}{\tau} \\ \frac{2^{-m}\ell}{\bar{v}} & \text{if } \bar{v} \geq \frac{2^{-m}\ell}{\tau}. \end{cases} \quad (2.3)$$

From Eq. (2.3), we have

$$\bar{v}t_0 \leq 2^{-m}\ell. \quad (2.4)$$

Therefore,

$$\text{dist}(P(R, T_1), P(R, T_2)) \leq \frac{1}{2}t_0\bar{v} + 2\frac{d_0}{p}t_h\bar{v} \quad (2.5)$$

In order to satisfy Eq. (2.1), we simply let $\frac{1}{2}t_0\bar{v} + 2\frac{d_0}{p}t_h\bar{v} \leq r$. That is,

$$\begin{cases} \tau\bar{v} + \frac{5.08\ell}{p}t_h\bar{v} \leq 2r & \text{if } \bar{v} < \frac{2^{-m}\ell}{\tau} \\ 2^{-m}\ell + \frac{5.08\ell}{p}t_h\bar{v} \leq 2r & \text{if } \bar{v} \geq \frac{2^{-m}\ell}{\tau}. \end{cases} \quad (2.6)$$

Approximately, Eq. (2.6) can be satisfied if

$$2^{-m}\ell + \frac{5\ell}{p}t_h\bar{v} \leq 2r. \quad (2.7)$$

2.3.1.2 Analysis of the Inductive Step

Consider the case of requiring multiple rounds of lookup-and-chase. Suppose the query looks up R 's location from a level- k_i location server in round i , and from a level- k_{i+1} server in round $i + 1$. To ensure the query makes progress toward R , we need to satisfy

$$k_{i+1} \leq k_i - 1. \quad (2.8)$$

Suppose the query returns R 's location information, $P(R, T'_1)$, in round i and reaches $P(R, T'_2)$ at time T'_2 . $k_{i+1} \leq k_i - 1$ holds if the following inequality holds:

$$\text{dist}(P(R, T'_1), P(R, T'_2)) \leq 2^{k_i-1}\ell. \quad (2.9)$$

Eq. (2.9) bounds the distance between the known location of round i and that of round $i + 1$, so the two locations are at most in two adjacent level- $(k_i - 1)$ squares. Therefore, the level of location server visited at round $i + 1$ is not greater than $k_i - 1$.

Similar to Eq. (2.2), we get

$$\Delta T' = T'_2 - T'_1 = \frac{1}{2}2^{k_i}t_0 + 2\frac{2^{k_i}d_0}{p}t_h. \quad (2.10)$$

So, we have

$$\text{dist}(P(R, T_1), P(R, T'_1)) \leq \frac{1}{2} 2^{k_i} t_0 \bar{v} + 2 \frac{2^{k_i} d_0}{p} t_h \bar{v} \quad (2.11)$$

In order to satisfy Eq. (2.8), we simply let $\frac{1}{2} 2^{k_i} t_0 \bar{v} + 2 \frac{2^{k_i} d_0}{p} t_h \bar{v} \leq 2^{k_i-1} \ell$. That is,

$$\begin{cases} \tau \bar{v} + \frac{5.08\ell}{p} t_h \bar{v} \leq \ell & \text{if } \bar{v} < \frac{2^{-m}\ell}{\tau} \\ 2^{-m}\ell + \frac{5.08\ell}{p} t_h \bar{v} \leq \ell & \text{if } \bar{v} \geq \frac{2^{-m}\ell}{\tau}. \end{cases} \quad (2.12)$$

Again, due to Eq. (2.4), Eq. (2.12) can be satisfied if

$$2^{-m}\ell + \frac{5\ell}{p} t_h \bar{v} \leq \ell. \quad (2.13)$$

2.3.2 Configuration of Protocol Parameters for DLSP

The above analysis provides insights into which parameters affect the packet-delivery ratio and how they can be configured to achieve the scalability of DLSP with respect to query delivery.

2.3.2.1 Configuration of ℓ

Consider the condition of the base case, Eq. (2.7), and that of the inductive step, Eq. (2.13). The condition of the base case is stronger than that of the inductive step if $\ell \geq 2r$. Moreover, both Eqs. (2.7) and (2.13) are independent of the field edge length, L . Therefore, as long as data can be delivered within a small region (level-0 squares) of edge length $\ell \geq 2r$, it can be delivered from an arbitrarily far away node. In fact, we need

$$\ell = 2r \quad (2.14)$$

because the overhead of location updates increases as ℓ increases (in Section 2.4).

2.3.2.2 Configuration of m

In Eq. (2.7), $\frac{5\ell}{p}t_h v$ is always positive since t_h is not negligible. So, m must be a positive integer. Again, the overhead of location updates is proportional to 2^m when the mobile's speed is above the threshold. Therefore, m should be set to 1, and the movement threshold is r .

2.3.2.3 Mobile's Speed Limit

From Eq. (2.7), if $m = 1$, $\bar{v} < \frac{r}{5\ell} \frac{p}{t_h} = \frac{p}{10t_h}$, which is a one-tenth of the packet-transmission speed. If the movement threshold for location updates gets smaller, the location updates become more frequent, and the mobile is allowed to move faster. However, $\bar{v} < \frac{2r}{5\ell} \frac{p}{t_h}$ must always hold, and the speed can never be greater than $\frac{p}{5t_h}$. So, the mobile's theoretic speed limit is a one-fifth of the packet transmission speed, no matter how frequently the location servers are updated.

2.3.3 Choice of Design Paradigm

GHLS (i.e., a centralized paradigm) can be considered as a trivial case of DLSP (i.e., a hierarchical paradigm), in which $\ell = L$. The analysis of GHLS is the same as that of the base case in DLSP, except that $d_0 \approx 0.5L$ because the mobile and its location server are considered two random points in the $L \times L$ square.

Suppose the movement threshold for updating the location server is $\bar{v}t_0 \leq d$. We need to satisfy

$$d + \frac{2L}{p}t_h\bar{v} \leq 2r. \quad (2.15)$$

When t_h is not very small, Eq. (2.15) may not hold for large networks and fast mobiles.

Based on Eqs. (2.15), (2.4), and (2.14), we can conclude that, regardless of the mobile's speed, the conditions of GHLS (i.e., the centralized paradigm) are stronger than those of

the hierarchical paradigm if $L < 2.5l$. So, the centralized paradigm is favorable for low mobile's speed, very low per-hop packet latency, or small/ median networks because of its simplicity and lower overhead [12]. For large networks with high mobility and non-trivial packet latency, the hierarchical paradigm should be used.

2.4 Analysis of Location-Service Overhead

In this section, we first analyze the overhead of location updates under DLSP and then propose a design optimization, called DLSP with a Selected Neighbor (DLSP-SN), which significantly reduces the location-update overhead.

2.4.1 Analysis of Location-Update Overhead

Let U denote the total overhead of location updates, and u_k the overhead of updating a level- k location server. The location-update frequency for level- k location servers is $t_k = 2^k t_0$. The average distance between R and a level- k location server ($LS_{k,j}^R(R, T)$) is $1.27 \cdot 2^k \ell$, and that between R and the level-0 location server $LS_{0,0}^R(R, T)$ is 0.5ℓ . Since there are at most 8 neighbor squares at each level, we have

$$\begin{aligned} U &\leq \sum_{k=0}^{h-1} 8 \cdot 1.27 \cdot 2^k \ell \frac{1}{t_k} + 0.5\ell \frac{1}{t_0} \\ &\leq (10.2h + 0.5) \frac{2^m \bar{v}}{p} \end{aligned} \tag{2.16}$$

where $h = O(\log(L \times L))$, and the total number of nodes, N , is proportional to $L \times L$ for a given node density. So, $U = O(\log(N))$. That is, DLSP is asymptotically scalable with respect to the protocol overhead. However, like GLS, DLSP suffers from high update overhead because there are multiple location servers at each level of the hierarchy.

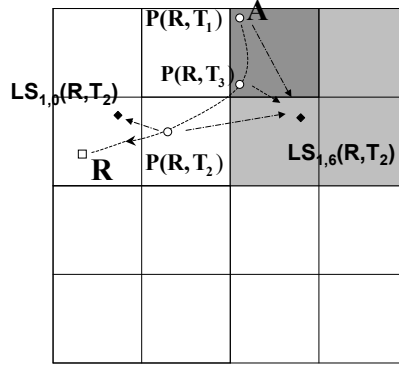


Figure 2.5: R sends updates to two level-1 location servers at $P(R, T_2)$, because $P(R, T_3)$ is in the selected neighbor square of $P(R, T_2)$.

2.4.2 Optimization of DLSP

Our optimization goal is to reduce the location-update overhead while preserving the high packet-delivery ratio. The key observation is that it is unnecessary to update the location servers in all neighbor squares. This is because, as a location query “chases” the mobile receiver, the mobile’s trajectory determines which location servers to communicate with.

This observation is illustrated in Figure 2.3. At time T_2 , R updates its level-1 location servers in the neighbor squares since it has crossed a boundary of level-1 squares. Therefore, at round 2, the query can obtain a more recent location, $P(R, T_2)$, and catch up with R . However, before such an update is available, a query is delivered to sensor node A , which is closest to R ’s previous location, $P(R, T_1)$. When R is not in the neighborhood of A , it needs to re-query R ’s location to relay the query. In such a case, the only level-1 location server contacted is one in the level-1 square in which A is located. More specifically, since A is in $S_{1,6}(P(R, T_2))$, the query relayed by A can only go through $LS_{1,6}^R(R, T_2)$, not the other four level-1 location servers. That is, only the update to the location server in the neighbor square, $S_{1,6}(R, T_2)$, is useful for delivering this query. So, the design optimization is called *Distributed Location Service Protocol with a Selected Neighbor* (DLSP-SN).

To illustrate how DLSP-SN works, let us zoom in the lower-left level-2 square of Fig-

ure 2.3 in Figure 2.5. Suppose R needs to send location updates to level-1 location servers at $P(R, T_1)$, $P(R, T_3)$, and $P(R, T_2)$ consecutively. At $P(R, T_3)$, it checks if its previous location $P(R, T_1)$ was in the level-1 square, $S_{1,0}(P(R, T_1))$. If so, it only updates $LS_{1,0}^R(R, T_1)$ (i.e., $LS_{1,6}^R(R, T_2)$). At $P(R, T_2)$, R finds that its previous location $P(R, T_3)$ is in the neighbor square, $S_{1,6}(P(R, T_2))$, so it sends updates to both $LS_{1,0}^R(R, T_2)$ and $LS_{1,6}^R(R, T_2)$. Note that the locations of two consecutive level- k updates must be in the same level- k square or two neighbor level- k squares, because the movement threshold for level- k updates, $2^{k-m}\ell$, is strictly less than the edge length of level- k square, $2^k\ell$.

The differences between DLSP and DLSP-SN are summarized as follows. First, suppose the highest level is h . Then, DLSP updates $LS_{0,j_1}^R(R, T)$ ($j_1 = 0, 1, \dots, 8$), and $LS_{k,j_2}^R(R, T)$ ($k = 1, 2, \dots, h - 1$ and $j_2 = 0, 1, \dots, 8$). DLSP-SN updates $LS_{k,0}^R(R, T)$ ($k = 0, 1, 2, \dots, h$), as well as the location server in the selected neighbor square. Second, suppose k_i and k_{i+1} are the levels of location servers through which a location query obtains the destination mobile's location at i and $i + 1$, respectively. In this case, DLSP requires $k_i > k_{i+1}$, but DLSP-SN does not have this restriction. To avoid endless chasing, DLSP-SN requires that, at each round, the query get more recent location information than the previous round.

DLSP-SN is less restrictive in the sense of obtaining location information, because it selects many fewer location servers than DLSP. As a result, DLSP-SN incurs more rounds and longer query paths.

2.5 Adaptation of Location Service

DLSP-SN reduces its update overhead, but may extend the query path length, increasing the data-delivery cost. This increase of data-delivery cost may become significant in case of continuous data streams commonly seen in sensor network applications. To achieve overall energy-efficiency with DLSP-SN, we propose an adaptive location-update scheme in which a mobile adaptively sends its location updates based on the varying distribution

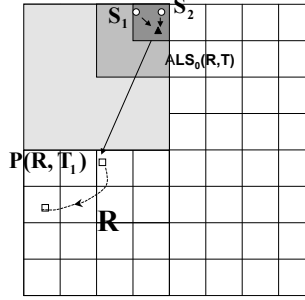


Figure 2.6: Location queries (or data packets) from S_1 and S_2 travel less hops during *round* 1 with adaptive location updates.

and rate of the data sources. We then analyze the parameter configuration for the adaptation to ensure a high query-delivery ratio and present a greedy algorithm to improve overall energy-efficiency. Finally, we summarize the comparison among the hierarchical location service protocols, DLSP, DLSP-SN, DLSP-ASN, and GLS.

2.5.1 Adaptive Location Updates

In a hybrid wireless network of stationary sensors and mobile actors, a mobile may receive data from multiple data sources located in the areas of interest. The overhead of querying the mobile's location to forward data from these sources may be expensive if they need to contact high-level location servers. Typically, the data sources in an area of interest are often spatially close to one another. Thus, the cost of location-query can be significantly reduced if the mobile's location can be retrieved from the common low-level location server. Therefore, to reduce the overhead of location-queries, a mobile selects and updates a few location servers near the data sources in DLSP-ASN.

Figure 2.6 provides an illustrative example. Suppose sensor nodes, S_1 and S_2 , reside in the same level-0 square $S_{0,0}(S_1)(= S_{0,0}(S_2))$, and continuously report data to a mobile R . Instead of sending location updates to S_1 and S_2 individually, R picks an adaptive location server, $ALS_0^R(S_1)$, in $S_{k,0}(S_1)$, and periodically sends updates to it as well as to the other location servers. When S_1 or S_2 sends R data, a location query is processed exactly the same as in Section 2.2 except for the first round. R 's location can be obtained

from $ALS_0^R(S_1)$, instead of from the level-2 location server, $LS_{2,j}^R(R, T_1)$, as shown in Figure 2.2. Thus, the data-delivery cost is reduced at the expense of extra adaptive location updates.

2.5.2 Condition for High Query-Delivery Ratio

Suppose R updates $ALS_0^R(S_1)$ at time T'_1 , and the location query reaches $P(R, T'_1)$ at time T'_2 . Let $T_a = 2^{k_a}t_0$ be the period of location updates to $ALS_0^R(S_1)$, and D be the distance between $P(S_1)$ and $P(R, T'_1)$.

Similar to the analysis of Eq. (2.10), we get

$$\Delta T' = T'_2 - T'_1 = \frac{1}{2}2^{k_a}t_0 + 2\frac{D}{p}t_h. \quad (2.17)$$

We simply let $\Delta T'\bar{v} \leq \frac{D}{2}$. That is,

$$2^{k_a-1}t_0\bar{v} + 2\frac{D}{p}t_h\bar{v} \leq \frac{D}{2}. \quad (2.18)$$

In Section 2.3, we derived Eq. (2.4) and the speed limit, $v < \frac{p}{10t_h}$ with the movement threshold r . In order to satisfy Eq. (2.18), we need

$$2^{k_a-2}\ell + \frac{D}{5} \leq \frac{D}{2}. \quad (2.19)$$

$$k_a \leq \log_2\left(\frac{D}{\ell}\right). \quad (2.20)$$

When k_a is small, there is higher update overhead but lower data-delivery cost; when k_a is large, there is less update overhead but higher data-delivery cost. So, k_a needs to be configured to achieve overall energy-efficiency.

Protocols	DLSP	DLSP-SN	DLSP-ASN	GLS
ID-to-LS mapping	Hash the mobile node ID into a location within a square, and the node closest to the location becomes a location server	Same as DLSP	Same as DLSP	Select the node whose ID is closest to the mobile node ID within a square
LS in neighbor squares	One LS in each of the eight neighbor squares	At most one location server from a neighbor square	Same as DLSP-SN	One LS from each of the three neighbor squares
Cross-boundary updates	Location updates can only be triggered by timeouts or exceeding the movement threshold	Same as DLSP, but the selected neighbor depends on whether or not a boundary of certain level is crossed	Same as DLSP-SN	Need to update the three neighbor location servers ^a from level-0 to level- k if the boundary of a level- k square is crossed
Data source adaptiveness	No	No	Yes A mobile may send additional location updates to the location servers near the data sources according to a greedy algorithm	No. A mobile node may send its location to the data sources at a fixed rate
Gridding effect	No	Yes	Not after the additional location updates are sent out	Yes
Multi-rounds	Yes, with restrictions (1-3) ^b	Yes, with restrictions (1-2) ^b	Same as DLSP-SN	No

Table 2.2: Comparison of hierarchical location services

^aIn GLS, one square considers its three adjacent squares belonging to the same parent square as its neighbors; in DLSP protocols, all the eight adjacent squares are considered neighbors.

^bRestrictions: (1) The query needs to obtain a newer location of the mobile at each round; (2) the query does not proceed if the location is obtained from a level-0 location server in the previous round; (3) the level of the location servers gets lower as the round progresses.

2.5.3 Analysis of Overall Energy-Efficiency

Let E denote the energy-efficiency without adaptive location updates, and E_a denote the efficiency with adaptive location updates. The mobile maintains a moving window to compute the average data rate, R_{data} , the average hop count, C_{hops} , and the average distance, D_{src} , from the two sources.

$$\Delta E = R_{data} \cdot \left(C_{hops} - \frac{D_{src}}{p} \right) - \frac{D_{src}}{p} \frac{1}{2^{k_a} t_0} \quad (2.21)$$

A mobile periodically searches for k_a in $[0, \log_2 \left(\frac{D}{\ell} \right)]$ such that ΔE is maximized or E_a is minimized.

In general, the rate and distribution of data sources cannot be described in a simple form. It is, therefore, very difficult to compute the optimal solution that combines data sources and sets k_a for each combination. The mobile can use some simple heuristics to find good solutions. For example, only the data sources in the same level-0 are combined at their level-0 location server. We can then use the above analysis to set k_a for each level-0 location server.

2.5.4 Comparison of Hierarchical Location Services

Different hierarchical location services are compared and summarized in Table 2.2.

2.6 Evaluation

We have performed extensive simulation to comparatively evaluate the performance of location-service protocols. For this purpose, we have implemented the DLSP protocols (DLSP, DLSP-SN, and DLSP-ASN) and GHLS in *ns-2* [2] (version 2.27), and also have ported GLS to the same version of *ns-2* we used for other protocols.

The following metrics are evaluated for the location service protocols: (1) Query Delivery Ratio—the percentage of location queries successfully delivered to the mobile receiver;

(2) Update Overhead—the number of update packets transmitted with each hop counted as one packet transmission; (3) Query Path Length—the number of hops each successfully-delivered query takes.

2.6.1 The Simulation Setup

The transmission range for radio communication is set to 100m based on the characteristics of MicaZ [1] devices. We assume the radio link is symmetric, and only collision may cause message loss. Typically, the raw radio of sensor nodes (e.g., Mica2, MicaZ) is lossy and asymmetric, but the underlying MAC or routing protocols provide reliable transmission via scheduling and retransmission. We use both 802.11 MAC and S-MAC in our simulation. We also use the two-ray ground propagation model.

Sensors are uniformly deployed over a square area, with density of 6.25 nodes per $100 \times 100\text{m}^2$. This high node density is chosen because in low node-density networks, geographic routing (e.g., GPSR) suffers from relatively high packet losses, which may distract the readers from our main focus on the performance of location services. Given this high node density, the average per-hop progress is approximately $0.7r$ or 70m. Our tests are run on networks of 400×400 , 800×800 , 1200×1200 , and $1600 \times 1600\text{m}^2$, which include 100, 400, 900, and 1600 sensor nodes, respectively. Since interactions among mobiles are not considered, only one mobile is simulated in our evaluation, and its movement follows the modified random way-point mobility model [78] in our base-case scenarios. The mobile's speed ranges from 4 to 40m/s, and its pause time is set to 0. We also simulate DLSP with random walk and Guass-Markov mobility models [9] to confirm that the proposed protocol functions regardless of the mobiles' movement pattern. We also simulated DLSP using the scenarios with 100×100 and $200 \times 200 \text{m}^2$ void areas to show its resilience to node failures. Finally, we evaluated DLSP with low-density networks.

We use GPSR [33] as a routing protocol throughout the evaluation of DLSP. The beacon period is set to 10s for stationary sensor nodes and 1s for the mobile. When a sensor node

receives a beacon from the mobile, it replies with a beacon after a random delay ranging from 0 to 1s. The movement threshold for triggering location updates in DLSP, DLSP-SN, GHLS, and GLS is set to 100m (i.e., $m = 1$). The timeout for triggering location updates for the location service protocols except for GLS (i.e., τ) is 8s. GLS does not have any timeout. Instead of using its instantaneous speed, the mobile uses its average speed over a moving window. Suppose R sends two consecutive updates to its level- k location servers at time T and T' . The average speed $\bar{v} = \frac{\text{dist}(P(R,T),P(R,T'))}{T'-T}$, although R 's trajectory may follow an arbitrary curve. To determine the timeout for the location information sent to a level- k location server, the mobile uses the average speed to predict the update interval $t_k = 2^k t_0$ with Eq. (2.3).

The edge length of the smallest square in the DLSP protocols (i.e., ℓ) is 200m. In GLS, the smallest square size is set to 100m, because all nodes in the same smallest square should be within two hops. The network size we tested, $1200 \times 1200\text{m}^2$, does not result in a perfect grid structure. In such a case, if an intended level- k square is not within the network boundary, it is substituted by a neighbor level- k square inside the boundary. For example, the level-2 square may be outside the boundary when the mobile is located at (900m,900m). Then, the level-2 square $\{(0,0), (800\text{m},800\text{m})\}$ becomes its replacement.

Ten sensor-node deployments are generated for each network size. With each deployment, we generate a movement scenario for each speed. All test results are the averages of 10 runs on all the deployments. Since the mobile's ID is the same in all tests, a seed is randomly generated in each run so that a sensor node can hash the mobile's ID into a different value for DLSP and GHLS. As for the workload, a sensor node is randomly chosen to send a location query to the mobile once every 2s during a period of 200s, i.e., 100 queries are sent. All tests for the same network size use the same workload. In GLS, every node should publish its location information to its location servers for the correct functioning of GLS. For fair comparison, we modify GLS such that the sensor nodes publish their location only during the initial warm-up period of 120s. These location updates during the warm-up

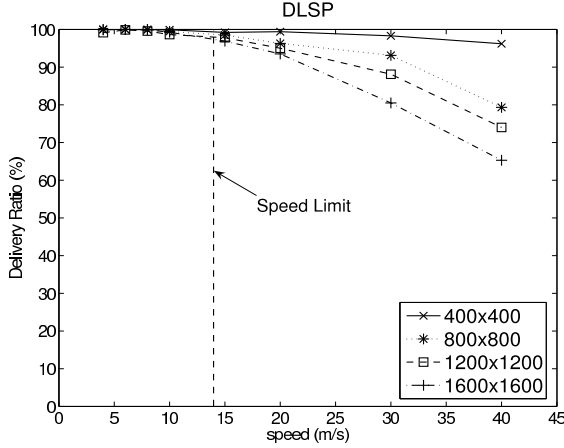


Figure 2.7: The query-delivery ratio of DLSP is higher than 96% for all network sizes if the mobile’s speed $\leq 15m/s$. The speed limit from our analysis is 14m/s.

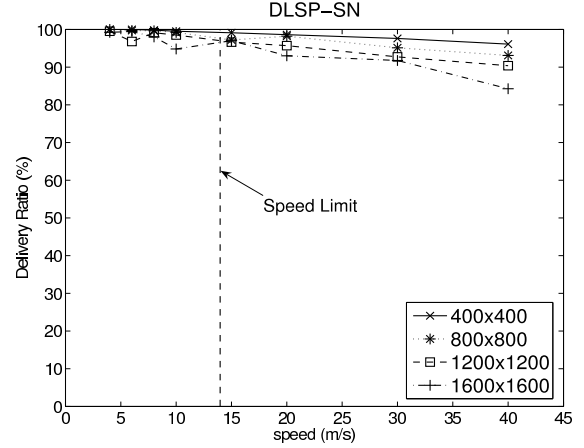


Figure 2.8: The query-delivery ratio of DLSP-SN is close to that of DLSP below the speed limit, and noticeably better in case of high speeds.

period are not counted in the update overhead.

For all protocols, the workload starts at 120s and the simulation ends at 300s. The surplus of 80s allows the last few queries to be delivered.

2.6.2 Simulation Results Using 802.11 MAC

Using the 802.11 MAC in *ns-2*, the transmission time plus the backoff delays ranges from 0.001 to 0.02s. Without a low-power MAC at hand, we add a fixed link-layer delay of 0.5s (or 0.25s). Thus, the actual per-hop latency ranges from 0.5 to 0.52s (or 0.25 to 0.27s), which resembles the per-hop latency in low-power MACs [43, 75]. Because the average per-hop progress of a packet is about 70m, the average packet-transmission speed is calculated to be 140m/s. Based on our analysis, the speed limit with the movement threshold of 100m is 14m/s.

2.6.2.1 Query-Delivery Ratio

Figure 2.7 shows that DLSP scales well if the mobile’s speed $\leq 15m/s$. In the network of 1600 nodes, the delivery ratios of both DLSP and DLSP-SN drop below 90% beyond

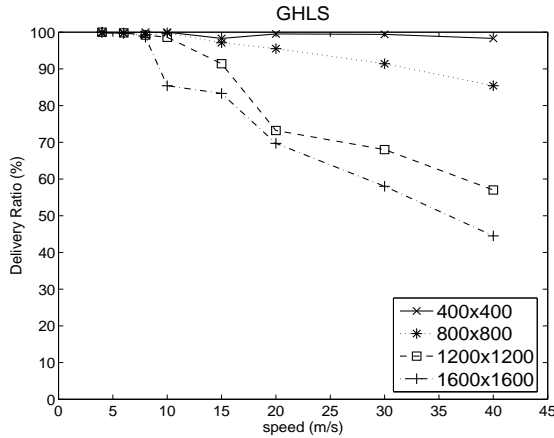


Figure 2.9: There is no single speed limit for different network sizes in GHLS because it does not scale.

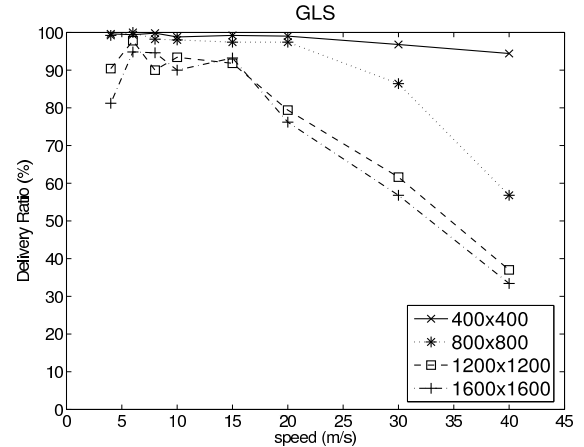


Figure 2.10: The delivery ratio of GLS degrades because many forward pointer messages are lost.

the theoretic speed limit, 28m/s. We have also run tests with different per-hop latencies and different movement thresholds. The results are consistent with our analysis, and thus omitted.

The query-delivery ratio of DLSP-SN, as shown in Figure 2.8, is close to that of DLSP below 20m/s and even higher than that speed because DLSP requires the query to obtain location information from a lower-level location server than the previous round, but DLSP-SN does not have this restriction and can take more lookup-and-chase rounds. Figure 2.9 shows that the delivery ratio of GHLS degrades significantly as the network size and the mobile's speed increase. This is because, as the per-hop latency is non-trivial, the term $\frac{2L}{p}t_h\bar{v}$ easily exceeds the bound, $2r$, in Eq. (2.15). When the query reaches the location obtained from the location server, the mobile has already moved too far away from that location to receive the query, and hence the message is dropped.

The delivery ratio of GLS, shown in Figure 2.10, degrades significantly as the network size and the mobile's speed increase, also because the mobile has moved too far away to receive the query when it reaches the location. GLS uses forwarding pointers to leave the mobile's trail for the query to chase the mobile. But the messages containing the forward-

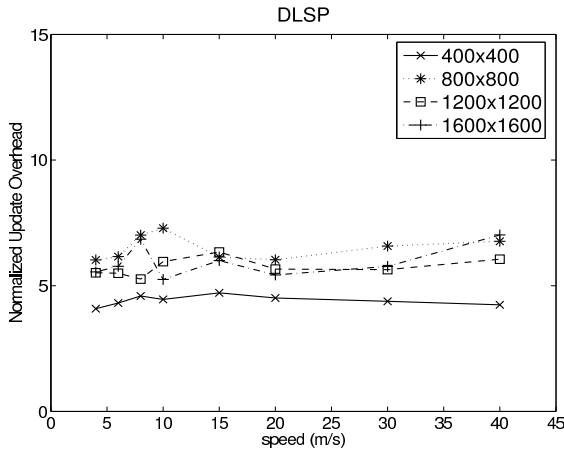


Figure 2.11: DLSP incurs a very high update overhead because there may be as many as 8 location servers at each level.

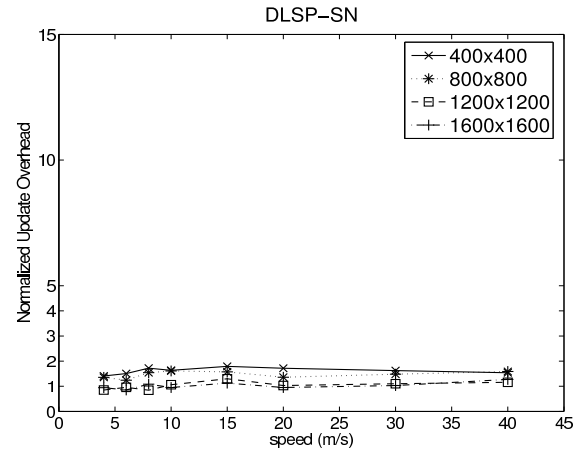


Figure 2.12: DLSP-SN reduces the update overhead by 70% or more. Its overhead is comparable to that of GHLS in a network of 900 nodes or more.

ing pointers are likely to get lost, particularly when the mobile moves fast, because the destination of these messages (i.e., the grid it moves out of) is in the opposite direction of the node's movement. By geographic forwarding, the mobile selects the neighbor closest to the destination. But such a neighbor is most likely to be out of the mobile's radio range. When a forwarding pointer is lost, the chain of forwarding pointers is broken, and the query has to be dropped.

GLS also suffers some performance degradation at a low speed for the following reason. Unlike the other location protocols we evaluate, location updates are triggered only by the movement threshold in GLS. So, when the mobile's speed is low, the update period is very long, especially for high-level location servers in large networks. Then, loss of a location update can cripple these location servers for a very long time. Queries will be dropped if they reach these servers. At high speeds, the delivery ratio of small networks is noticeably better than that of large networks, because it is easier for a query to catch up with the mobile within smaller areas.

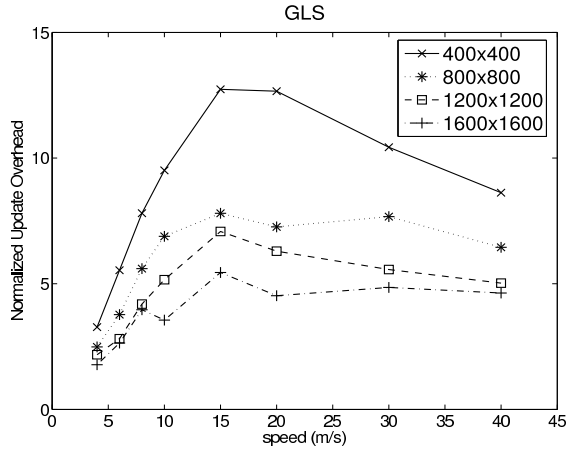


Figure 2.13: GLS incurs a very high update overhead because each level has 3 location servers, and boundary-crossing incurs additional overhead.

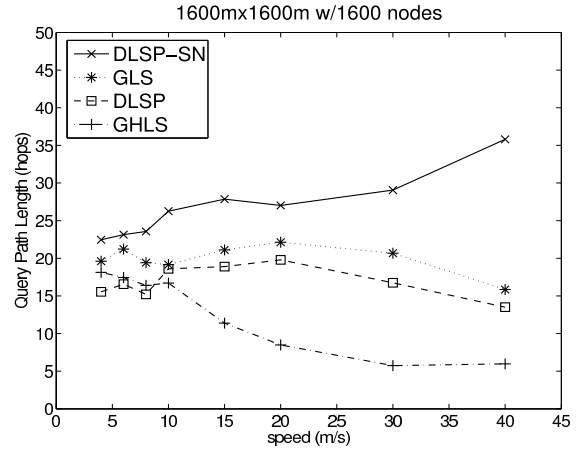


Figure 2.14: DLSP-SN has longer query paths due to gridding effect.

2.6.2.2 Location-Update Overhead

Because GHLS is shown in [12] to incur the least update overhead, we normalize the update overheads of DLSP, DLSP-SN, and GHLS with respect to that of GHLS, as illustrated in Figures 2.11–2.13. We obtained the results from the same tests for the query-delivery ratio. All the normalized overheads are relatively insensitive to the mobile’s speed, since the tests of all protocols use the same movement threshold for triggering location updates. As the mobile’s speed increases, the update overhead increases accordingly for all protocols.

Compared to DLSP, DLSP-SN reduces the update overhead by at least 70%, as shown in Figures 2.11 and 2.12. More importantly, the normalized overhead of DLSP-SN decreases as the network size increases because the normalized overhead of DLSP is $O(\frac{\log(N)}{N})$ (overhead of DLSP-SN is $O(\log(N))$ and that of GHLS is $O(N)$). For this reason, GLS exhibits a similar trend in Figure 2.13. However, the trend is not clear for DLSP, which can be explained as follows. Because of the network boundary, the number of location servers at any level increases as the network size grows. For example, the average number of level-0 (level-1) location servers increases from 4 to 6.25 (from 0 to 3) as N changes from 100 to

400. So, the trend is offset by the increase of overhead due to additional location servers.

In Figure 2.13, the overhead of GLS increases almost linearly at low speeds for the following reason. GLS does not use any timeout for sending updates, so its update overhead always increases linearly with the mobile's speed. In GHLS, the timeout is 8s and the movement threshold is 100m, and hence, at low speeds, the mobile sends location updates every 8s, and the overhead of GHLS is constant even when the mobile's speed increases. Therefore, the normalized overhead of GLS increases linearly at low speeds. Let us compare GLS with DLSP-SN. The overhead of DLSP-SN is at least 75% less than that of GLS, since it updates fewer location servers at each level and incurs fewer updates when the mobile crosses a square boundary. Let us compare GLS with DLSP in Figures 2.13 and 2.11. GLS is shown to incur a much higher overhead than DLSP for $400 \times 400m^2$ networks, because GLS updates the same number of level-0 location servers (4) as DLSP does for this network size, and it incurs more overhead in case of boundary-crossing. As the network size grows, DLSP selects more location servers than GLS, so its overhead catches up with or exceeds that of GLS.

2.6.2.3 Query-Path Length

The results plotted in Figure 2.14 are also from the same tests for the query-delivery ratio. Due to the gridding effect, the query-path length of DLSP-SN is 40 – 45% longer than that of DLSP in large networks.

In Figure 2.14, the query-path length of GHLS decreases sharply beyond the mobile's speed of 10m/s, because more than 30% of queries (most of them take long paths) are dropped and thus not counted. Similarly, the query-path lengths of DLSP and GLS decrease noticeably at 30 and 40m/s. These speeds are consistent with Figures 2.7, 2.9 and 2.10. DLSP-SN results in longer query-paths than GLS, because DLSP-SN uses fewer location servers than GLS. So, DLSP-SN suffers more from the gridding effect. The results of smaller networks show the same trend with smaller gaps.

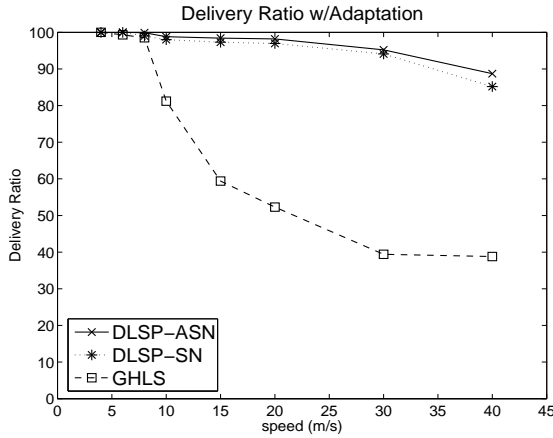


Figure 2.15: The delivery ratios of DLSP and GHLS match the results in previous figures.

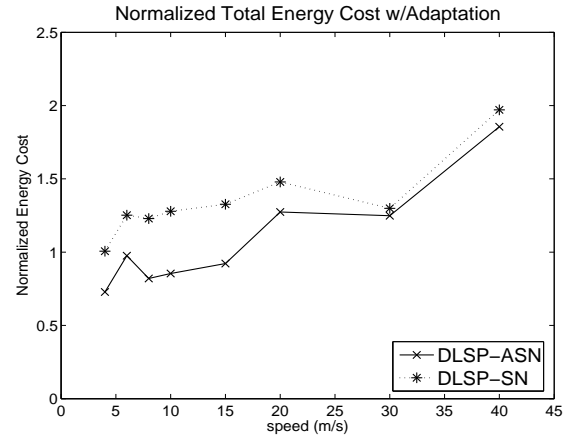


Figure 2.16: The energy cost of DLSP-ASN is even less than GHLS when the speed is below 15m/s, when both provide high packet-delivery ratios.

2.6.2.4 Adaptation

To evaluate how DLSP-ASN improves overall energy-efficiency over DLSP-SN, we use the same deployments and movements as in previous tests, but change the workload such that only two sensor nodes in the same level-0 square send data to the mobile at the same constant rate.

Figures 2.15 and 2.16 show the results from a network of 1600 nodes and the data rate of 0.5 message per 1 second for each node.

Figure 2.15 shows that, with adaptive location updates, DLSP-ASN has a slightly higher delivery ratio than DLSP-SN, because, in the first round, each query travels fewer hops in DLSP-ASN than in DLSP-SN. So it takes less time for a query to reach the mobile's known location, and thus, the mobile moved away less from the location. Starting at the second round, the query has a higher chance to be delivered successfully. Figure 2.16 shows the total energy cost normalized by the total cost of GHLS. Here we use the number of transmissions as the energy cost since we use the same transmission power for all packets. The adaptive mechanism can improve the overall energy-efficiency by as much as 40%.

For the range of 4 to 15m/s, the total energy cost of DLSP-ASN is comparable to, or even lower than, that of GHLS. This is because most queries are delivered in one round. During the first round, a query obtains the mobile’s location information within a small square in DLSP-ASN, but in GHLS, it has to travel more hops to a randomly-picked location server within the largest square. As the speed increases, the improvement diminishes because DLSP-ASN also needs to take more rounds to deliver the queries. In the tests of smaller networks and lower data rates, DLSP-ASN shows less improvement on overall efficiency as expected.

2.6.3 Simulation Results Using S-MAC

In order to validate our analysis of DLSP on a MAC with real low-power duty cycling, we simulated DLSP using S-MAC [76]. S-MAC is inspired by PAMAS [61] and uses RTS-CTS to reduce channel contention. S-MAC periodically sleeps, wakes up to receive and transmit packets if any, and then returns to sleep. Each active period is a constant period, and thus, the length of the sleep period determines the length of each frame (i.e., the active period plus the sleep period). To match the per-hop latency with our 802.11 MAC-based simulation, we set the sleep period such that the length of the S-MAC duty cycle is 0.5s. Other parameters of S-MAC such as slot time are kept as default, resulting in 20.8% duty cycle. This duty cycle is rather high, but we keep the default parameters of S-MAC while setting the per-hop delay as 0.5s for a fair comparison.

Moreover, because S-MAC is designed for static sensor networks, we need to slightly modify it to deal with mobility — if a sensor node receives a beacon from a mobile, it stays awake for a short period (in our simulation, this period is 2.5s). With this modification, the neighbor sensors of the mobile are given enough wakeup time to send their replies and avoid severe collision, which could occur without the modification. The mobile node does not observe S-MAC sleep-scheduling, so it can communicate with sensor nodes with different sleep schedules. This may be justified because the mobile is usually much less

Network size	Average per-hop latency	Standard deviation	Movement threshold
400m × 400m	0.251s	0.271	27.9m/s
800m × 800m	0.373s	0.281	18.8m/s
1200m × 1200m	0.410s	0.280	17.1m/s
1600m × 1600m	0.439s	0.313	16.0m/s

Table 2.3: Average per-hop latency of DLSP using S-MAC. The average per-hop latency and its standard deviation vary with the network size. The movement thresholds can thus be derived from our analysis using Eq. 2.13 for different network sizes.

power-constrained than sensors.

If a packet is lost, the sender tries to send it again (up to 3 times) in the next active period. Therefore, the actual per-hop latency varies with sleep scheduling and packet re-transmission. The results presented next are from the test runs using the same deployments and movements as in the previous simulation.

Unlike the DLSP simulation with 802.11 MAC with fixed delay of 0.5s, DLSP with S-MAC can have a delay shorter than its frame length (which is set to 0.5s) for the following reasons. First, the sensors surrounding the mobile node stay awake longer than other sensor nodes, so the latency between these sensors and the mobile is much less than that between two sensors under low-power duty cycling, which is approximately 0.5s. Second, at the origin of each packet, the per-hop latency is, on average, half of a duty cycle. As the network size increases, location updates and queries take more sensor-to-sensor hops, so the average per-hop latency increases. The mean and standard deviation of the per-hop latency and the speed limit derived from Eq. 2.13 are shown in Table 2.3.

Figures 2.17–2.19 plot the query-delivery ratio of DLSP, DLSP-SN, and GHLS, respectively, using S-MAC. With S-MAC, the performance of DLSP protocols (DLSP and DLSP-SN) also validates our analysis — DLSP protocols scale well if the mobile’s speed is under the limit as shown in Table 2.3, and degrade as the mobile’s speed grows beyond the movement threshold. Compared to Figures 2.7, 2.17 shows that the performance of DLSP with S-MAC is slightly better than that of DLSP with 802.11-MAC, while the performance

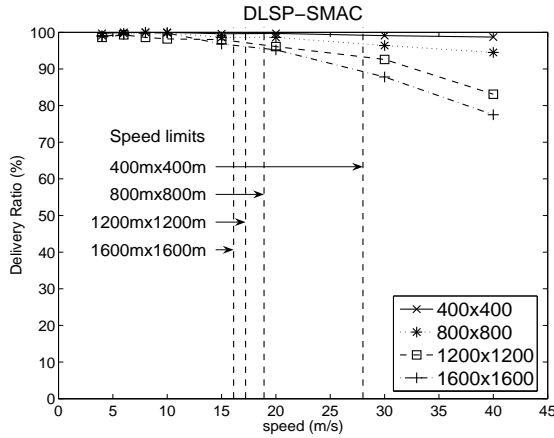


Figure 2.17: The query-delivery ratio of DLSP with S-MAC in a 1600m×1600m network. DLSP with S-MAC scales well if the mobile’s speed is below the threshold shown in Table 2.3.

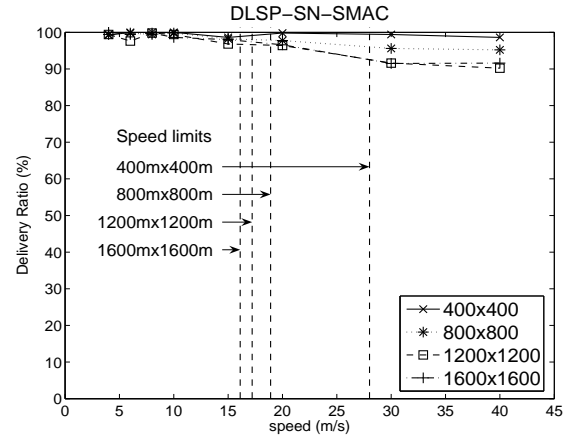


Figure 2.18: The query-delivery ratio of DLSP-SN with S-MAC in a 1600m×1600m network. DLSP-SN with S-MAC also scales well if the mobile’s speed is below the movement threshold.

of DLSP exhibits similar trends regardless of the underlying MAC protocol. This performance improvement is attributed to the fact that the per-hop latency with S-MAC is below 0.5s.

2.6.4 Results with Additional Mobility Models

We also evaluated DLSP with two additional mobility models: random walk mobility model and Gauss-Markov mobility model [9]. The random walk model has strong randomness as in the random way-point model. However, in the random walk model, mobile nodes randomly choose their speed and direction at each fixed interval instead of randomly choosing the destination in the random way-point model. In the Gauss-Markov mobility model, the speed and direction of mobile nodes are correlated over time and modeled as a Gauss-Markov stochastic process. The temporal-dependency of the Gauss-Markov model is determined by two parameters: σ is the standard deviation of the randomly-generated speed and direction at each interval, and α is the memory-level parameter which determined the randomness of the mobility model. The details of these mobility models can be

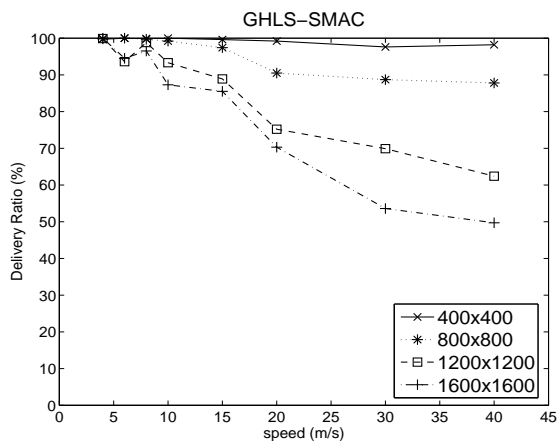


Figure 2.19: GHLS with S-MAC shows a similar trend as GHLS with 802.11 MAC. Since there is no single speed limit for different network sizes in GHLS, the performance degrades even at a lower speed for large networks.

found in the survey paper [9].

Figures 2.20 and 2.21 plot the performance of DLSP with different mobility models. Here we present a subset of our test results to show the effect of different mobility models with different parameters. For the random walk model, the interval duration is set to 20s and 40s and the interval duration is set to 10s to 20s with $\alpha = 0.5$ and $\sigma = \pi/2$ for the Gauss-Markov model. The mobile's speed ranges from 4 to 40m/s as in our previous simulation. It is shown in Figures 2.20 and 2.21 that DLSP scales well if the mobile's speed is under the threshold with any mobility model, which confirms our analysis.

However, at a high speed, it is observed that the degree of performance degradation differs from one mobility model to another, and from one configuration to another, because the performance of location services is affected by other parameters of mobility models, even if the (average) speed is the same. For example, the interval duration of the random walk model affects the performance of the protocol; the longer the duration of the interval, the further the mobile moves. Then, location queries that have been forwarded to the mobile's previous location will be less likely to be in the proximity of the mobile, and the delivery ratio may degrade. This effect is more pronounced when a mobile moves at a high speed in a large network, in which it hits the network boundary less frequently. For exam-

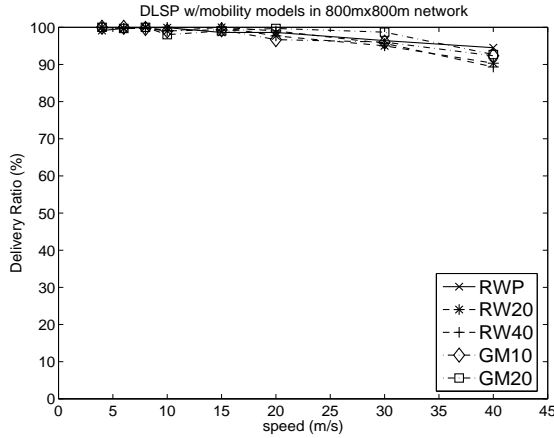


Figure 2.20: The random way-point model (RWP), the random walk model (RWP) with the duration of 20s (RW20) and 40s (RW40), and the Gauss-Markov model with the duration of 10s (GM10) and 20s (GM20) are simulated with DLSP in an $800\text{m} \times 800\text{m}$ network.

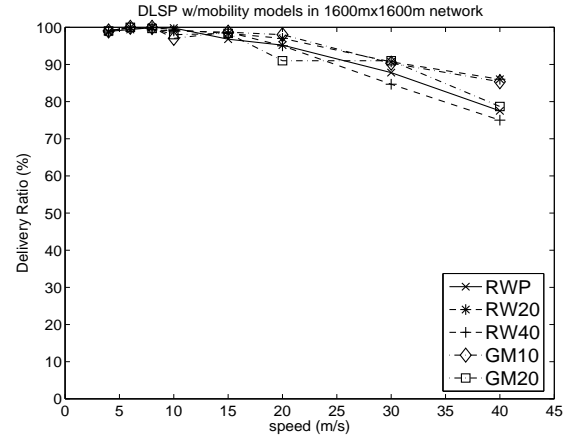


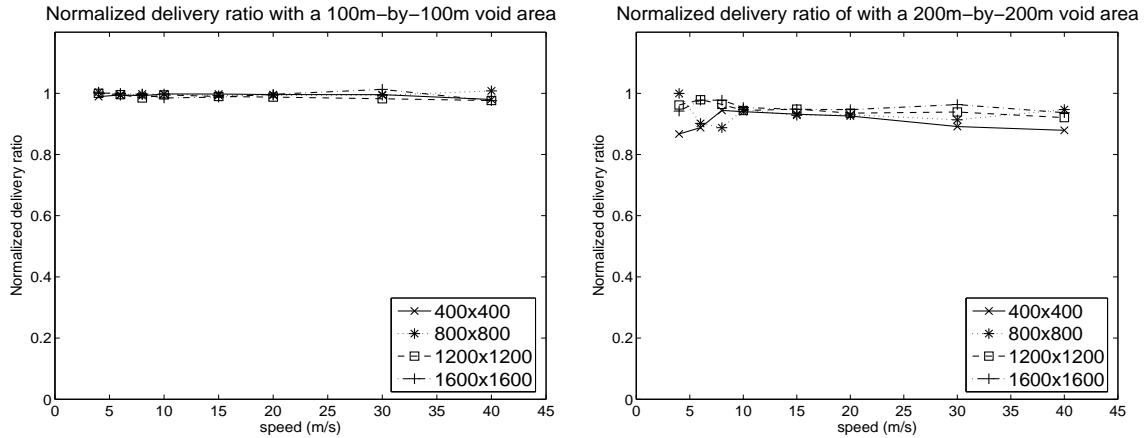
Figure 2.21: The random way-point model (RWP), the random walk model (RWP) with the duration of 20s (RW20) and 40s (RW40), and the Gauss-Markov model with the duration of 10s (GM10) and 20s (GM20) are simulated with DLSP in an $1600\text{m} \times 1600\text{m}$ network.

ple, in Figure 2.21, it is shown that the random walk mobility model with a 20s duration (RW20) outperforms the same model with a 40s duration (RW40) at 40m/s. So does the Gauss-Markov mobility.

There are previous efforts to develop the common metrics that can interpret the parameters of different mobility models [58, 81], but not a single good metric has been developed yet, and most of them focused on routing protocols, not on location services. Development of a universal measure of mobility models for location services is beyond the scope of this work.

2.6.5 Results on Robustness Against Node Failures

We evaluated the robustness of DLSP when some sensor nodes fail. By modifying the scenarios used before, we introduced a void area that contains no functional node. We picked the void area such that the mobile node passes through the area at 30 seconds in simulation time, i.e., the mobile goes through the void area at least once. The size of the



(a) The normalized delivery ratio when a void area of $100\text{m} \times 100\text{m}$ is introduced. (b) The normalized delivery ratio when a void area of $200\text{m} \times 200\text{m}$ is introduced.

Figure 2.22: The delivery ratios with void areas are normalized to that of the scenario without any void area. These plots show that the delivery ratio of DLSP degrades slightly when a void area is introduced. The delivery ratio degrades more as the void area gets relatively larger, i.e., the network becomes smaller or the void area becomes bigger or both.

void area is chosen to be of 100×100 or $200 \times 200 \text{ m}^2$.

Figure 2.22 shows the delivery ratio with a void area, which is normalized to that with no void area shown in Figure 2.17. When a $100 \times 100 \text{ m}^2$ void area is introduced, the delivery ratio drops slightly (up to 2.39%) as shown in Figure 2.22(a). Figure 2.22(b) shows the normalized delivery ratio when a $200 \times 200 \text{ m}^2$ void area is introduced. With the $200 \times 200 \text{ m}^2$ void area, the average degradation of delivery ratio is higher, ranging from 4.43% to 9.16%. The delivery ratio decreases as network size increases (i.e., the relative size of the void area decreases). These figures show that DLSP performs well even with a void area.

The performance degradation is due to the following two reasons: (1) some location update/query messages are more likely to be lost while the mobile is in a void area, and (2) some update/query messages may have to detour around the void area, causing some message loss (decrementing TTL down to zero) or extending their end-to-end delay and hence making it harder for them to catch up with the mobile.

If the size of a void area is relatively large, according to its random movement, the

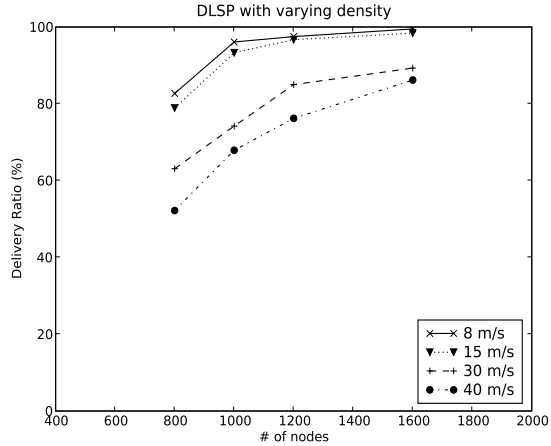


Figure 2.23: The delivery ratio of DLSP degrades as the density of the deployed network decreases, and the speed of the mobile increases.

mobile stays longer inside the void area. Because the mobile has limited or even no connectivity to sensor networks in a void area, some location-update from and location-query messages to the mobile are likely to be lost, resulting in more performance degradation.

Once the mobile enters a void area, its sojourn time there is determined by the path it takes; it stays longer in the void area when going through the center of the area, than when traversing only the boundary of the area. Therefore, when the mobile moves at a low speed, there are more variations in the sojourn time inside the void area, and thus more fluctuations at lower speeds in Figure 2.22(b).

Note that both TTDD and Bread Crumb style approaches will not function correctly if some faulty nodes break the forwarding path. For instance, in the above scenario, the forwarding path is broken by the void area as the mobile goes through it, so the packets generated by some sensor nodes cannot be delivered to the mobile.

2.6.6 Results on Robustness with Low Densities

We extended our evaluation on the robustness of DLSP with low-density networks. We generated networks with 800, 100, 1200, and 1600 sensor nodes within $1600 \times 1600m^2$, which are equivalent to the density of 3.125, 3.9062, 4.6875, and 6.25 nodes per $100 \times$

Number of nodes in 1600m×1600m area	800	1000	1200	1600
Average per-hop progress (m)	62.71	71.11	75.94	80.88

Table 2.4: Average per-hop progress with varying numbers of nodes in 1600m×1600m networks.

100m². The networks with less than 800 nodes are often disconnected, and thus excluded in our evaluation.

As shown in 2.23, the delivery ratio degrades as the node density is decreased or as the mobile’s speed is increased. This is because, as the network gets sparser, the average per-hop progress becomes smaller and the messages travel longer paths. It therefore becomes harder for messages to catch up with the mobile destination. This effect can be severer when a mobile moves with higher speeds.

This result also confirms our analysis; DLSP achieves a high packet-delivery ratio when the average per-hop progress is above 70m/s (the speed used in our analysis) and a mobile’s speed is below its speed limit, 15m/s. The average per-hop progress with the different node density is shown in Table 2.4. In networks with 1000 or more nodes, the average per-hop progress is above 70m/s. In such networks, the delivery ratios of DLSP for the mobile’s speed of of 8m/s and 15 m/s are 98.40% and 96.70%, respectively.

2.7 Conclusion

In this chapter, we presented a distributed location service protocol (DLSP) which considers the non-trivial per-hop latency caused by low-power duty cycling in sensor networks. Through a rigorous analysis of DLSP, we derive the condition for achieving a high packet-delivery ratio, and show how to configure the protocol parameters to ensure the scalability of DLSP. DLSP is shown to be scalable if the mobile’s speed is below a certain fraction of the packet-transmission speed, which depends on a movement threshold. The theoretical mobile’s speed limit is a one-fifth of the packet-transmission speed.

We evaluate DLSP with extensive simulation using two MAC protocols and three mobility models. The evaluation results confirm our analysis. We also proposed an optimization technique, DLSP-SN, that can reduce the location-update overhead by 70% or more, while its query-delivery ratio is even better than DLSP when the mobile's speed is high. In order to make a tradeoff between update and data-delivery costs, we presented a greedy adaptation mechanism, DLSP-ASN, which can significantly improve overall energy-efficiency. DLSP is also shown to be robust in the scenarios with void areas or node failures.

CHAPTER III

DISTRIBUTED HOLE DETECTION

3.1 Introduction

Recently, WSNs are being deployed in various applications such as environmental monitoring, emergency rescue, object tracking, traffic monitoring and control, healthcare applications, and building-integrity monitoring.

A hole in a WSN can be defined as an area which is not covered by a communication or sensing range of any sensor node in the network. A formal definition of a hole is given in Section 3.4. Holes in a WSN can be formed for various reasons. First, holes form due to the characteristics of the deployment area. If a sensor network is deployed in a field or urban setting, obstacles such as lakes or buildings will create holes. Second, holes may be formed due to events. For example, in a sensor network for detecting a fire in a forest, holes may represent the area where fire has occurred. Third, holes may be generated by faulty and depleted nodes. Finally, holes may be formed when an active attacker destroys or jams an area.

The detection of such holes in a WSN is important because 1) the holes themselves can represent valuable information such as characteristics of deployment areas or the event of interest, and 2) the holes can significantly affect the performance of many protocols that use location information. For example, in geographic forward routing, detouring around a hole, such as a perimeter mode of a greedy perimeter stateless routing (GPSR) [33], can be

a very expensive process. Also in data centric storage (DCS) [24, 27, 42, 56], the election of storage nodes may not be possible if the hashed location for a certain event is within certain holes. In such a case, the performance of DCS can be poor or the protocol may not even function.

The current approaches to hole detection can be categorized into *range-free* and *range-based* approaches. The former [21, 41] exploits only connectivity information for hole detection, while the latter [18] exploits geographic location information from sensor nodes. Although range-free approaches do not require a localization service, they are inefficient for detecting newly-generated or enlarged holes because they require expensive network-wide flooding procedures to detect any change in network topology. On the other hand, range-based approaches [18] require a localization service. The localization service is not an extra overhead for various sensor network applications, since they too require the geographic location of sensor nodes. However, an unrealistic unit-disk model is adopted in [18], which does not discuss location estimation errors or link asymmetry.

We propose a distributed hole detection algorithm that utilizes location information. The proposed algorithm is designed for applications that require knowing the geographic location of sensor nodes and prompt detection of newly-generated or enlarged holes, for such applications as the fire detection. The real-time availability of the information of areas affected by fire is important. The proposed algorithm will depend only on local information of node locations for detecting holes in a WSN. Also, the proposed algorithm will be able to tolerate the location errors and asymmetry of the communication ranges among sensor nodes.

The contributions in this chapter are threefold as follows. First, we propose a distributed algorithm, TRAVERSE, to detect the hole boundaries. It exploits the information of the realistic radio and localization models. Second, we suggest geographic forward routing with hole avoidance (GFRHA) to detour packets around holes. GFRHA uses the hole information detected by TRAVERSE to route packets before they encounter the holes, to

reduce path lengths and energy consumption. Finally, we evaluate TRAVERSE and GFRHA with qualitative and quantitative metrics. We first evaluate TRAVERSE for topologies with holes of various shapes, and then for varying network density, or with varying parameters of the radio model. We also evaluate GFRHA against a well-known geographic forwarding algorithm, GPSR, to show its performance gain in the presence of holes.

The rest of this chapter is structured as follows. In Section 3.2, we summarize the related work. After introducing the assumptions in Section 3.3, we present the details of our distributed hole detection algorithm in Section 3.4. In Section 3.5, we discuss GFRHA as an application of the proposed protocol. Section 3.6 shows the qualitative and quantitative evaluations of our approach. Finally, we conclude this chapter in Section 3.7.

3.2 Related Work

In the range-free hole-detection algorithms, the location of sensor nodes is not used. Instead, the connectivity information is used to detect holes. In the range-based algorithm, the location of sensor nodes is used to determine the boundary of each hole on the network.

Range-free approaches [21,41] flood the network from a small number of beacon nodes. Holes are identified using hop-count discrepancies from those beacon nodes. A few additional flooding procedures are necessary to tighten the boundary of the detected holes. This approach is claimed to be more efficient, since it does not require a localization service and the number of flooding procedures is limited [41]. However, detecting newly generated or enlarged holes with this approach may not be efficient because it requires a few network-wide flooding procedures to identify new boundaries of holes upon changes in network topology.

Range-based approaches [18] require the location information of each node, since their detection mechanism depends on the location information of sensor nodes. However, the localization service is not an extra overhead for various sensor network applications, since they too require the geographic location of sensor nodes. Thus, location information is

already available without any overhead for those applications. For example, the aforementioned fire-detection application will require the geographic location of the sensor nodes *where* a fire occurred. However, in [18], an unrealistic unit-disk model is adopted, which does not discuss location estimation errors or link asymmetry.

A hole detection problem also appeared in graph theory [29, 50]. However, the definition of a hole in graph theory is not same as that of our problem. In graph theory, a *hole* is defined as a chordless cycle with five or more vertices, where a *chordless cycle* is defined as a sequence of k distinct vertices, v_0, v_1, \dots, v_{k-1} in which there is an edge from v_i to $v_{(i+1) \bmod k}$ (for all $i = 0, \dots, k - 1$), and no other edge between any two of these vertices. When nodes and links between them are represented as vertices and edges, respectively, the holes in the sensor networks are identified as holes in graph theory. However, a chordless hole may not correspond to any hole in a WSN. Even though a chordless hole corresponds to a hole in the WSN, the chordless hole may not be a tight bound of a hole in a WSN. Thus, we modified the definition of hole in graph theory to fit our problem. Our formal definition of hole will be given in Section 3.4.

Motion planning [37] is one of the fields in robotics that has several similarities with our problem, where a problem of navigating robots avoiding obstacles is studied. Typically, motion planning takes two phases: mapping and planning. A map of a given area is obtained in the mapping phase, and actual movement pattern is evaluated in the planning phase. A map of the given area is often obtained by using multiple sensor-readings, or by exploration of automated robots. Then, an optimal path to a destination location is evaluated using the obtained map.

Our hole-detection is similar to the mapping phase, and GFRHA is similar to the planning phase; we first find holes (obstacles) in the given area, and then, route messages instead of navigating robots avoiding the detected holes. However, there are several differences between motion planning and our problem. In motion planning, mapping and planning is done by resourceful robots. In the mapping phase, they directly interact with

multiple sensors, or explore the area by themselves, and in the planning phase, they evaluate the optimal (or near-optimal) path to the destination using a global map obtained in the mapping phase. In our problem, since sensor nodes are resource-limited and have only limited local views instead of a globe view of the deployment area, they should collaborate to detect holes, and use local views to route messages around holes.

Nonetheless, there are algorithms, called *bug algorithms*, that use only limited local views as in our algorithms proposed in this chapter. Among bug algorithms, *VisBug* is similar to GFR; in *VisBug*, robots are navigated in the direction of a destination until they encounter an obstacles, and then around the obstacles using only local information. Also, *TagentBug* is similar to our algorithm, GFRHA; in *TangentBug*, robots are navigated in the tangential direction of an obstacle if it lies between the current position and the destination. The difference between *TangentBug* and our algorithms are twofold. First, in *TRAVERSE*, sensor nodes *distributively* detect holes, while robots can directly detect the boundary of obstacles by using a visibility sensor in *TagentBug*. Second, the detected hole information should be disseminated to nearby sensor nodes, while this procedure is not required since robots have the obstacle information obtained with their own visibility sensors.

3.3 System Assumptions

3.3.1 Radio Model

In WSNs, wireless channels show irregularities on radio performance as in other wireless channels [49, 82]. The irregularities are very common in wireless communication, and they are caused by many factors, such as different path losses, depending on propagation directions, radio transmission power, and interferences with other nodes. These irregularities result in non-uniform transmission ranges, asymmetric communication links, etc.

The unit-disk model is a simple disk model, but cannot capture the dynamics of wireless channels. Under the unit-disk model, the radio transmission range is a perfect circle; all the

nodes in the network have a uniform transmission range, and there is a link between two nodes if they are located within the transmission range. Thus, this model cannot represent the realistic performance of a WSN.

Here, we adopt the *log-normal shadowing* radio propagation model [49] to capture the irregularities of wireless channels, in which the received signal strength is modeled with the log-normal distribution. More specifically, the reception power P at distance r from the transmitting node with the transmission power p_0 is defined by

$$P = p_0 \left(\frac{r_0}{r} \right)^\alpha 10^{X/10},$$

where r_0 is the reference distance for the antenna far-field, α the path loss exponent, and $X \sim N(0, \sigma^2)$, where σ is the shadowing deviation. This model is identical to the unit-disk model when $\sigma = 0$. The *threshold distance* is defined as one from which the received signal strength starts to drop below the threshold power, under which the receiver cannot decode signals when $\sigma = 0$. As in [49], we also define the *connection function*, $\phi(r)$, as the probability that a receiver at distance r from the sender can decode the signal. The connection function for the log-normal distribution is given by

$$\begin{aligned} \phi(r) &= Pr \left[X \geq \frac{10\alpha \ln(r/r_t)}{\ln(10)} \right] \\ &= \frac{1}{2} - \frac{1}{2} \operatorname{erf} \left(\frac{10\alpha \ln(r/r_t)}{\sqrt{2} \ln(10) \sigma} \right). \end{aligned}$$

Since our proposed algorithm requires two-way communications, we assume that there exists a link between two nodes with the probability of $\phi(r)^2$ when the distance between them is r .

3.3.2 Localization Service Model

Localization services in sensor networks have gained popularity because they provide location information essential to numerous sensor network applications. Localization services estimate the location of each sensor node using the relative distance or direction among sensor nodes and optional anchor nodes with exact location information. Relative distance or directions among neighboring nodes are obtained using difference-in-time-of-arrival, received signal strength, or connectivity. Typically, localization service iterates the estimation process several times to achieve a high level of precision in location estimation as required by the applications. Also, there may exist anchor (or beacon) nodes which have the exact location information loaded manually or obtained by using GPS-like devices. These anchor nodes provide their exact location information to sensor nodes in their vicinity, and this location information acts as the seed of the location information for normal sensor nodes. Using anchor nodes reduces the errors of the location estimation and/or the number of iterations to achieve the same level of precision in location estimation.

Here, we assume that the location estimation error can be modeled as a normal distribution. In other words, the majority of location estimations for the sensor nodes are close to the exact locations of the sensor nodes. Also, we assume that the standard deviation of the normal distribution is smaller than, or comparable to, the average communication range of sensor nodes. If the location estimation errors are too large, not only our hole detection algorithm, but also other routing protocols or applications running atop the localization service, will not function correctly. Thus, this assumption is reasonable for most WSN applications.

3.4 Distributed Hole Detection

3.4.1 Overview

We first define a hole in WSNs using graph theory. Nodes and links between nodes are represented as vertices and edges, respectively. On the graph, a hole is defined as a cycle with certain properties.

Based on this definition of a hole, we present an algorithm called TRAVERSE to detect the boundary of each hole. The algorithm is designed to be distributed so that it can be invoked efficiently and immediately upon each topology change. Also, it is designed to function with errors in location estimation, or the realistic radio model, such as the log-normal radio propagation model. The process of detecting holes is composed of three steps. First, we identify nodes that may be on the boundary of holes, called *boundary candidate* nodes. The condition for the candidate nodes will be discussed in the following subsection. Second, we identify the boundary of each hole by starting from the candidate node. TRAVERSE is designed to identify the boundary of each hole. Third, we detect enlarged or newly-generated holes by invoking TRAVERSE upon topology change.

The rest of this section is organized as follows. The definition of a hole in WSN is given in Section 3.4.2. We describe the identification of candidate nodes in Section 3.4.3, followed by a description of handling special cases in Section 3.4.4. The main algorithm, TRAVERSE, is introduced in Section 3.4.5. Finally, we describe the detection of a new hole or the change of a hole in Section 3.4.6.

3.4.2 Definition of a Hole

Here, we formally define a hole before discussing hole detection. We first define some terminologies, and use them to define a hole.

We introduce a graph representation of a sensor network for concise description of our problem. A deployed sensor network can be represented as a graph $G = (V, E)$, where

sensor nodes and links between sensor nodes are represented as vertices and edges, respectively. Since geographic location of vertices in a graph G is important for hole definition, we also consider G as a subset of \mathbf{R}^2 , where the vertices in G have the same geographic location, or 2-D coordinates, as they have in a deployed sensor network. The deployed sensor network can be considered as the graph G 's geometric realization of \mathbf{R}^2 . We define a hole with both geographic- and graph-representation of the deployed network.

We now define terminologies needed for hole definition.

Definition 1. Let C be a sequence of vertices of length k , v_0, v_1, \dots, v_{k-1} . We define C as a non-intersecting cycle if there is an edge from v_i to $v_{i+1 \bmod k}$ (for all $i = 0, \dots, k-1$) and no edge in the cycle intersects with another edge.

Definition 2. A non-intersecting cycle C divides the plane into two regions. We define the region on the right side of the cycle as the *inside* of the cycle if we traverse the cycle in the same order of the given sequence of the cycle. The other region is defined as the *outside* of the cycle.

Now we define a chordal path as follows.

Definition 3. For a non-intersecting cycle C , consider a path P with the following conditions. First, P is a sequence of vertices, $w_0, w_1, \dots, w_{\ell-1}$. Second, there exist non-adjacent vertices v_i and v_j such that $w_0 = v_i$ and $w_{\ell-1} = v_j$. Third, for all p ($0 < p < \ell - 1$), there does not exist any q ($0 \leq q \leq k - 1$) such that $w_p = v_q$. If there exists a path P satisfying all of the above conditions, we define such a path as a chordal path of the cycle C .

We can now define a hole in a WSN with the above terms as follows.

Definition 4. We define a non-intersecting cycle C as a hole if it has no chordal path inside the cycle. Also, we define the edges of the cycle as the boundary of the hole.

For a given hole, we also define the following terminologies.

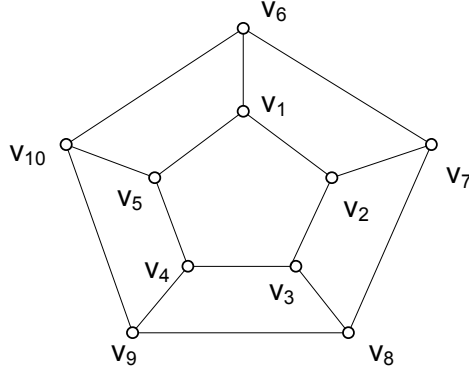


Figure 3.1: This figure shows examples of holes.

Definition 5. A hole is defined as an *inner hole* if the order of the vertices in the cycle is clockwise. The boundary of an inner hole is defined as an *inner boundary*. Similarly, we define a hole as an *outer hole* if the order of the vertices in the cycle is counterclockwise, and its boundary as an *outer boundary*. Inner boundaries define the boundaries of holes inside the deployment area, and outer boundaries define the boundaries of the network deployment area.

Definition 6. We define node v_i and node v_k as the incoming node and the outgoing node for node v_j , respectively, when there is a partial path such as $\dots, v_i, v_j, v_k, \dots$ in a hole boundary.

We now clarify the definition of a hole with an example shown in Figure 3.1. For example, a cycle v_1, v_2, v_3, v_4, v_5 is a hole since there is no chordal path inside the cycle. Also, this cycle is an inner hole since the order of vertices is clockwise. On the other hand, a cycle v_1, v_5, v_4, v_3, v_2 is not a hole since there are chordal paths inside the cycle; a path v_1, v_6, v_7, v_2 is one such chordal path.

Now let us consider a cycle $v_6, v_{10}, v_9, v_8, v_7$. Since there is no chordal path inside the cycle, this cycle is a hole. Note that vertices v_1, v_2, \dots, v_5 are outside of this cycle. This cycle is an outer hole, and it defines the boundary of the deployment area.

Depending on the application or the network service which uses the boundary information, very small holes are insignificant. For example, the performance of geographic

routing protocols are not affected by very small holes. Thus, it may be useful to have thresholds for a hole such that only holes relevant for the application are identified. We define a hole of a length k or more as a k -length hole. Similarly, we can define A -area hole as a hole of size equal to or greater than A , where the area of a given hole is defined as the area of the inside (outside) for an inner (outer) hole.

3.4.3 Identification of Candidate Nodes

As a preparation process of TRAVERSE, we identify the boundary candidate nodes. Boundary candidate nodes are the nodes which may lie on the boundary of holes. Then, TRAVERSE will be initiated from each candidate node.

From the definition of a k -length hole, it is obvious that the boundary of a k -length hole is an ℓ -side polygon, where $\ell \geq k$. In such a polygon, we have the following property.

Lemma III.1. *The sum of angles inside an ℓ -gon is given as $\pi \cdot (\ell - 2)$. Thus, there is at least an inner angle that is equal to, or greater than, $\pi \cdot (\ell - 2) / \ell$. Since $\pi \cdot (\ell - 2) / \ell \geq \pi \cdot (k - 2) / k$ if $\ell \geq k$. Therefore, there is at least an inner angle that is equal to, or greater than, $\pi \cdot (k - 2) / k$ among nodes on the boundary of a hole of length of $\ell (\geq k)$.*

We define a candidate node based on Lemma III.2.

Definition 7. Let v_0 be a node with p neighbors, v_1, v_2, \dots, v_p . Without loss of generality, we assume that v_1, v_2, \dots, v_p are in the counterclockwise order from v_0 . We also let $v_{p+1} = v_1$. We define the node v_0 as a candidate node if there exists i , $1 \leq i \leq p$ such that $\angle v_i v_0 v_{i+1} \geq \pi \cdot (k - 2) / k$, where k is the threshold of a hole. Here, we also define v_i and v_{i+1} as an incoming node and an outgoing node of the candidate node. Note that a candidate node may have more than one pair of incoming-outgoing nodes.

From the definition of candidate node, we have the following property.

Lemma III.2. *For each hole in a WSN, there exists at least one candidate node, v , in the hole boundary. Also, v and v 's incoming and outgoing nodes belong to the hole boundary.*

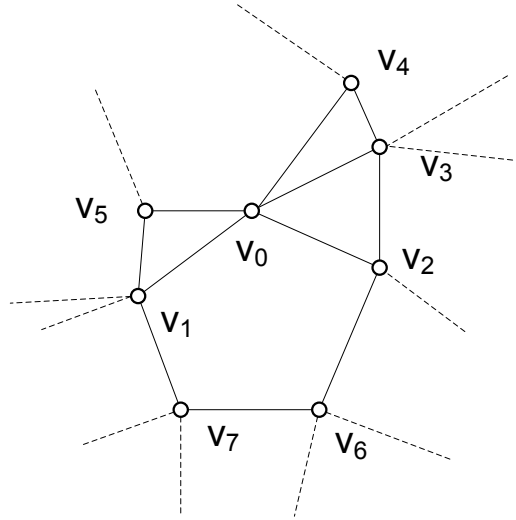


Figure 3.2: This figure shows examples of candidate nodes.

Proof. From Lemma III.1, at least one of inner angles of a hole is equal to, or greater than, $\pi \cdot (k - 2)/k$. Since every node that has such angles at it is identified, there exists at least one candidate node for each hole boundary. \square

Thus, candidate nodes can be identified using information about immediate neighbors. Note that when a node on a hole boundary is identified as a candidate node, its incoming node and outgoing node are also in the boundary of the hole. Also, note that a node may identify itself even though it is not in a hole boundary. This may happen when the length of the minimum cycle including the identified node and its incoming and outgoing nodes is smaller than the threshold k . Also, it may happen to a node that belongs to BRIDGE or CAPE, which will be defined in Section 3.4.4.

Figure 3.2 shows the example of a candidate node. We will use a node v_0 as an example node. It first sort its neighbor nodes with the counterclockwise angular order. Here, the result will be $v_1, v_2, v_3, v_4,$ and v_5 . When $k = 5$, $\angle v_1 v_0 v_2$ and $\angle v_4 v_0 v_5$ are greater than $\pi \cdot (k - 2)/k = 0.6\pi = 108^\circ$. Thus, v_0 is identified as a candidate node, and v_1 - v_2 and v_4 - v_5 are identified as incoming-outgoing pairs of the candidate node v_0 . We may need to invoke TRAVERSE more than once from the candidate node v_0 since it has more than one

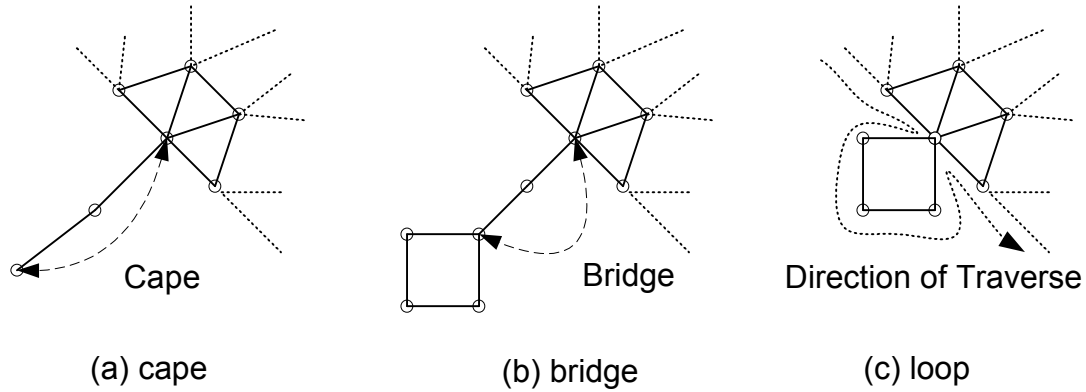


Figure 3.3: The special cases handled by the TRAVERSE algorithm.

pairs of incoming-outgoing nodes.

3.4.4 Handling Special Cases

After identifying the candidate nodes, we handle some special cases before invoking the hole traverse algorithm.

First, we identify nodes which have only one neighbor. From each such nodes, we start traversing following the neighbor of the node until we find a node which has more than two neighbors. We call this path CAPE. Figure 3.3(a) shows examples of CAPES with the length of two. CAPES may exist on the boundaries of holes or network area, and the number of CAPES may increase as the density of the network decreases. We exclude the nodes in CAPES with the exception of the last one, which has more than two neighbors, when identifying the boundaries of holes since these nodes will give the dead-ends.

Second, we remove the candidate node information if a node has only two neighbors. This node belongs to either a CAPE or a BRIDGE. BRIDGE as shown in Figure 3.3(b) is defined as a path between two boundaries of different holes if only one path exists between the two boundaries. The detailed discussion of BRIDGE will follow in the following subsection. If this node belongs to a CAPE, this node will not be on the boundary of any hole, as explained above. If this node belongs to a BRIDGE, this node will be identified as a node on the boundary by starting TRAVERSE from another node. In both cases, it is not

necessary to start TRAVERSE from nodes which have only two neighbors. Thus, we do not start TRAVERSE from these nodes.

Finally, we remove the hole of length three. For every candidate node, we check if the incoming node of the candidate node is a neighbor of the outgoing node of the candidate node. In other words, the hole formed by the candidate node is a simple triangle. Thus, we eliminate this case since the hole caused by such a candidate node is trivial.

3.4.5 Identification of hole boundary

After identifying candidate nodes, we identify a boundary for each hole by traversing from candidate nodes. Basically, we follow the boundary of holes using the right hand rule as in [18]. However, we need to enhance the traversing method to accommodate the realistic radio model.

We present the TRAVERSE algorithm to identify the boundary of holes. In essence, TRAVERSE forwards a message starting from a candidate node using the right-hand rule to follow the boundary of a hole in a clockwise direction. When starting TRAVERSE, we apply the right-hand rule from the incoming node of the candidate node, which will result in an outgoing node. Note that a candidate node can have more than one pair of incoming–outgoing nodes. In such a case, we may need to invoke TRAVERSE for each pair of incoming–outgoing nodes. For example, in Figure 3.2, v_0 will initiate TRAVERSE with $v_1 - v_2$ and $v_4 - v_5$ as incoming–outgoing node pairs. After initiating TRAVERSE, we repeat the use of the right-hand rule until we reach the starting node. If we reach the starting node while traversing a hole, the path generated by TRAVERSE is identified as the boundary of the hole, and TRAVERSE will terminate. In the example shown in Figure 3.2, the boundary for the $v_1 - v_2$ pair will be found by the order of v_0, v_2, v_6, v_7, v_1 , and v_0 by using the right-hand rule. This algorithm is similar to BOUNDHOLE algorithm in [18], but has different rules in handling special cases such as edge intersections and loops.

In TRAVERSE, we do not allow edge intersections. If the link between the current node

and the next node to follow dictated by the right-hand rule intersects any of the link in the path of the current traverse, we do not follow the link. Instead we apply the right-hand rule repeatedly until we find a link which does not intersect any of the links in the path of the current traverse. It is possible that every outgoing link intersects with the current traverse path. In this case, we abandon the last node in the path, and go back to the second last node in the path. At the second last node, we find the next best node other than the last node in the path, and follow the node. This process is called *back tracking*. The length of cycles identified by TRAVERSE may be smaller than the threshold k . Information about such small cycles is not required by applications, and thus, it is abandoned.

Now, we will show the property and the correctness of TRAVERSE.

Lemma III.3. *When TRAVERSE is invoked at a candidate node on a hole, it finds the hole containing the candidate node and its incoming–outgoing node pair.*

Proof. A node that belongs to either BRIDGE or CAPE does not invoke TRAVERSE. Thus, TRAVERSE is invoked only when it and its incoming and outgoing nodes belong to the boundary of a hole. Note that a hole may be shorter than the threshold k , which should be checked after identifying the hole.

TRAVERSE will first follow the outgoing node of the given candidate node by the right-hand rule. Finding the next node using the right-hand rule is repeated until the starting candidate node is reached. Since, in TRAVERSE, edge intersection is not allowed when selecting the next node, it will follow the hole boundary without breaking it. Also, due to the back tracking, TRAVERSE will continue to follow the hole boundary in case there is no node to follow, which may happen when all the edges from a certain node are intersecting the hole boundary.

Now, we will prove there is not any chordal path inside the cycle. Let us assume that there exists a chordal path P, w_1, w_2, \dots, w_p , inside a cycle C, v_1, v_2, \dots, v_k , identified by TRAVERSE. Let w_1 be v_i , which is one end of the chordal path P . For concise representation, we also let v_0 and v_{k+1} be v_k and v_1 , respectively. Since the chordal path is inside the cycle

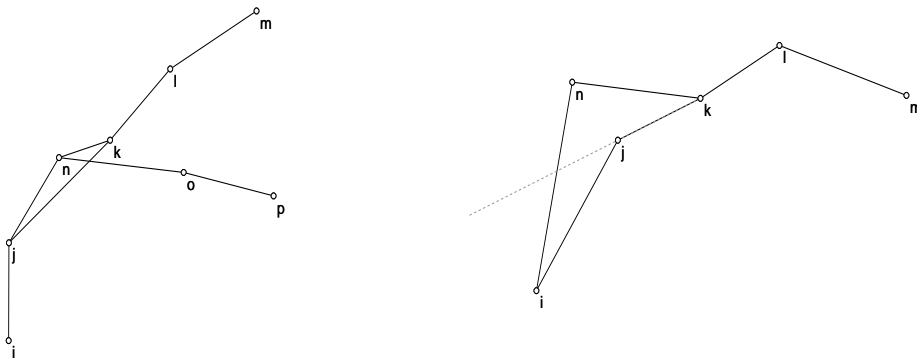
C from the assumption, i.e., the nodes in P are in the right side of the cycle, $\angle v_{i-1}w_1w_2 = \angle v_{i-1}v_iw_2 < \angle v_{i-1}v_iv_{i+1}$. However, in such a case, the next node chosen by TRAVERSE at the node v_i should have been w_1 instead of v_{i+1} by the right-hand rule. This contradiction comes from the assumption that there exists a chordal path. Therefore, there does not exist a chordal path in the cycle identified by TRAVERSE. \square

Now we can prove the correctness of TRAVERSE.

Theorem III.4. TRAVERSE finds every hole in the deployed network.

Proof. From Lemma III.2, it is proved that TRAVERSE will be initiated from at least one node from every hole in the network. Then, as proved in Lemma III.3, TRAVERSE identifies a cycle without chordal paths. Thus, the cycle identified by TRAVERSE is a hole if its length is greater than the threshold k . Therefore, with the identification of candidate nodes and TRAVERSE, every hole in the network is identified. \square

Also, we find the next node to traverse by looking at up to two-hop neighbors to find tight bounds. Under the unit-disk model, it may suffice to consider only 1-hop neighbor as in [18]. However, in a real scenario, a topology as shown in Figure 3.4 may exist in the network due to the location estimation error or non-uniform radio transmission range. In such a case, there may be a tighter bound than the hole boundary found by TREAVERSE using only 1-hop neighbor. Note that the latter boundary is also a hole by definition. Thus, we consider the location of up to two-hop neighbors, and the node as the next traversing node which has a neighbor in the traversing direction. For example, in Figure 3.4(a), TRAVERSE considers up to two-hop neighbors when selecting the next node to follow. When the current path is $\dots - i - j$, node n will be selected as the next node to follow since its neighbor o is preferred to node l by the right-hand rule. However, a certain two-hop neighbor of the current node which seems better by the right-hand rule may not be a preferable choice. In Figure 3.4(b), when the current path is $\dots - i - j - k$, node i , a two-hop neighbor of k is preferred to node l or node m by the right-hand rule. However, selection of this node is



(a) When the current path is $\dots - i - j$, node n will be selected as the next node to follow since its neighbor o is preferred to node l by the right-hand rule. (b) When the current path is $\dots - i - j - k$, the node l is selected as the next node to follow instead of node n because node i , a neighbor of node n , goes back to the node in the current path.

Figure 3.4: Examples of cases to consider two-hop neighbor lookups when TRAVERSE selects the next node to follow.

not preferred since it goes back to the previous path. To avoid such a case, we check if the two-hop neighbor is not on the left-side of the following path. For example, if k chooses n as its next node to follow, node i is on the left-side of the segment $k - n$. Thus, node i through node n is not a preferable choice to follow.

While traversing, we may form a loop in the path as shown in Figure 3.3(c). This case often occurs when we traverse the network boundary. In this case, we remove the loop from the current traverse path, and the loop is identified as a boundary of another hole. After separating the identified loop into another boundary of a hole, we continue the traversing from the node where the loop is found using, again, the right-hand rule.

A special case of the boundary may include the BRIDGE. BRIDGE is defined as a path between the boundaries of different holes if only one path exists between them as shown in Figure 3.3(b). A BRIDGE is identified by TRAVERSE when it detects a loop, and it cannot find any other link to follow but the link in the traverse path. In this case, we trace back our traverse path until we can find another link to follow. Then, we continues TRAVERSE from that node, and the path in the BRIDGE is removed from the boundary.

3.4.6 Detection of Topology Changes

TRAVERSE will be invoked shortly after the initial deployment to identify the routing holes introduced by the environment, such as terrain or non-uniform deployment. However, while the sensor networks are operating, the topology of the sensor networks may change because of faulty nodes, events in the network, or active attack. Thus, new holes may be generated or the existing holes may be enlarged. These topology changes should be recognized, and the boundary information should be updated as necessary.

In most sensor network protocols, each sensor nodes periodically broadcasts *heart-beat* packets to ensure its availability to its immediate neighbors. When a node misses consecutive heart-beat packets more than a predefined threshold from one of its neighbors, it regards the neighbor node failed, and removes it from its neighbor list.

When a node detects a failure of its neighbor, TRAVERSE can be invoked in the following cases to reflect the change in topology of the sensor networks. First, TRAVERSE will be invoked if a node becomes a candidate node after missing one or more of its neighbors. In this case, TRAVERSE will run normally as in the initial hole detection phase.

Second, TRAVERSE can be invoked if one of the nodes in a boundary of a hole detects its outgoing node failed. In this case, we set an *update* flag to enforce the hole detection since the nodes in the boundary already have the boundary information.

3.5 Geographic Forward Routing with Hole Avoidance

3.5.1 Overview

We now discuss utilizing the hole boundary information identified by TRAVERSE. As an example application utilizing hole information, we modify the geographic forward routing (GFR) protocol such that packets are detoured around holes. As a baseline GFR protocol, we will use GPSR [33].

While a packet is forwarded near a hole by GPSR, it can be the case that the node which

holds the packet does not have any neighbor node closer to the destination location. In such a case, GPSR needs to start an expensive hole detouring algorithm. For example, in such a case, GPSR enters perimeter mode, and routes the packet to the nodes using the right-hand rule in a planarized graph.

However, packets can be detoured before they encounter a hole instead of invoking expensive perimeter-mode forwarding, if the boundary of holes identified by TRAVERSE are known in advance. When a node forwards a packet, it can check if there exists a hole between the node and the destination location. In such a case, it can detour the packet around the hole instead of greedily forwarding the packet to the direction.

In the rest of this section, we discuss the utilization of hole information with more details in Section 3.5.2, and then, show examples of the routing while detouring packets to avoid holes in Section 3.6.2.

3.5.2 Detouring Messages Using Hole Information

We propose geographic forward routing with hole avoidance (GFRHA) as a potential application of the hole information. GFRHA detours packets around holes before they encounter a hole to avoid expensive perimeter-mode forwarding. To achieve this, we first disseminate the identified hole information around the hole. Then, we detour the packet utilizing the disseminated information as necessary.

When the boundary of a hole is identified by TRAVERSE, the summary of the boundary information is disseminated to sensor nodes near the hole. After identifying a hole, we approximate the identified hole as a circle which contains all the nodes on the boundary of the hole. Then, we disseminate the summary of the hole, i.e., the coordinates of the center and the radius of the approximated circle, to the nearby sensor nodes. More specifically, we disseminated the summary information only to sensor nodes near the hole using controlled flooding; when a sensor node receives such information, it rebroadcasts it only when it is within a certain threshold distance from the center of the circle.

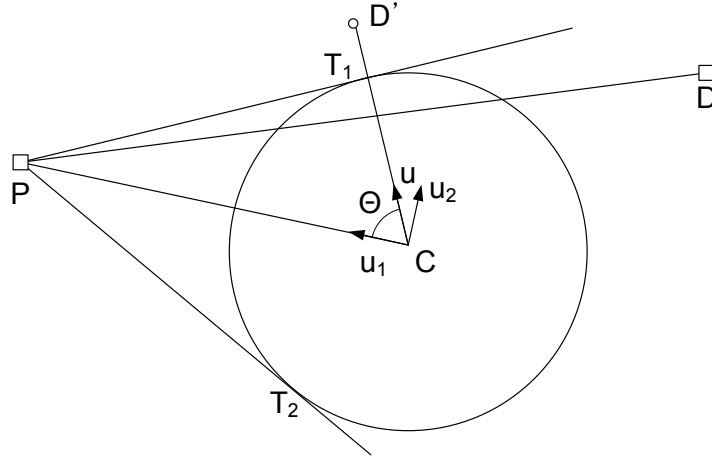


Figure 3.5: This figure shows examples of holes.

While forwarding packets, GFRHA detours packets utilizing hole information as necessary. If there exists a hole between the current forwarding node and the destination location, GFRHA detours a packet around the hole. More specifically, GFRHA detours the packet to the tangential point closer to the destination.

Figure 3.5 shows this in detail. Let us assume that a node P has a packet destined to D , and it has the hole-summary information such that the hole is centered at the point C and its radius is r . When selecting the next hop to forward, node P checks if the hole is on the way to the destination by evaluating the distance between the line \overline{PD} and the center of a hole, C . If the distance is smaller than R , i.e., the hole is on the way to the destination, node P detours the packet around the hole by sending the packet to the temporary destination D' . The location of D' is obtained as follows. Node P can draw two tangential lines to the circle, and let T_1 and T_2 be the points of contact between the tangential lines and the circle. Without loss of generality, let T_1 be the contact point closer to the destination D . If we let \vec{u} be a unit vector such that $\vec{u} = \frac{\overrightarrow{CT_1}}{|\overrightarrow{CT_1}|}$ and $\overrightarrow{CD'} = (R + r) \cdot \vec{u}$, where R is the average radio transmission range.

Vector \vec{u} can be evaluated as follows. First, let \overrightarrow{CP} , $\overrightarrow{CT_1}$, and θ such that

$$\begin{aligned}\overrightarrow{CP} &= \ell \cdot \overrightarrow{u_1}, \\ \overrightarrow{CT} &= r \cdot \overrightarrow{u}, \\ \theta &= \angle PCT_1,\end{aligned}$$

where $\overrightarrow{u_1}$ and \overrightarrow{u} are unit vectors.

Since $\overline{PT_1} \perp \overline{CT_1}$, $\overrightarrow{CP} \cdot \overrightarrow{CT_1} = r^2$. From this, we get $\ell \overrightarrow{u_1} \cdot r \overrightarrow{u} = lr \cos \theta = r^2$. Thus, $\overrightarrow{u_1} \cdot \overrightarrow{u} = \cos \theta = r/\ell$.

Now let $\overrightarrow{u_2}$ a unit vector such that $\overrightarrow{u_1} \perp \overrightarrow{u_2}$, $\overrightarrow{u} = \alpha \overrightarrow{u_1} + \beta \overrightarrow{u_2}$.

We can get α and β as follows.

$$\begin{aligned}\overrightarrow{CP} \cdot \overrightarrow{CT_1} &= \ell \overrightarrow{u_1} \cdot r (\alpha \overrightarrow{u_1} + \beta \overrightarrow{u_2}) \\ &= \alpha r \ell \overrightarrow{u_1} \cdot \overrightarrow{u_1} + \beta r \ell \overrightarrow{u_1} \cdot \overrightarrow{u_2} \\ &= \alpha r \ell \\ &= r^2\end{aligned}$$

Thus,

$$\alpha = \frac{r}{\ell} \quad \text{and} \quad \beta = \pm \frac{\sqrt{\ell^2 - r^2}}{\ell}.$$

Thus,

$$\overrightarrow{u} = \frac{r}{\ell} \overrightarrow{u_1} \pm \frac{\sqrt{\ell^2 - r^2}}{\ell} \overrightarrow{u_2}.$$

If the current node P or the destination location D is in the circle C , it just uses the perimeter mode instead of detouring because there may not exist a path to D' .

3.6 Evaluation

3.6.1 Distributed Hole Detection

We evaluate our hole detection algorithm, TRAVERSE, with various scenarios to evaluate its performance qualitatively and quantitatively. First, we present the quantitative results of TRAVERSE that show the boundaries identified by the algorithm on the deployed area. Then, we show the qualitative results of the proposed algorithm.

Throughout the simulation, we set the transmission range of sensor nodes to 100 m, which is adopted from the characteristics of MicaZ [1]. When we simulate with the log-normal shadowing radio propagation model, the threshold distance is set to 100 m. Also, the deployment area is set to a 2000 m \times 2000 m field. Different numbers of sensor nodes are uniformly deployed in the deployed field depending on the scenarios. The average degree of the sensor nodes is determined by the number of nodes in the area and the transmission range of the sensor nodes. Note that the performance of TRAVERSE depends on the average degree and the relative locations of sensor nodes. However, we use these parameters to show the results of more realistic scenarios.

First, we show the holes with various shapes detected by TRAVERSE in Figure 3.6. In these examples, arbitrary holes are generated on the network where the average node degree is 20, i.e., a sensor node has an average of 20 neighbors. Here, the small squares represent sensor nodes, while the thick red lines represent boundaries of the identified holes. The threshold for TRAVERSE is set to 4, so not only the large hole at the center but also small holes are identified.

Figure 3.7 shows the result of TRAVERSE when the average degree of nodes is varied. We make an artificial hole in the center of the deployment area with the radius of 500 m, one fourth the length of the network boundary. In these figures, the small squares represent sensor nodes, and thick red lines represent the boundaries identified by TRAVERSE. As shown in Figure 3.7, TRAVERSE finds the tighter boundary as the average degree increases.

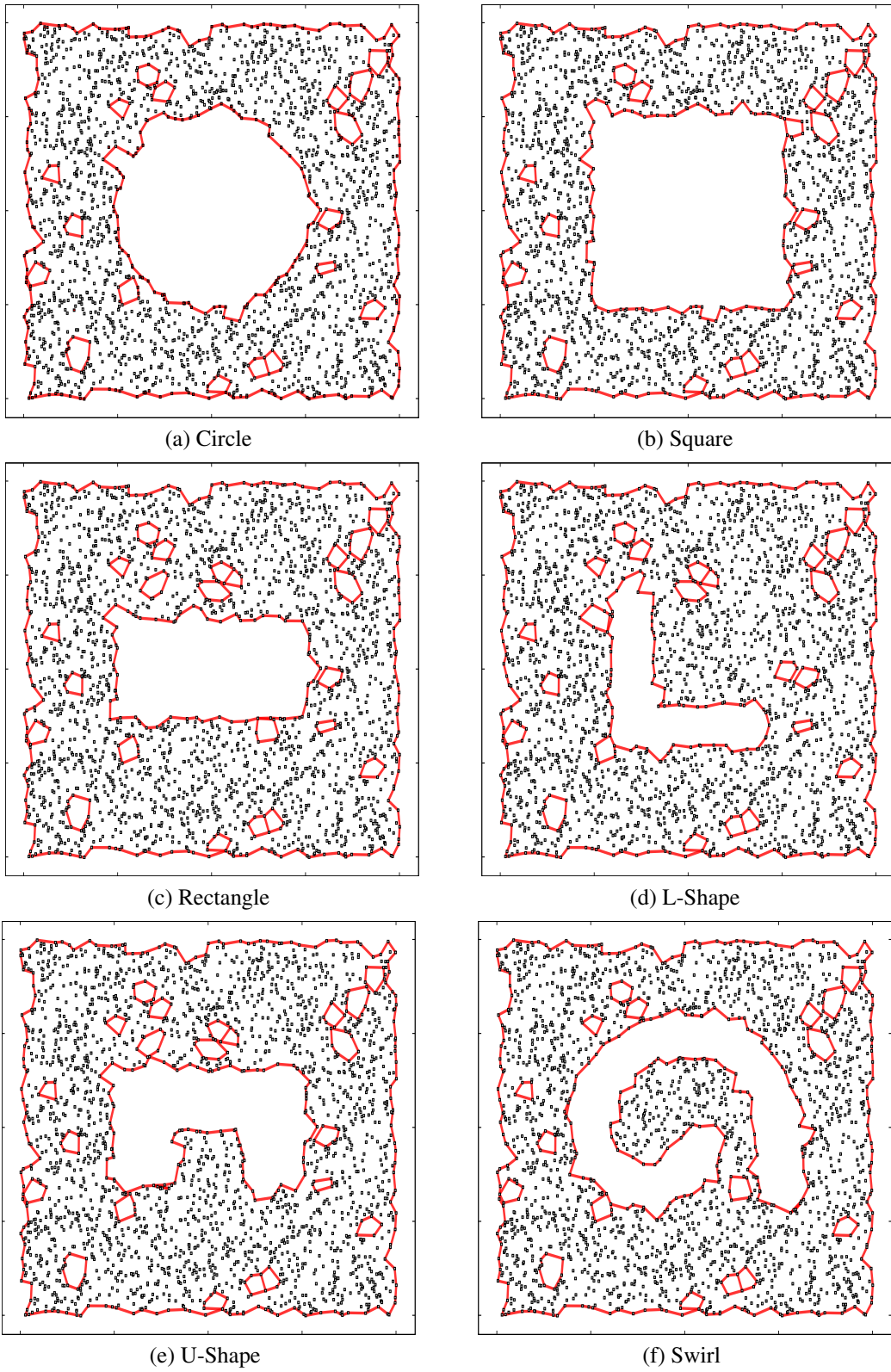


Figure 3.6: The result of TRAVERSE for the networks with holes of various shapes.

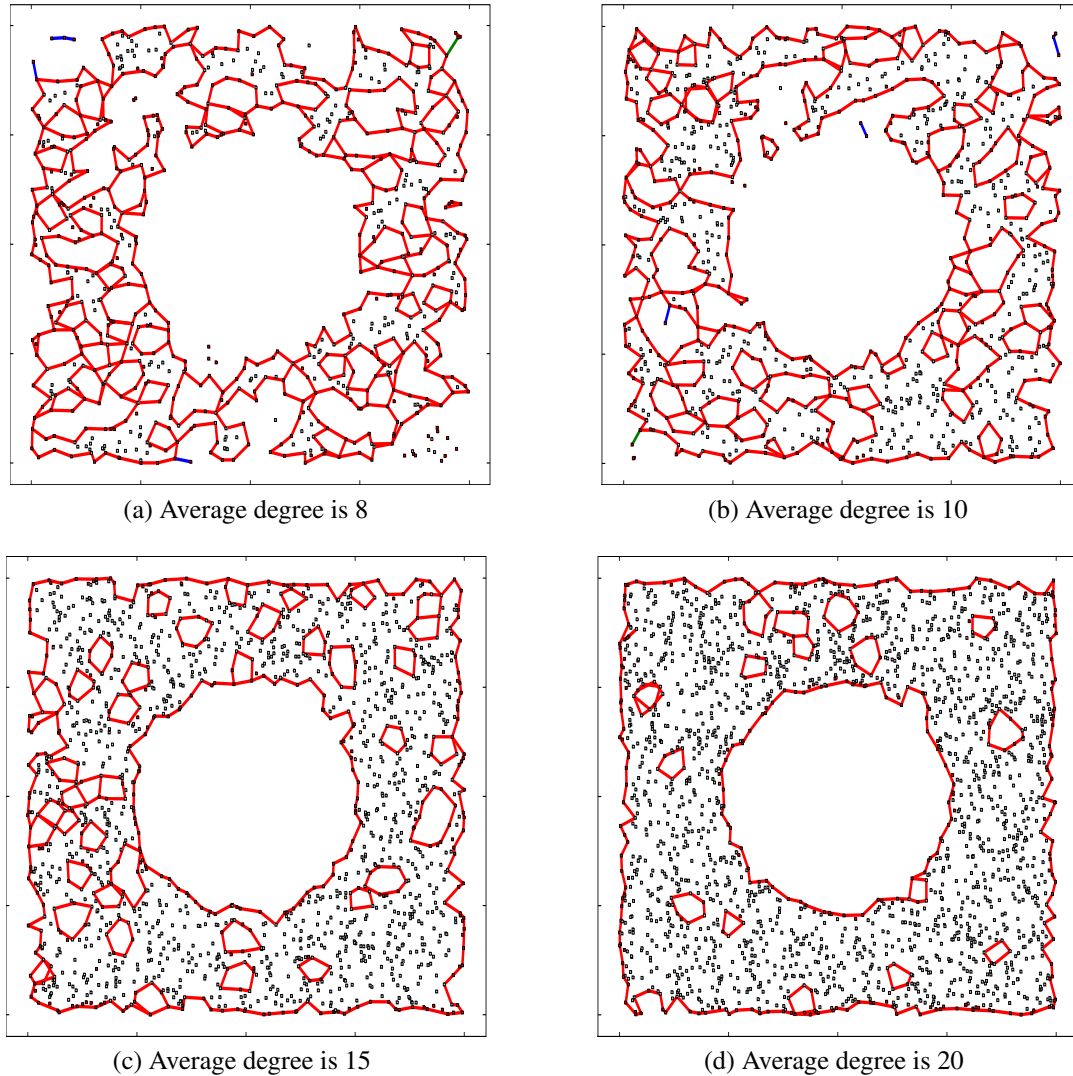


Figure 3.7: The result of TRAVERSE for the networks with varying average degree when an artificial circular hole exists in the center of the deployment area. The small squares represent the node in the deployed area, and the thick lines represent the boundaries identified by the proposed algorithm. As the average degree increases, the boundaries found by TRAVERSE get tighter since more nodes exist close to the boundaries of the central hole and the network boundary.

Because there exist more nodes at the boundary of the central artificial hole and the network deployment area, the tighter and smoother boundary can be found by the algorithm. Also, the number and the size of small holes decrease as the average node degree increases as shown in Figure 3.7. When the average node degree is small, i.e., the density of the network is low, it is more likely that there exist areas that are not within the transmission range of any node.

Figure 3.8 shows the boundaries identified by TRAVERSE when we changed the parameter of the log-normal shadowing radio propagation model. When the σ value of the radio propagation model is increased, the transmission range of each node varies more. We set the threshold for the connection function to 0.9. In this adoption of the log-normal shadowing model, there may exist connections between nodes which are apart from each other longer than the average transmission range, but most of the links are shorter than the average transmission range. As a result, the average node degree is decreased. Thus, the boundaries identified by TRAVERSE are less tight and more small holes are identified by the algorithm.

The results of TRAVERSE when errors exist in the location estimation for sensor nodes are shown in Figure 3.9. As the location estimation errors get larger, the performance of the proposed algorithm will be poorer; the boundaries identified by the algorithm may be so tight, the boundaries of some holes may not be identified, or the boundaries of some non-holes may be identified. The figures in Figure 3.9 show the boundaries identified by the proposed algorithm when the location estimation errors follow the normal distribution with deviations of 5, 10, 15, and 20, respectively. Table 3.1 shows the size of the area of the outer boundaries of the network. For the outer boundaries, the tighter boundary will result in larger area size since the hole is located outside of the network deployment area. As shown in Table 3.1, the area confined by the boundary gets smaller as the standard deviation of the location error increases. This happens because the TRAVERSE algorithm may not choose the best node to follow due to the location estimation errors. However, the

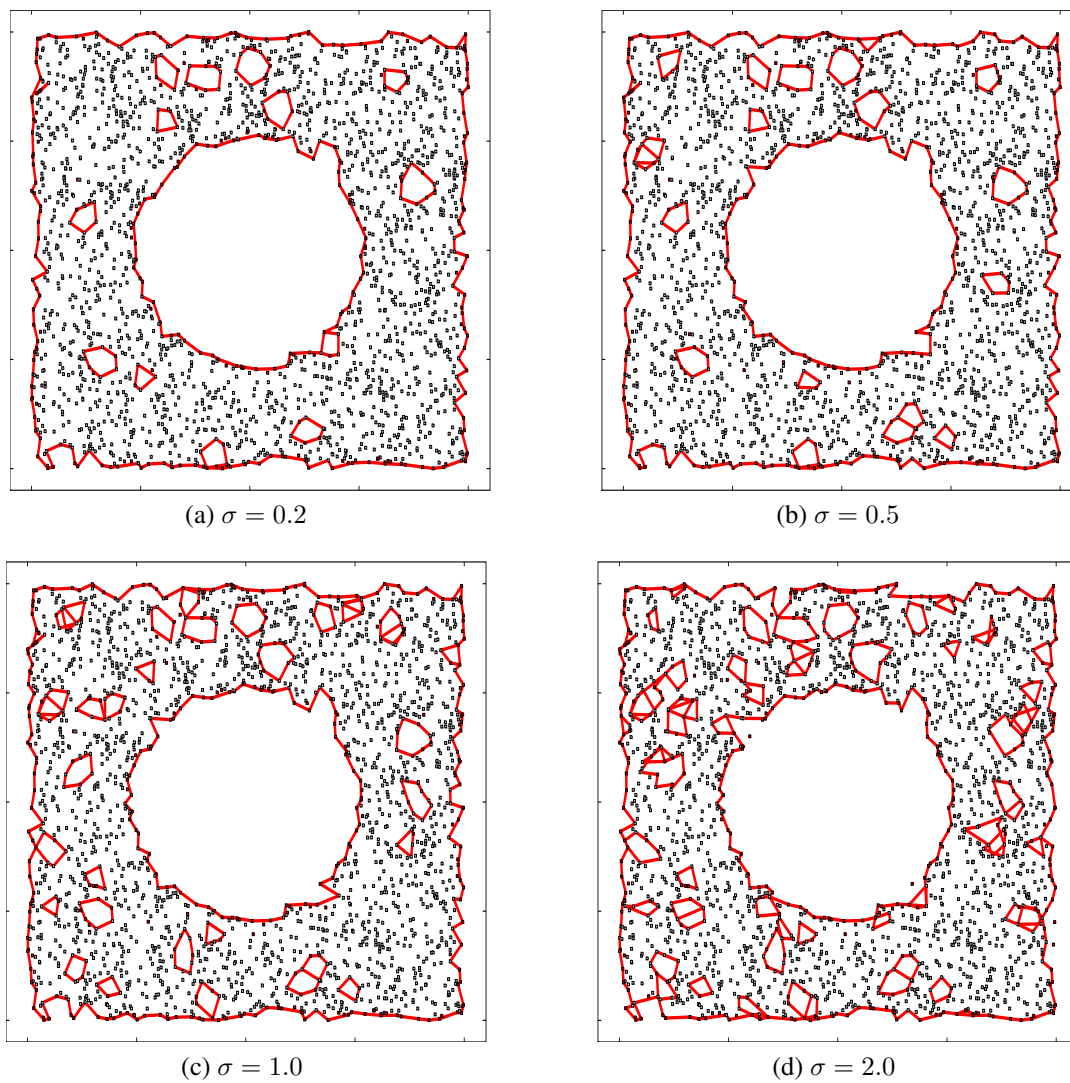


Figure 3.8: The result of TRAVERSE for the networks with varying parameters for the log-normal shadowing radio propagation model. As the value of σ is increased, the average node degree is decreased, resulting in looser boundaries and more small holes in the deployment area.

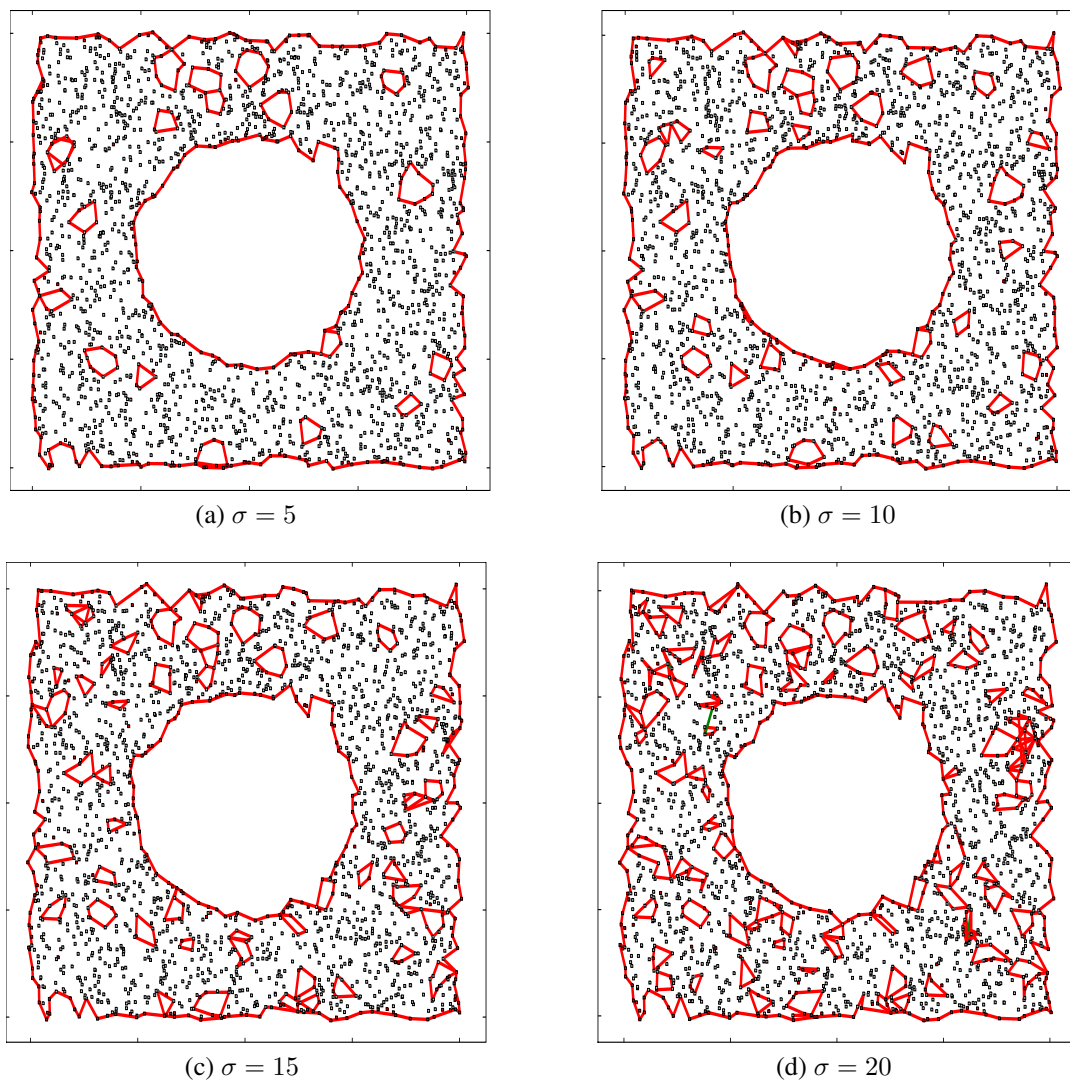


Figure 3.9: The result of TRAVERSE for the networks with varying parameters for the location errors. As the value of σ is increased, the average node degree is decreased, resulting in looser boundaries and more small holes in the deployment area.

σ for location error	area (10^6m^2)	difference (%)
0	3.800	0
5	3.787	0.34
10	3.774	0.68
15	3.772	0.74
20	3.758	1.1

Table 3.1: The size of the area confined by the outer boundaries identified by TRAVERSE when the standard deviation of the normal distribution for the location estimation errors vary. As the location estimation error increases, the size of the hole area is slightly decreased.

difference between the case with no error is only 1.1% even for the case with $\sigma = 20$.

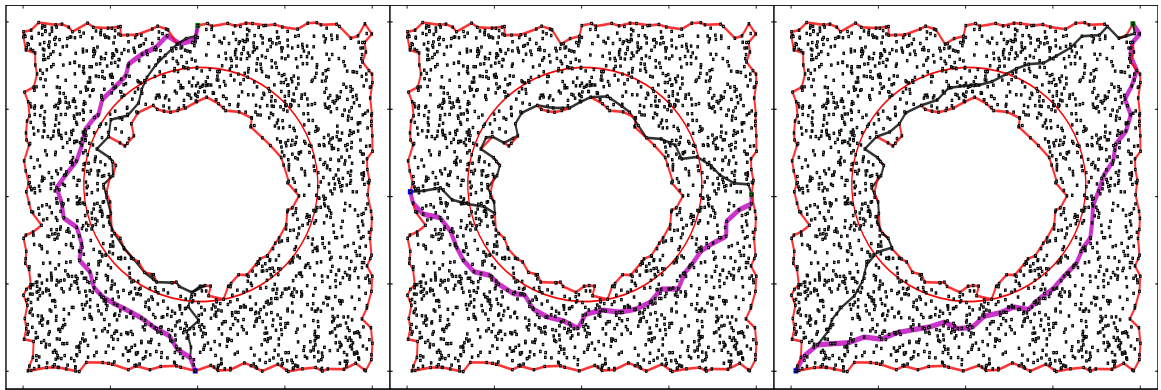
3.6.2 Geographic Forward Routing with Hole Avoidance

We evaluate GFRHA by comparing the paths taken by GPSR and GFRHA for the same source node and the destination location. The topologies shown in Figure 3.6 are used to evaluate GFRHA. We first compare the path lengths for three packets from one end of the network to another end of the network to show the exemplary cases, and we compare the path lengths of random traffic.

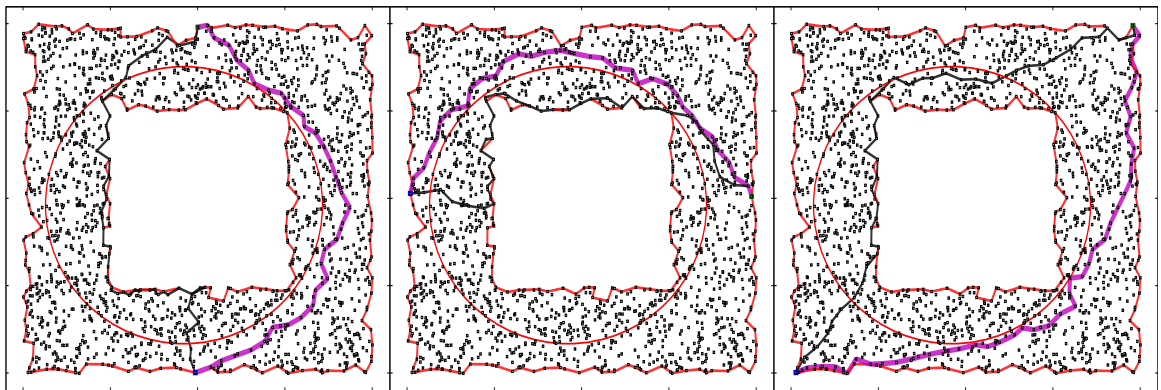
Three packets are generated for each of the topologies, and the paths generated by GPSR and GFRHA are shown in Figures 3.10 and 3.11. As in Figure 3.6, the boundaries of holes are drawn in these figures along with the paths generated by GPSR and GFRHA; think blank lines represent the paths generated by GPSR, while thick magenta lines represent the paths by GFRHA. The source nodes of left, middle, and right figure are middle-bottom, left-middle, and left-bottom, respectively, while the destination of left, middle, and right figure are middle-top, right-middle, and right-top, respectively.

As shown in Figures 3.10 and 3.11, GPSR routes greedily to the destination and detours around the hole after a packet encounters a hole, i.e., when there is no node in one-hop neighbor closer to the destination, while GFRHA detours a packet around a hole in advance to avoid such an expensive detouring using perimeter-mode.

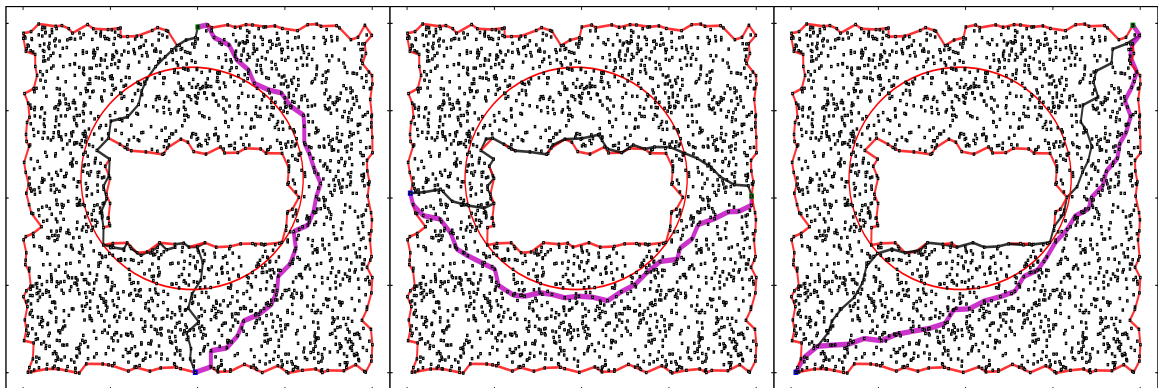
The path lengths taken by GPSR and GFRHA and their differences are shown in Ta-



(a) Detouring circle

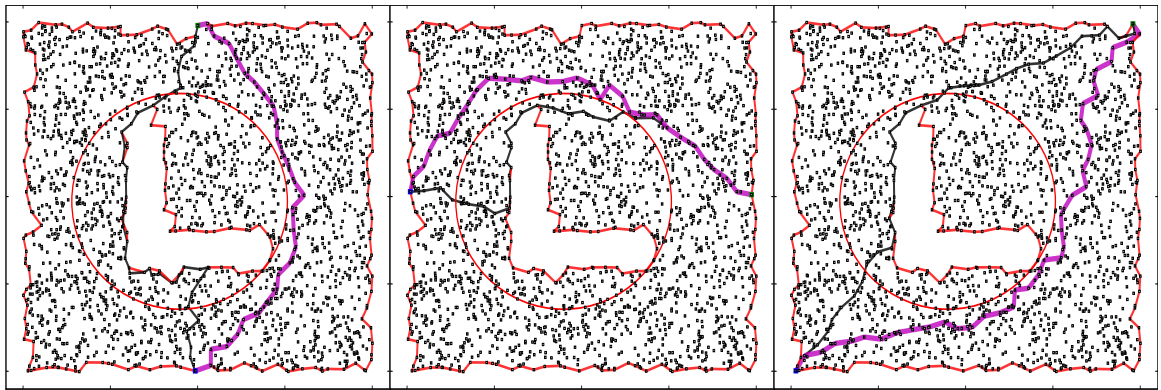


(b) Detouring square

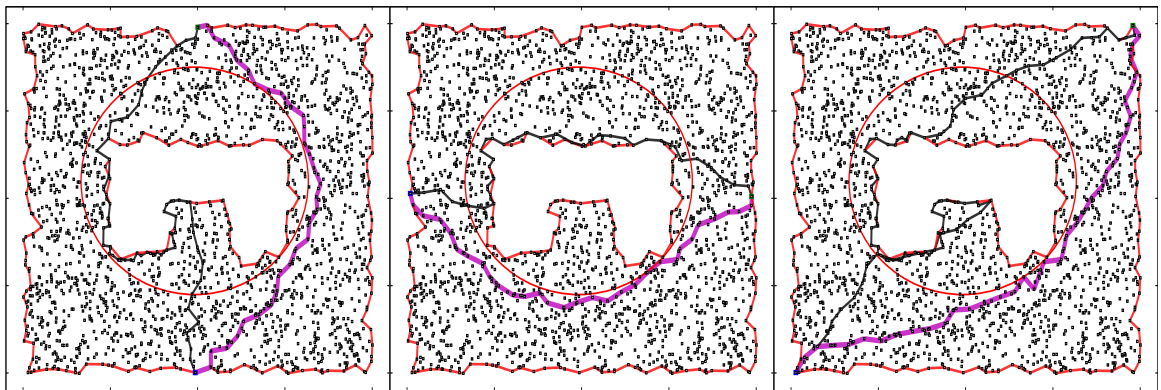


(c) Detouring rectangle

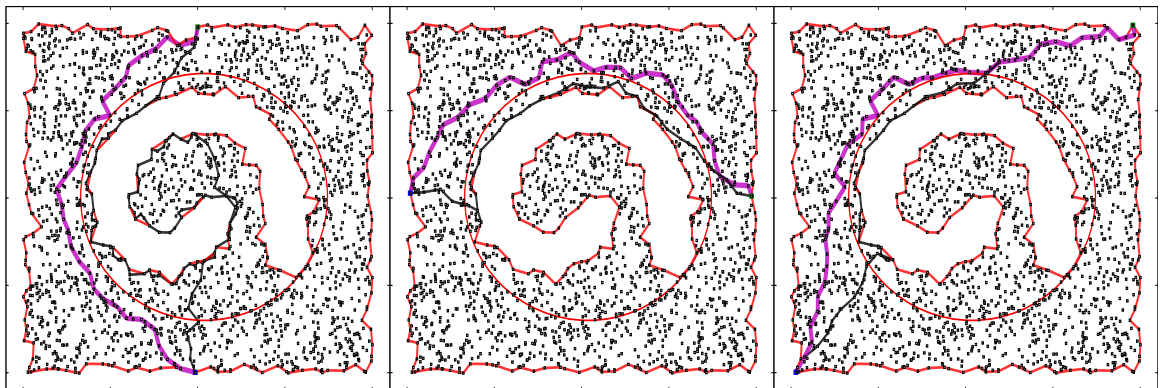
Figure 3.10: An example of routing with hole-avoidance. In each figure, the boundaries of holes are drawn along with the summary of a hole by red line. Also the paths taken by GPSR and GFRHA are represented by a thin black line and a thick magenta line. The sources of left, middle, and right figure are middle-bottom, left-middle, and left-bottom, respectively. The destination of left, middle, and right figure are middle-top, right-middle, and right-top, respectively.



(a) Detouring L-shape



(b) Detouring U-shape



(c) Detouring swirl

Figure 3.11: An example of routing with hole-avoidance. In each figure, the boundaries of holes are drawn along with the summary of a hole by red line. Also the paths taken by GPSR and GFRHA are represented by a thin black line and a thick magenta line. The sources of left, middle, and right figure are middle-bottom, left-middle, and left-bottom, respectively. The destination of left, middle, and right figure are middle-top, right-middle, and right-top, respectively.

ble 3.2. As shown in the table, the performance gain of GFRHA over GPSR significantly differs depending on the shape of the hole and source and destination locations.

We also evaluate the performance comparison between GFRHA and GPSR with random traffic. We randomly select 100 source and destination pairs from the given topologies, where all the source and destination nodes are selected from outside of summarized holes. Figure 3.12 shows the average path length for the random traffic when there are different shape of holes as in Figure 3.6. Again, it is observed that the differences in path lengths taken by GPSR and GFRHA are heavily dependent on the shape of holes. This is mainly because the shape of a hole can significantly affect the number of hops in the perimeter mode when a packet encounters the hole. For example, a packet can take much longer hops to detour a hole if it is a u-shaped or a swirl-shape hole than if it is a circular-shaped hole. On the other hand, the path length does not change much with GFRHA if the summarized hole is similar because packets are detoured before they encounter the hole.

It is anticipated that the performance gain is greater if holes are summarized as convex hulls, and not as circles. However, there is a trade-off between reducing energy consumption in routing and disseminating hole summaries. If we use convex hulls to summarize hole information, the data we need to disseminate the hole summary will be increased, i.e., we consume more energy in disseminating hole information. However, the study of such trade-off is beyond the scope of this work. Here, we show the applicability of information generated by TRAVERSE by other network protocols.

3.7 Conclusion

We present the TRAVERSE algorithm to identify the boundary of each hole in the deployment area of sensor networks. In TRAVERSE, boundaries of holes are identifies as follows. First, we identify candidate nodes, which are nodes that have two adjacent neighbors separated more than by a predefined threshold degree. Second, we start TRAVERSE from those candidate nodes to follow the boundaries of the holes using the right-hand rule,e

Shape of hole	From mid-bottom to top-bottom			From mid-left to mid-right			From left-bottom to right-top		
	Path length		Difference (%)	Path length		Difference (%)	Path length		Difference (%)
	GPSR	GFR-HA		GPSR	GFR-HA		GPSR	GFR-HA	
Circle	38	32	15.79	40	31	22.50	43	37	13.95
Square	50	33	34.00	47	33	29.79	43	42	2.33
Rectangle	50	31	38.00	38	30	21.05	40	36	10.00
L-shape	45	29	35.56	34	30	11.77	40	40	0
U-shape	71	31	56.34	38	30	21.05	104	38	63.46
Swirl	137	32	76.64	43	33	23.26	49	41	16.33

Table 3.2: The path lengths taken by GPSR and GFRHA, and their differences (%). Depending on the shape of the hole and the locations of sources and destinations, the performance gain (or loss) by GFRHA over GPSR significantly differs.

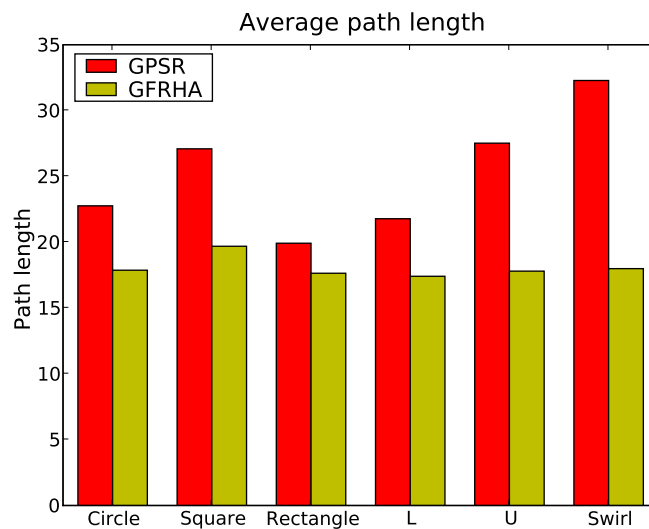


Figure 3.12: The average path length for the random source-destination pairs with different shapes of holes.

with modifications for handling exceptions.

In this chapter, we show the performance of TRAVERSE both qualitatively and quantitatively. We show the identification of holes with various shapes to present the qualitative evaluation of the protocol. We also show the performance of the protocol under the realistic log-normal shading radio model, or with the estimation errors by the localization service.

Finally, we show the application of TRAVERSE. We propose geographic forward routing with hole avoidance (GFRHA) by modifying GPSR to utilize hole information. By utilizing hole information, GFRHA detours packets around holes before packets encounter a hole and enter into the expensive perimeter-forwarding mode of GPSR. Evaluations show that GFRHA can significantly reduce the path lengths depending on the shape of holes and the locations of source and destination.

CHAPTER IV

ATTACK-RESILIENT COLLABORATIVE MESSAGE AUTHENTICATION

4.1 Introduction

Data Centric Storage (DCS) [24, 27, 42, 56] is a prominent data-storage and query-processing mechanism on Wireless Sensor Networks (WSNs). Resource-limited sensor nodes collaboratively identify events of interest, and report them to storage nodes at predefined locations according to the type of event or the range of sensed data. Queries of stored event information can then be issued, typically by mobile users, from anywhere in the network, and are forwarded to the relevant storage nodes. At storage nodes, the queries are processed and the query results are sent back to the issuer(s). DCS is preferable to External Storage (ES) at the base station, especially when there are many types of event to detect and report, and not all event types are queried often in a large network [56]. Also, the time of accessing DCS can be much shorter than that of accessing ES when storage nodes are located close to those who need to access them. This can be achieved by replication of storage nodes.

Security support for DCS, as for other WSN applications, is important since WSNs usually operate in an unattended and hostile environment. Secured DCS ensures that no fabricated information is inserted into the storage system and no unauthorized user is al-

lowed to access the stored data. The main challenge in securing DCS is how to verify the authenticity of messages from remote locations since event-report, event-query and query-response messages often need to travel multiple hops to remote nodes in a WSN.

Securing DCS, however, is very difficult, especially when attackers launch node-capture attacks. Since sensor nodes operate in an unattended environment and may also be physically exposed to attackers, it is relatively easy for attackers to capture and then reverse-engineer them to extract their secret (keying) information. In such a case, attackers can subvert the entire system by compromising even a single sensor node. The attacker may fabricate seemingly valid packets using the keying material extracted from the compromised node to insert false data into the network. Depending on the type of the forged message, the attacker may (1) report false events to storage nodes, (2) report false responses to mobile nodes, or (3) make unauthorized accesses to the storage node by issuing queries.

Detecting forged messages is extremely difficult if they are generated using the valid keying material, especially when they came from remote nodes. Research has been conducted about the detection of data forgery using reputation systems and statistical methods [23,55,67], but the results are effective only for local data forgery, and not for messages sent from remote nodes. Even expensive signing with public keys [46,68] cannot handle this problem when messages are generated using valid (stolen) keying materials. En-route filtering mechanisms [57,71,74,80,83] provide data-forgery detection even in the presence of compromised nodes. However, these mechanisms depend on the existence of a base station, and cannot be applied directly to DCS, where data is sent to storage nodes at arbitrary locations.

In this thesis, we propose *Attack-Resilient Collaborative Message Authentication* (ARCMA) to secure DCS, especially under node-capture attacks. ARCMA focuses on authentication of event-report, event-query, and query-response messages that may take multiple hops to reach their destinations. Specifically, in ARCMA, a set of sensor nodes cooperate to evaluate a *Collaborative Message Authentication Code* (CMAC) for the messages sent

to, and received from, remote nodes. As a traditional MAC, a CMAC is evaluated both at the sender and the receiver sides, and only those messages with valid CMACs are accepted by the receiver. Since the keying material of sensor nodes may be exposed under node-capture attacks, sensor nodes must collaborate to provide necessary protection against such attacks. This is akin to the sensor nodes' collaboration (to overcome their limitations in sensing capability) to identify the events of interest to the underlying applications.

The main contributions of this work are summarized as follows. First, we propose a novel attack-resilient message authentication mechanism, called ARCMA, in which each node belongs to one of k groups, and a message is collaboratively authenticated and verified by k nodes, each from a distinct group. To achieve this, each node maintains an *Authentication Tree* (AT), which is a spanning tree formed with k nodes, each from one of k distinct groups, and collaborates with all the nodes in its AT to evaluate CMAC for message authentication. We also encrypt messages with location-dependent keys to validate their origin.

Second, we show how ARCMA can be applied to authenticate messages associated with DCS operations. We show how each parameter can be set for (1) event-report messages which are typically generated by a set of cooperating sensor nodes in proximity, (2) event-query messages which are generated by mobile users, and (3) query-response messages which are sent back to the mobile users. Most previous work focused on securing event-report messages destined for the base station, and does not consider how to secure the processing of queries issued by mobile users.

Third, we present heuristics to construct ATs and to assign sensor nodes to different groups. Since a global view is not available, or too expensive to obtain in a WSN, we propose two distributed heuristic algorithms to build ATs, MIN and OPT. We also provide a group-assignment protocol, in which sensor nodes in the neighborhood assign their groups such that different group numbers can be assigned.

Finally, we analyze the security of ARCMA and evaluate its performance. We show that

the security of ARCMA does not degrade as long as less than k nodes are compromised. Also, we evaluate the overhead of constructing ATs and exchanging extra messages for message authentication for design parameter k and node density.

The rest of this chapter is organized as follows. The related work is summarized in Section 4.2. Section 4.3 describes the system model and assumptions used throughout the chapter, and the key management for the proposed protocol is described in Section 4.4. Then, ARCMA is detailed in Section 4.5, followed by descriptions of the authentication-tree construction in Section 4.6 and group assignment in Section 4.7. Section 4.8 presents the security analysis and the performance evaluation of ARCMA. Section 4.9 concludes this chapter.

4.2 Related Work

DCS [24, 27, 42, 56] was proposed to store and query the information (e.g., events of interest) collected in a WSN. The events of interest detected by the WSN or their metadata are reported to storage nodes whose locations are pre-determined based on the type or range of the sensed data, and queries for this information are delivered to, and processed at those storage nodes.

Various key management protocols have been proposed to support the security of WSN applications. Key management in a WSN is a challenging problem due to the large network size and the severe resource limitation in each node. For symmetric key sharing, several key pre-distribution schemes [13, 14, 17, 32, 44] have been proposed that assign a partial set of keys or keying material to each sensor node so that each pair of neighboring nodes can establish a shared key with a high probability. TinyPK [68] and ECDLP [46] are the implementations of public-key cryptography for WSNs.

However, the security of DCS cannot be achieved by just encrypting/signing messages with the keys generated by the above key management protocols. In DCS, event-report and event-query messages typically take multiple hops to reach remote storage nodes. Thus,

the securing DCS requires authenticating these messages. However, node-capture attacks are relatively easy to mount in WSNs, and an *insider attack* using the keying material extracted from the captured nodes can be catastrophic if the attacker can generate any event-report, event-query, or query-response message. In such a case, all of the above-mentioned schemes will become futile.

R-DCS [25] replicates storage nodes for scalability and resilience, but it cannot tolerate active attacks including node-capture attacks. *p*DCS [60] provides security and privacy on DCS by using a keyed hash function to map the storage nodes, but it cannot also prevent fabricated event-reports after node-capture attacks.

Several protocols have been suggested to provide secure event reports under node-capture attacks. Secure aggregation [55, 67] and en-route filtering [5, 57, 71, 73, 83] are suggested to prevent the reporting of invalid information only to an uncompromisable base station, and the base station has all the keying material to validate any packet. In these protocols, each sensor node has either a pairwise key with the base station or a set of keys randomly selected from a large key pool. On the other hand, the base station has either pairwise key with all the sensor nodes, or all the keys from the key pool. When sending event information, a sensor node authenticates the event message with one of the keys it has. In en-route filtering, such event messages can be statistically filtered when they are invalid; a forwarding node may verify the messages if it has the same key used for authenticating the messages. Since a sensor node has only a subset of the key pool, it may be possible that an invalid packet may be forwarded to the base station. Thus, the final verification of the event messages should be handled by the base station. These protocols are not applicable to DCS, where any easily-attacked sensor node should be able to receive and verify event messages as a storage node. If each sensor node has all the keying material to validate any incoming packet, it is equivalent to having one common key shared by every node. In this case, the whole system is subverted when only one node is compromised.

A reputation-based system such as [23] was proposed to detect the reporting of false

information. In such a system, the reputation of a sensor node is determined by its behaviour that is monitored by other sensor nodes. If the reputation of a certain sensor node is below a threshold, the node is ignored by other nodes. For example, other nodes do not forward packets originating from low-reputation nodes. In such a system, if the reputation of a sensor node is maintained only locally, an attacker may insert invalid packets by compromising only one node and moving to a new location after the reputation of the compromised node becomes lower than the threshold. To share a reputation of a sensor node globally, the reputation of a specific node should be stored in a predefined location, e.g., the location of the reputation storage can be evaluated using a hash function as the location of storage nodes is determined in DCS. However, securing such reputation update is not trivial, and such updates are too expensive for battery-powered and low-bandwidth sensor nodes. Also, reputation systems proposed for sensor networks [23] assume that each sensor node verifies the messages generated by its neighbors in a promiscuous mode, and build each other's reputation. However, wireless links are typically asymmetric, and thus, a node cannot always hear all of its neighbors. Also, the requirement that every message should be interpretable by intermediate nodes between the source and the destination may create security holes. That is, a message's content may be exposed to the attacker if one of the nodes on its path was compromised.

Zhang *et al.* [79] proposed a countermeasure against node-capture attacks on mobile sinks. Their solution focused on an application scenario in which mobile sinks are used to retrieve the sensed data, and their main goal is to prevent unauthorized data access via a compromised *mobile sink*, not compromised sensor nodes. They allow the least privilege to a mobile sink such that it can access the authorized information. To do so, they assumed the existence of an uncompromisable and resourceful base station, which has a pairwise key to every sensor node. The base station provides mobile sinks with security credentials, which can be verified by sensor nodes using their keys shared with the base station.

ARCMA differs from the above approaches in that it can authenticate messages sent to

any other locations, and it does not assume any uncompromisable base station. Besides, ARCMA provides k -collusion resistance, i.e., the security of the system does not degrade if less than k nodes are compromised, like most of the secure aggregation or en-route filtering [5, 57, 73, 83].

4.3 System Model

4.3.1 Sensor Network Model

DCS is placed on a WSN, which is usually composed of a large number of inexpensive sensor nodes with limited memory, computation and communication capacities. Sensor nodes are usually battery-powered, and hence, energy is a precious, scarce resource. Hardware-supported tamper-proofing is usually not a feasible solution for sensor nodes due to its higher hardware cost.

We assume sensor nodes to have been deployed densely such that events of interest can be detected by a set of cooperating sensor nodes near the locations of their occurrence. More specifically, we require a network dense enough so that an event can be detected by at least k nodes. The conditions of network-density and relevant sleep-scheduling algorithm for this requirement is discussed in [36]. There are other compelling reasons for dense deployment, such as fault-tolerance and short-range communication. Detected events will be sent to (possibly remote) storage nodes, where information about the event is stored or possibly aggregated with other information. The storage nodes are nothing but sensor nodes, which are selected *a priori* according to a pre-defined rule. An event-report message may traverse a large number of hops if the storage nodes are located far away from its occurrence.

External mobile nodes, which may be carried by users or attached to ground/air vehicles, may interact with nearby sensor nodes, issuing queries for the information of interest. Sensor nodes will forward the queries issued by mobile nodes to the storage nodes that will

then reply with the queried information. The mobile nodes usually have more (computation, communication and energy) resources than sensor nodes.

The existence of a base station is *not* assumed in ARCMA as in many other works [5, 55, 57, 67, 71, 73, 79, 83]. Using a base station as a trusted third party, solutions to many security problems can be simplified. However, adoption of a base station has the following problems. First, it is not always guaranteed to have stable communication to a base station. Second, it may be expensive to communicate with a base station since it can be located far from most of deployed sensor nodes. For example, DCS is more efficient than ES using a base station in terms of the communication cost when there are many event types and frequent queries [56]. Finally, a base station can be the single point of failure. If the base station of a deployed network is faulty or compromised, the whole system would not function. Thus, in the previous work, the existence of an uncompromisable base station is assumed. In ARCMA, we did not assume the existence of a base station at all.

In designing ARCMA, we assume existence of the following three common services: localization [8, 30, 38, 59], time synchronization [16, 22, 63, 64], and geographic forwarding routing [7, 33]. All of these services are basic and usually required for other sensor network applications than DCS; localization and time-synchronization services are required to provide the location and the time of each identified event, and geographic forwarding routing is required to forward event-report and query messages. ARCMA exploits these “already available” services without incurring additional costs.

4.3.2 Attack Models

WSNs are inherently vulnerable to various security attacks because they usually operate in an unattended and hostile environment. We assume that attackers are resourceful and mobile, and launch several types of attacks. Attackers can launch outsider or insider attacks. An outsider attack may be *passive* such as eavesdropping communications or performing traffic analysis, or *active* such as inserting, modifying, or dropping packets. Adversaries

can launch a stronger type of (insider) attack, such as node-capture attacks in which sensor nodes are captured and compromised to extract their keying material. A node-capture attack is relatively easy to mount in WSNs since sensor nodes operate in an unattended environment, and are therefore likely to be exposed to attackers. The main focus of this chapter is to secure DCS against node-capture attacks.

We assume that attackers of DCS want to (1) disable the targeted DCS by inserting false data so that the legitimate users will receive incorrect data, (2) report false data to the legitimate query issuers, or (3) access the stored data for unauthorized purposes. An attacker can achieve all of these goals by inserting false messages into the system. For example, if an attacker can generate valid-looking, i.e., generated with valid keys, event-report messages so that the false event information is stored at the storage nodes, all the users who issue queries will receive the false event information. Similarly, the attacker can report false data to queries or access stored data by inserting false messages.

The proposed protocol in this work, therefore, focuses on preventing an attacker from inserting false messages into the system. In the proposed protocol, we guarantee that attackers cannot insert any false message, i.e., the security does not degrade, as long as less than k nodes are compromised.

Also, even when k or more than k nodes are compromised, to generate a false message originating from a certain area, the attacker has to compromise at least one node from k different areas. This fact limits the attackers' ability to insert false messages. For example, an attacker cannot forge an event-report message from a certain area if he does not compromise at least one node from the area unless he compromises k nodes from different k areas.

We, however, assume that the network is safe for a short while after the deployment, during which the initialization can be performed. This is realistic, since it takes time for attackers to learn the existence and operation of a WSN, and to compromise sensor nodes.

4.4 Key Management

In this section, we present a key management that adopts polynomial-based key pre-distribution for the proposed protocol. The polynomial-based key pre-distribution is adopted since its security does not degrade if less than a certain number of nodes are compromised. This means that an attacker does not obtain any information of the polynomial if the number of compromised nodes is below a threshold.

4.4.1 Polynomial-based Key Pre-distribution

We first summarize polynomial-based key pre-distribution [6], on which the key management of ARCMA relies.

A $(k-1)$ -degree¹ bivariate polynomial is defined as

$$f(u, v) = \sum_{i,j=0}^{k-1} a_{ij} u^i v^j$$

over a finite field F_q , where q is a prime number large enough to accommodate a cryptographic key. When a bivariate polynomial is symmetric (i.e., $f(u, v) = f(v, u)$), we define a share of the polynomial of node s as $f(s, v)$, which is a $(k-1)$ -degree univariate polynomial. By distributing a share of the polynomial to every sensor node, any two nodes in the network can set up a pairwise secret by exchanging only their node IDs. For example, two nodes s and r share a secret by replacing the variable of their share of the polynomial with the correspondent's ID, i.e., $f(s, r) = f(r, s)$. The common secret between any two nodes is proven to be safe if less than k shares of the $(k-1)$ -degree polynomials are revealed to the adversary, i.e., less than k nodes are compromised.

¹We use $(k-1)$ -degree polynomials instead of k -degree polynomials as in most literature to simplify notations in the later sections.

4.4.2 Key Distribution

ARCMA uses three sets of bivariate polynomials to generate keys for different purposes: pairwise-key, group-key, and spatial-key polynomials.

1. Pairwise-Key Polynomial, $f_p(u, v)$: is used to generate the pairwise key between any two sensor nodes in the neighborhood, or between a mobile node and a sensor node. Each polynomial variables will be replaced by the node ID.
2. Group-Key Polynomial, $f_g(u, v)$: is used to evaluate the MACs of messages. One variable of the group-key polynomial will be replaced by group number, and the other by the node ID. To prevent the collusion attack since the polynomial is commutative, we set the mobiles' ID greater than k .
3. Spatial-Key Polynomial, $f_s(u, v)$: is used to generate encryption-keys for messages forwarded to remote locations. Since the destinations of such messages are specified as their location (not ID) in DCS, the variables are replaced with the location information of the sender and the receiver of a given message.

When sensor nodes are deployed, they are preloaded with a common master key K_0 . The coefficients of the above three-polynomials are derived from this key using the common keyed hash function $H_K()$. The coefficient a_{ij} of f_p are evaluated as

$$a_{ij} = \begin{cases} H_{K_0}(i \cdot k + j + B) & \text{if } i \leq j \\ a_{ji} & \text{otherwise} \end{cases}$$

where B is set to 0. By setting B to k^2 and $2 \cdot k^2$, the coefficients of two other polynomials f_g and f_s are evaluated.

The master key K_0 will be permanently removed from the memory of sensor nodes after evaluating coefficients of the polynomials.

4.4.3 Key Assignment

Once deployed, sensor nodes evaluate their share of pairwise-key polynomial by replacing one of the variable with their own ID. Then, they discover their one-hop neighbors, and establish pairwise keys with them. Each sensor node broadcasts its own ID, and the pairwise key can be simply evaluated using the pairwise-key polynomial using the neighbor's ID.

After discovering its neighbor nodes, each sensor node generates a random number that is used for the cluster key. The cluster key of a node is used to encrypt local broadcast messages sent by a specific node. The cluster key can be encrypted with the pairwise key and delivered to all neighbors individually. Let CK^s be the cluster key of sensor node s .

Once local relations are secured, the underlying localization protocol can be evoked. The pairwise keys and cluster keys established in the above process may be used to encrypt or decrypt messages of the localization protocol, if necessary. After the location of each sensor node is discovered through the localization service, each sensor node evaluates its share of spatial-key polynomial.

When evaluating the spatial-key polynomial, quantized coordinates are used instead of the raw coordinates. Since the exact coordinates of remote nodes are, in general, not known *a priori*, the exact coordinates of the destination cannot be used with the spatial-key polynomial to obtain a matching key both at the source and the destination. (In the geographic forwarding routing, knowledge of the exact coordinates are not necessary since a packet is handled by the sensor node that is the closest to the destination.) Thus, we use the *quantized* coordinates, and the spatial-key is associated with the quantized coordinates, rather than the exact geographic location. The quantized location (L_s) of a sensor s located at (x, y) is defined as $L_s = \lfloor \frac{x}{\ell_0} \rfloor \lfloor \frac{y}{\ell_0} \rfloor$. Here, the quantization index ℓ_0 determines the granularity of the quantization. Then, s 's share of the spatial-key polynomial can be evaluated to be $f_s(L_s, v)$. The use of the quantized coordinates is equivalent to dividing the whole network area into squares whose edge length is ℓ_0 , and the lower-left corner of a grid is

$f_p(u, v)$	Pairwise-key polynomial
$f_g(u, v)$	Group-key polynomial
$f_s(u, v)$	Spatial-key polynomial
K_0	Master key used to derive the coefficients of bivariate polynomials
CK^s	Cluster key of sensor node s
L_s	Quantized location of sensor node s , defined as $\lfloor \frac{x}{\ell_0} \rfloor \lfloor \frac{y}{\ell_0} \rfloor$ when (x, y) is s 's raw coordinate
ℓ_0	Quantization index to determine the granularity of quantization
N^s	Set of s 's neighbors
G_i	Set of sensor nodes in group i
AT^s	Authentication tree maintained by sensor node s
AT_i^s	Sensor nodes in G_i and in AT^s , $1 \leq i \leq k$
$\{M\}_K$	Encrypted message M using key K
$MAC(K, M)$	Message authentication code (MAC) of message M using key K

Table 4.1: Notations used for ARCMA

used for the coordinates of the sensor nodes in the grid.²

Group assignment is simultaneously performed with the aforementioned localization. Each group can be assigned a node by the group-assignment protocol described in 4.7. Once a group number is assigned, each node evaluates its share of f_g .

After evaluating the shares of three polynomials using the above process, the master key K_0 is permanently removed from the memory of the sensor nodes.

Each mobile node also has its share of the pairwise-key and group-key polynomials by replacing one of the variables with its ID, i.e., mobile node m will be loaded with $f_p(m, v)$ and $f_g(m, v)$. The mobile node need not hold any information about the spatial-key polynomial.

Table 4.1 summarizes the notation shown in this section and later sections.

²The grid explained here is similar to the level-0 grid of DLSP shown in Chapter II, but the sizes of the grids are not necessarily the same.

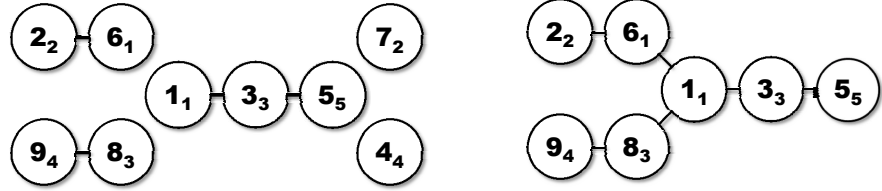
4.5 Attack-Resilient Collaborative Message Authentication (ARCMA)

4.5.1 Overview

In ARCMA, sensor nodes collaboratively authenticate messages sent to, and received from, remote nodes. The traditional message-authentication method relies on MAC, which is evaluated as a one-way keyed hash function. However, this method is not sufficient for WSNs because it is relatively easy for the adversary to capture nodes on WSNs. With valid keying materials extracted from the captured nodes, the adversary can then insert a message with a valid MAC. To prevent such attacks, ARCMA requires messages to be authenticated collaboratively by a set of sensor nodes. More specifically, each sensor node belongs to one and only one of k distinct groups, and members of each group share a group-key polynomial to generate a common key to evaluate MACs. When authenticating a message, k nodes from k distinct groups, one from each group, evaluate MACs using group-keys, and the CMAC is evaluated by XORing these MACs. Like a traditional MAC, the CMAC is evaluated at the sender side and concatenated to the message. Then, the CMAC is re-evaluated at the receiver side for its verification. Using CMACs, messages can be authenticated even under node-capture attacks since the attacker must know all k group keys to fabricate a valid MAC.

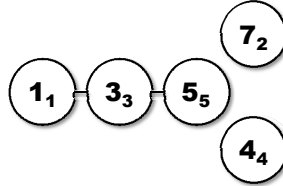
To evaluate a CMAC, each sensor node needs to know at least one node for each of k groups in its neighborhood. Thus, each node maintains an AT, a structure to maintain information on nodes for each of k groups. AT is a spanning tree with at least k nodes. Using its AT, a sensor node can evaluate or verify the CMAC. For convenience, the AT maintained by node s is represented by AT^s , and sensor nodes in AT^s are represented as AT_i^s , where i is the group the node belongs to. Each sensor s node maintains the following information in its AT: the node ID for AT_i^s , the next hop to AT_i^s , and the number of hops to AT_i^s for each group i ($1 \leq i \leq k$).

Figure 4.1 shows an example of ATs. Figure 4.1(a) depicts a given topology, where



(a) An example topology. Vertices and edges represent nodes and connectivity between nodes, respectively. The main number and the subscripted number in a vertex represent the ID and group number of the node, respectively.

(b) A (possible) authentication tree for node 1.



(c) Another possible authentication tree for node 1.

Figure 4.1: Example of authentication trees: This figure shows ATs in a given topology when $k = 5$

vertices and edges represent nodes and connectivity, respectively. The ‘main’ number and the number in parentheses in a vertex represent the node ID and its group number when $k = 5$. Figures 4.1(b) and 4.1(c) show possible AT^1 .

4.5.2 Collaborative Message Authentication

We now describe how messages are exchanged when sensor node s located in L_s sends a message M to another sensor node r located in L_r . In summary, s computes a CMAC for M and encrypts them with a proper spatial-key. When r receives M , it evaluates the CMAC after decrypting it, and checks if the evaluated CMAC and the received CMAC match. It accepts the message only when the two CMACs match.

Messages at the sender’s side are exchanged as follows.

1. s sends M to the nodes in AT^s . s sends M with ID id , timestamp ts , and its location, L_s , to all the nodes in its AT. Here, id is a parameter other than group number for the group-key polynomial, the timestamp is used to prevent replay attacks, and the

location is used to provide the authenticity of the location of reported data. P_M is a proof of message which is used to prevent the compromised node from asking the message authentication for forged messages. Depending on the type of a given message, these fields will be filled in with different values. This will be detailed in Section 4.5.3.

$$s \rightarrow AT_i^s : \{id|M|ts|L_s|P_M\}_{f_p(s,AT_i^s)} \text{ for } 1 \leq i \leq k$$

2. s receives MACs evaluated by the nodes in AT^s . The nodes in AT^s evaluate the MAC for the given message with the timestamp and the location of s , and then return it to s . Note that this is processed only when a valid proof P_M for the given message M is provided.

$$AT_i^s \rightarrow s : \{\text{MAC}(f_g(i, id), M|ts|L_s)\}_{f_p(s,AT_i^s)}$$

3. s computes the CMAC by XORing the MACs it received. s evaluates a CMAC as follows:

$$\begin{aligned} \text{CMAC} &= \text{MAC}(f_g(1, id), M|ts|L_s) \oplus \\ &\quad \text{MAC}(f_g(2, id), M|ts|L_s) \oplus \cdots \oplus \\ &\quad \text{MAC}(f_g(k, id), M|ts|L_s). \end{aligned}$$

4. s encrypts M with its spatial key, and sends it to r . s concatenates the timestamp, its location and CMAC to the message, and sends the concatenated message to r using the underlying routing protocol.

$$s \rightarrow r : L_s, L_r, \{M|ts|L_s|\text{CMAC}\}_{f_s(L_s, L_r)}$$

When r receives the message, it evaluates the CMAC using its own AT, similarly to the CMAC evaluation at the sender side, as follows.

1. r sends M to the nodes in AT^r . r decrypts the message with $f_s(L_s, L_r)$, and sends it to the nodes in its AT. Here, the proof of message is not required since r 's location is different from s 's location, L_s .

$$r \rightarrow AT_i^r : \{id|M|ts|L_s\}_{f_p(r, AT_i^r)} \text{ for } 1 \leq i \leq k$$

2. r receives the MACs evaluated by the nodes in AT^r . When the nodes in r 's authentication tree, AT^r , receive the message, they evaluate the MAC for the given message with the group-key and return it to r .

$$AT_i^r \rightarrow r : \{\text{MAC}(f_g(i, id), M|ts|L_s)\}_{f_p(r, AT_i^r)}$$

3. r evaluates the CMAC and accepts the message only if CMACs match. Upon receiving replies from the nodes in AT^r , r evaluates the CMAC for the given message by XORing the received MACs. Only if the CMAC from s matches the CMAC it computed, will r accept the message.

In the above process, the same message M is transmitted to all the nodes in AT^s and AT^r . This will be very expensive, thus calling for an optimization to reduce the number of message transmissions. Without optimization, the cost of exchanging messages to evaluate the CMAC increases linearly with k . However, we need not send the same message to all the nodes individually, since the message is known to the local nodes. So, we can use a local broadcast using s 's cluster key, CK^s . If a node needs to forward such a message

asking for MAC, i.e., it has child node(s) in AT^s , it can again send the message using its own cluster key. When MACs are received, the intermediate nodes in a node's AT can XOR all the MACs it receives from its children, and then report the XORed MAC to its parents. When s receives such reports from its children, it can compute the CMAC by XORing them. The CMAC obtained from this optimization will be the same as that obtained by XORing individual MACs at s since XOR is transitive. When the CMAC is verified by r , a similar step can be taken.

A CMAC mismatch indicates a compromise. If the CMAC computed by r does not match the CMAC from s , at least one node in either AT^r or AT^s did not report a proper MAC. In such a case, r can send the same message M to all the nodes in AT^r individually without optimization. Then, r can send all of the MACs to s . Upon receiving such a message, s also requests nodes in AT^s to re-evaluate the MACs. If the MACs for a certain group do not match, either the nodes of a group in AT^s or AT^r , or both, are compromised. In such a case, both nodes are revoked. This revocation process is expensive since the same message should be sent to all the nodes in AT^s and AT^r . However, this type of attack is *not* effective from an attacker's standpoint not only because the attack is easily detectable but also because the compromised nodes are revoked upon their first attack.

4.5.3 Securing DCS Operations Using ARCMA

We now describe how ARCMA can be used for securing DCS messages: event-report, event-query, and query-response messages. Regardless of message types, messages are transmitted to remote locations. So, the collaborative authentication described in the previous subsection can be used. However, different proofs of messages for CMAC evaluation are required for different types of messages.

4.5.3.1 Reporting Sensed Data

Sensor nodes cooperate to identify events of interest; an event will typically be detected by multiple sensor nodes, and their sensor readings will be aggregated for detection accuracy.

When such an event is reported to the corresponding storage nodes, the report message must be authenticated to guarantee the authenticity of the report. ARCMA can be used for this purpose, and the information about the event can be used as the proof of the message. Node density in a WSN is determined so that any region is covered by more than a certain number of nodes [36] for an event of interest to be detected with a desired level of accuracy since each sensor node has only limited sensing capability. By adjusting the sensor node density, we can, therefore, make an event detectable by at least k nodes which can participate in authenticating the event to be reported to the corresponding storage node. These nodes evaluate MAC only when the information in the event-report message is consistent with the information they have, i.e., they use the information about the event as a proof of the message. The *id* field of ARCMA messages is filled with the ID of the sensor node that composes the event-report message.

The storage node verifies the authenticity of each event-report message using its own AT, and stores only validated messages. Once verified, the reported event is stored by all the k nodes in the receiver's authentication tree as replicas. These replicas are later used as the proof of message for query-response messages.

4.5.3.2 Processing Queries Issued by Mobile Users

An external mobile user may query the sensor network to retrieve the data stored in DCS. Such queries are routed via multiple hops to the storage nodes, and then the corresponding results are generated and sent back to the mobile user. In this scenario, both the query and the result should be verifiable.

A valid query should be generated only by a legitimate mobile user. So, a mobile user

should be authenticated first before issuing queries to the network. However, it should be authenticated by multiple nodes rather than just by one node. When authenticated, the mobile user will be issued a token, which is a security credential it can present to the sensor nodes that belong to the same group as the token-issuer. After collecting k tokens, the mobile user can issue a query by presenting tokens as the proof of event-query, i.e., the query is validated by the security credentials issued by k different sensor nodes.

Mobile node m can be authenticated by sensor node s by exchanging three-way handshakes. First, m sends s its ID and a nonce, N_m . When s receives such a message, it also generates a nonce, N_s . Then, s sends its own ID along with N_m and N_s after encrypting it with a pairwise key between s and m , $f_p(s, m)$. Note that both s and m can evaluate the pairwise key using the pairwise-polynomial after exchanging their IDs. Then, m sends the nonce generated by s after encrypting it with $f_p(s, m)$. Now, s and m can mutually authenticate each other.

$$\begin{aligned}
 m \rightarrow s & : m, N_m \\
 s \rightarrow m & : s, \{N_s | N_m\}_{f_p(s, m)} \\
 m \rightarrow s & : \{N_s\}_{f_p(s, m)}
 \end{aligned}$$

Then, s sends m a token, $T_g(m)$, if it belongs to group g . $T_g(m)$ is defined as

$$T_g(m) \equiv s|g|m|ts|\{s|g|m|ts\}_{f_g(g, m)}$$

This token is valid only to the nodes in group g , and only m can present this token to the sensor nodes since only m can evaluate the pairwise-keys with arbitrary sensor nodes. Here, ts is a timestamp to indicate the time when the token is issued, and may be used by sensor nodes to reject stale tokens.

$$s \rightarrow m : T_g(m)$$

When m needs to issue a query, Q , it sends a query message to one of the nearby sensor nodes with the k tokens it has collected as the proof of message. Also, it evaluates CMAC for the query which can be evaluated with its share of the group-key polynomial. Here, CMAC is evaluated with the timestamp of the current time and the location of s . CMAC is evaluated by the mobile user to reduce the overhead of sending an invalid query. A legitimate mobile user can evaluate CMAC, and there is no reason for it to generate an invalid CMAC.

$$m \rightarrow s : ts|L_s|\{Q|ts|L_s|CMAC\}_{f_p(m,i)}|T_g(M)$$

where $1 \leq g \leq k$, and $CMAC \equiv MAC(f_g(m, 1), Q) \oplus MAC(f_g(m, 2), Q) \oplus \dots \oplus MAC(f_g(m, k), Q)$.

Then, s sends tokens and collects MAC for the given query, Q .

$$s \rightarrow AT_i^s : \{Q|ts|L_s|T_g(m)\}_{f_p(s, AT_i^s)}, \text{ where } 1 \leq i \leq k$$

The nodes in AT^s verify the token, which is the proof of the event-query message, and send s either MAC for the query message or INVALID message.

$$AT_i^s \rightarrow s : \{MAC(f_g(m, i), Q|ts|L_s)\}_{f_p(s, AT_i^s)} \text{ or INVALID.}$$

If all the tokens are valid, s can evaluate CMAC by XORing MACs it has collected. Then, it checks if the evaluated CMAC and the CMAC received from the mobile user match. Only when they match, does s send the query, Q , to the storage nodes.

When the query is received by r , which is a storage node, it first verifies the message using AT^r ; then r composes the query-response, R , for the valid query. The reply message

is again authenticated using AT^r , and the query-response message R itself is used as the proof of message; all k nodes should store the same event as a replica of the event, and they verify R by comparing it with the stored events. Then, the query-response message is encrypted with the pairwise-key between r and m , $f_p(r, m)$; the encrypted message is evaluated using the pairwise-key polynomial so that the clear text of message is only readable by m .

$$r \rightarrow m : r, \{R|ts|L_r|CMAC\}_{f_p(r,m)}$$

When m , the query issuer, receives this message, it evaluates CMAC using its share of the group-key polynomial, and accepts it only when a valid CMAC is concatenated to the reply message.

4.6 Authentication Tree Construction

Since a global view is not available at any given sensor node, we present two simple heuristic algorithms to construct ATs without incurring high overhead. The first heuristic, called MIN, builds a minimum-depth tree by selecting the shortest-distance node from a certain group for the AT. This heuristic adds a small amount of information in a periodic beacon message, commonly used in sensor network applications like health monitoring, node discovery, and route discovery. In each periodic beacon message, a node advertises the groups it has discovered by using a k -bit vector. When a sensor node notices that some bits are not set in a neighbor's beacon while the corresponding bits are set in its own bit vector, i.e., its neighbor has not yet discovered the nodes in certain groups that it has already discovered, it announces the information about them in its next beacon message. When a sensor node detects such information in its neighbor's beacon, it updates its AT. Using these steps, a t -hops-away node can be discovered within t beacon periods, as in a distance-vector routing protocol. The pseudo-code of this heuristic is given in Algorithm 1.

Algorithm 1 The pseudo-code of MIN heuristic

```
sub Send Broadcast
loop
   $bcast \leftarrow$  new broadcast message
  for all  $i$  s.t.  $AT_i$  is available and request[ $i$ ] is set do
    Add the information of  $AT_i$  to  $bcast$ 
  end for
  Broadcast  $bcast$ 
  Sleep(broadcast period)
  Clear request
end loop
sub Receive Broadcast
for all node information  $I$  in the received message do
   $i \leftarrow$  the group number of  $I$ 
  if  $AT_i$  is not available then
    Set  $AT_i$  with the information of  $I$ 
  end if
end for
 $n \leftarrow$  the node ID of the sender of the receive broadcast
for all  $i$  s.t.  $AT_i$  is available and  $AT_i^n$  is not available do
  Set request[ $i$ ]
end for
```

The second heuristic, called OPT, tries to minimize the number of transmissions in the optimized AT operation. For example, the MIN heuristic yielded the results in Figure 4.1(b) for a given topology Figure 4.1(a). This AT requires four transmissions since nodes 1, 2, 7, and 8 need to transmit a message for an AT operation. On the other hand, the AT shown in Figure 4.1(c) for the same topology requires only three transmissions for an AT operation. Even though the nearest nodes are not chosen for groups 4 and 5, a transmission by node 3 can cover both groups in this example. The OPT heuristics works as follows. After discovering one's neighbor, each node keeps two sets of nodes; transmission set (T) and candidate set (C). The transmission set contains the nodes which will relay the message in AT operations. First, each node puts itself in T, and its neighbors into C after calculating the out-degree, which is defined as the number of new groups of each neighbor if it is added. At each iteration, the node with the maximum out-degree will be moved from C to T, and the neighbors of the node will be added to C. When there is no node that has a positive out-

Algorithm 2 The pseudo-code of OPT heuristic

```
sub Construct AT
 $T \leftarrow \{s\}$ 
 $C \leftarrow N^s$ 
 $\forall c \in C$ , calculate  $d(c)$ 
repeat
  Find  $m$  s.t.  $m \in C \wedge \forall c \in C, d(m) \geq d(c) \wedge d(m) > 0$ 
  if  $m$  is found then
     $T \leftarrow T \cup \{m\}$ 
     $C \leftarrow (C - \{m\}) \cup (N^m - T)$ 
     $\forall c \in C$ , update the out-degree of  $c$ .
  else
    Send a route request for missing groups
  end if
  Wait for the reply
until  $AT^s$  is fully-constructed
sub Receive Route Request
for all  $i$  s.t. group  $i$  is requested do
  if  $AT_i$  is available then
    Add this information in reply
  end if
end for
Send reply
sub Receive Route Reply
for all route info  $r$  do
  if The group of node  $r$  is missing in  $AT^s$  then
    Find  $m$  that is farthest  $\wedge m \in T$ 
    Increase  $d(c)$  where  $c \in C \wedge m \in path(c)$ 
  end if
end for
c.f.  $d(s)$  represents the degree of sensor node  $s$ 
```

degree in C , a sensor node will request the route for the missing groups. Upon receiving such a request, a sensor node replies if it has access to the group. The pseudo-code for this heuristic is given in Algorithm 2.

4.7 Group Assignment Protocol

Group assignments of sensor nodes significantly affect the functionality and performance of ARCMA, where one node from each of k groups should collaborate together. Thus, the group assignment should guarantee uniform distribution of groups across the deployment area.

In ARCMA, groups can be distributively assigned at each grid. A sensor node determines its quantized coordinates, i.e., the grid it belongs to after it obtains its geographic location and deployment area information through a localization service. Then, sensor nodes in a grid discover each other by exchanging their own IDs and their neighbors' IDs within the grid. After that, the node with the smallest node ID in the grid assigns groups to sensor nodes. In doing so, it can uniformly assign group numbers to sensor nodes. More specifically, if there are $i \cdot k + j$ nodes in the grid, where $i \geq 0$ and $0 \leq j < k$, the sensor nodes with minimum ID assigns at least i nodes to each of k groups. When there are less than k nodes in the grid, sensor nodes in the grid will have limited capability to send or receive authenticated messages; they may find sensor nodes from the missing groups in the neighbor grids. However, an event-report message may not be authenticated in the grid when less than k nodes observe a given event.

4.8 Evaluation

4.8.1 Security Analysis

We analyze the security of ARCMA against the various attacks described in Section 4.3.2. Since all the messages are encrypted with the relevant keys, the proposed protocol is safe

from passive or active outsider attacks as long as proven cryptography is used. Also, replay attacks are prevented since all the messages including tickets contain time-stamps. Thus, our analysis will focus on node-capture attacks, where valid keying materials are exposed to attackers.

Also, ID spoofing and Sybil attacks can be prevented by using the bivariate polynomials. Without knowledge of the pairwise-key polynomial, the attacker cannot generate the secret keys for the spoofed IDs. Therefore, the attacker cannot launch a Sybil attack with spoofed IDs.

Now we focus on security analysis when an attacker launches node-capture attacks. In this case, the attacker has the valid keying information so that the naive encryption will not prevent the attacker from inserting false messages. We first consider the case where the attacker compromises less than k nodes, and then, the case where the attacker compromises k or more nodes.

When less than k nodes are compromised: Let us consider the case where the attacker compromises less than k nodes. In such a case, the attacker has the full control of the compromised nodes and the full knowledge of the keying material in the nodes. Using these keying materials, the attacker can launch different attacks depending on how the compromised nodes are used in the system.

There are a few options that the attacker can choose with the compromised nodes. The first option is to stay silent when the compromised nodes are asked to evaluate a MAC by a certain node which has the compromised nodes in its AT. The second option for the attacker is to report a wrong MACs when the compromised nodes are asked to evaluate a MAC. Another option for the attacker is to try to generate a message by asking other nodes to evaluate MACs to compose a false message. This type of attack will be the most attractive to the attacker since the attacker can generate any message to subvert the system. For example, the attacker may generate event-report messages to report false events, or event-query messages to retrieve detected events. Here we discuss how ARCMA prevents

such attacks.

Lemma IV.1. *The security of ARCMA does not degrade, i.e., the integrity of the system remains the same if less than k compromised nodes remain silent when requested for MAC evaluation.*

Proof. Here, the requesting node may be either a sender or a receiver. In this case, the requesting node can wait for the time being, and after a timeout, it can consider that the nodes are dead and recruit other nodes from the group where the compromised nodes belong, using the reconstruct algorithm. Note that for the requesting node, this case is exactly the same as the case where the compromised nodes becomes faulty or have depleted their batteries. Therefore, invalid information cannot be inserted into the system using this attack, although a delay may be caused. \square

Lemma IV.2. *The security of ARCMA does not degrade, i.e., the integrity of the system remains the same if less than k compromised nodes report wrong MACs.*

Proof. In this attack, CMAC will be composed using the wrong MACs. Therefore, the CMAC evaluated at the sender's side and the CMAC evaluated at the receiver's side will not match. Therefore, the receiver will detect the CMAC mismatch, and it will reject the message. \square

In the attack where compromised nodes report wrong MACs, the messages authenticated with wrong MACs are rejected by the receiver as explained in Lemma IV.2. However, the receiver does not know which nodes caused the CMAC mismatch. The identification of the compromised nodes and revocation of the nodes can be performed by sending individual MACs and adopting the honeybee technique [53]. When the receiver detects CMAC mismatch, it sends the MACs evaluated by the nodes in its AT to the sender without XORing MACs. The sender can now check the groups whose MACs mismatch. The sender notifies the group numbers whose MACs mismatch to the receiver. Then, the nodes of such groups both at the sender's side and the receiver's side are discarded by the sender and the

receiver because we know one of the nodes for such groups are compromised, but we do not know which one is compromised. If the attacker selects this option, the attacker can delay CMAC evaluation of only one message since the compromised node will be excluded after the first attempt. This type of attack is not very efficient from the view point of the attacker.

Lemma IV.3. *An attacker cannot generate a message with false information by requesting MAC evaluation if less than k nodes are compromised.*

Proof. Although this type of attack may be most preferable by an attacker, this type of attack is prevented by the use of appropriate proof of messages as shown in 4.5.3. When an attacker compromises less than k nodes, he must contact at least one uncompromised sensor node to evaluate CMAC since CMAC-evaluation requires the collaboration of k nodes from distinctive groups. For example, when the attacker asks the nearby uncompromised sensor nodes to evaluate MAC for a false event-report message, the uncompromised sensor nodes will not respond to such a request since they have not detected such an event. Thus, the attacker cannot authenticate false event-report messages when he compromised less than k nodes. Similarly, the attacker cannot authenticate false query-response messages since uncompromised nodes will not collaborate to evaluate CMAC for false query-response messages since the events in such false messages are not stored in those uncompromised nodes. Also, the attacker cannot authenticate false event-query messages since he cannot present k tokens as the proof of event-query messages when he compromised less than k nodes. □

Theorem IV.4. *When an attacker compromises less than k sensor nodes, the security of the system does not degrade.*

Proof. According to Lemma IV.1, IV.2 and IV.3, the security of ARCMA does not degrade, i.e., an attacker cannot insert invalid messages into the system, if less than k sensor nodes are compromised.

In these attacks, the security of the system does not degrade at all in the sense that the attacker cannot insert any false message. These attacks may be considered as denial-of-service (DoS) attacks since they can delay the system or deplete the batteries of some nodes. But, these attacks are easily detected, thus the same attack cannot be repeated using the same compromised node. \square

When k or more nodes are compromised: Let us consider the case where k or more than k nodes are compromised. In such a case, the attacker may know all the coefficients of one or more of three polynomials.

Lemma IV.5. *The pairwise-key polynomial is exposed after k nodes are compromised, since each sensor node has a different share of the pairwise-key polynomial. Thus, the local traffic encrypted using the key generated by the pairwise-key polynomial will be exposed to the attacker.*

Lemma IV.6. *The group-key polynomial is exposed after k nodes from distinctive groups are compromised, since sensor nodes in the same group have the same share of the group-key polynomial.*

Here, we can discuss the number of nodes that an attacker should compromise to obtain the group-key polynomial. If the attacker randomly compromises sensor nodes, the attacker needs to compromise $O(k \log(k))$ nodes to compromise at least sensor node from all the k groups.³ After the group-key polynomial is exposed, the attacker can now evaluate the valid CMAC for any given message. Thus, he may be able to insert valid-looking messages. However, even after the group-key polynomial is exposed to the attacker, the attacker may not be able to insert any message if the spatial-key polynomial is not exposed. For example, the attacker cannot insert a fake event-report message for a certain location without the spatial-key for the location because it cannot properly encrypt the message with the valid spatial-key.

³This problem is the same with the well-known coupon collector's problem.

Lemma IV.7. *The spatial-key polynomial is exposed after k nodes from different quantized locations are compromised, since sensor nodes with the same quantized location have the same share of the spatial-key polynomial.*

Due to the above property, an attacker should go to k different locations, and compromise at least one node from those locations. After that, the attacker can encrypt or decrypt any message using keys generated from the exposed spatial-key polynomial. Thus, the attacker can read all the messages on ARCMA.

If the attacker also knows the group-key polynomial in addition to the spatial-key polynomial, the attacker can also insert any message because the attacker can now evaluate the valid CMAC for a given message using the group-key polynomial, and encrypt the message with the valid spatial-key generated with the spatial-key polynomial.

Theorem IV.8. *For the complete subversion of ARCMA, the attacker should compromise k nodes from distinctive groups, and k nodes from different locations, i.e., locations with different quantized locations.*

Proof. From Lemma IV.5, IV.6, and IV.7, it is shown that an attacker cannot generate any message without compromising k nodes from distinctive groups, and k nodes from different locations. In this case, an attacker obtains all three polynomials, and can generate any message without being detected. □

4.8.2 Performance Evaluation

We now focus on the evaluation of memory usage and the CMAC evaluation cost of ARCMA.

4.8.2.1 Memory Requirement

A sensor node has only limited memory. Even though this may become a lesser problem in the future due to the decreasing cost and increasing density/capacity of memory, the

memory will still be a limited resource for sensor nodes or a larger memory may consume the battery power much faster.

Each sensor node needs to store three polynomials, each of which has k terms, each being a member in F_q , where q is a prime number large enough to hold the security keys. In ARCMA, only symmetric cryptographic functions are used, and a 128-bit key size will be sufficient. Thus, each sensor node needs the memory of $3 \cdot k \cdot 128$ bits = $384 \cdot k$ bits.

Each sensor node also maintains an AT. For each of the k groups, the ID of the node, the ID of the next-hop node, and the number of hops should be stored. When 16-bit node IDs are used (as in TinyOS [3]) and the maximum hop count is less than 255, the storage requirement for the AT at each node is $(2 \cdot 16 + 8) \cdot k$ bits = $40 \cdot k$ bits.

The intermediate nodes in an AT need to store the information about the nodes in its own subtree. A k -bit vector should be stored for this purpose. Since each node will, on average, be an intermediate node of $k - 1$ other nodes, the node needs $k \cdot (k - 1)$ bits.

The total memory requirement for ARCMA is the sum of the above three requirements, resulting in $k^2 + 423 \cdot k$ bits. When $k = 20$ for example, the memory requirement is about 1.1 Kbytes.

4.8.2.2 CMAC Evaluation and AT construction Costs

We evaluate the two heuristics to build ATs in terms of the CMAC evaluation and AT construction costs. The CMAC evaluation cost is defined as the average number of transmissions to deliver a message to all the nodes of the AT. We average the number of transmissions by dividing it by the number of groups in an AT to show the cost of reaching one node (or group). The construction cost is defined as the average number of iterations and route request/reply messages per group to build the ATs.

We also show the cost of reconstructing the AT when a sensor node is removed from the network because it is either faulty or compromised. When such a problem node is removed from the network, all the nodes in the AT that have the problem node on their paths to the

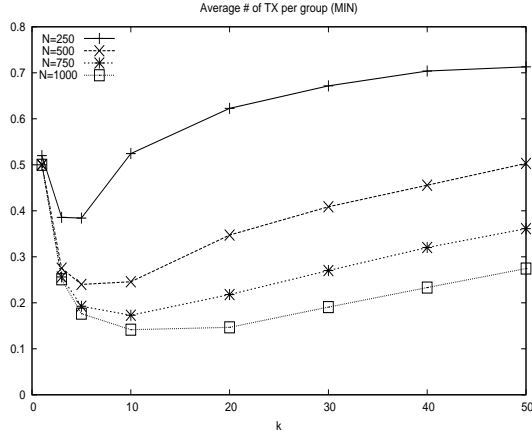


Figure 4.2: The average number of transmissions per group increases as k increases in MIN.

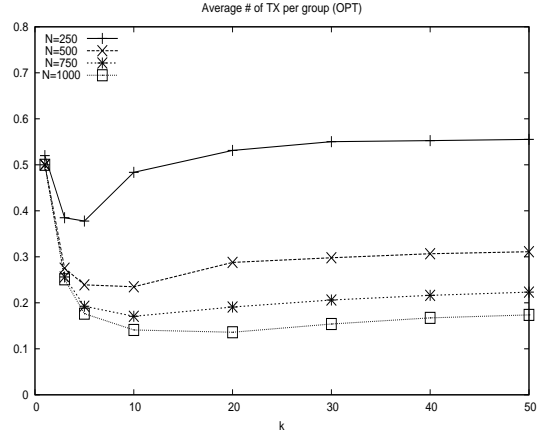
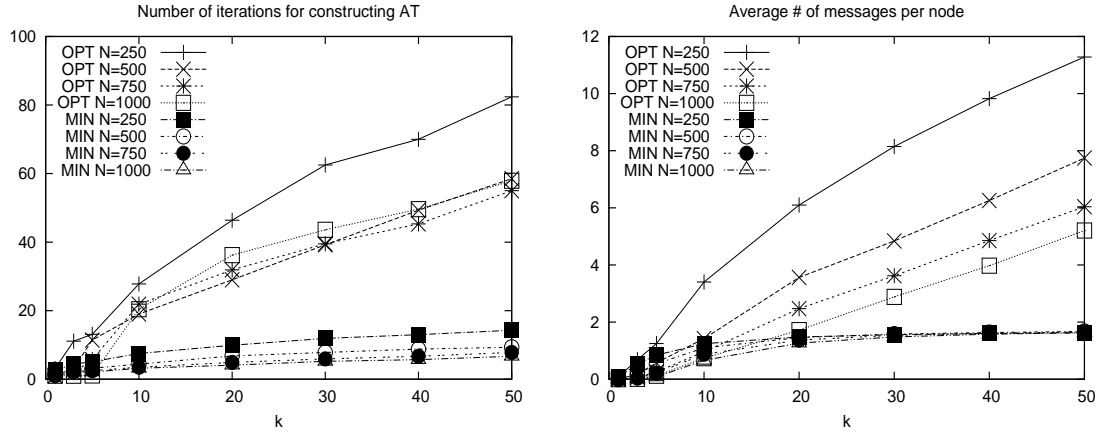


Figure 4.3: The average number of transmissions per group increases at a much slower pace as k increases in OPT.

AT's root should also be removed. Then, ATs should be reconstructed without using the problem node for the subsequent CMAC evaluations. We will adopt the number of nodes affected by the problem nodes and the number of iterations necessary to reconstruct the ATs as the metrics to evaluate the AT reconstruction cost.

The simulation parameters are set as follows. We assumed the transmission range (R) of the sensor node to be 100 m (equal to that of MicaZ [1]). All simulations are conducted in a 1000 m \times 1000 m coverage area unless specified otherwise. The number of nodes (N) in the area is varied to be 250, 500, 750, and 1000. The average number of neighbors can be calculated as $\pi R^2 \times N/1000^2$, thus varying the average number of neighbors from 7.85 to 31.4. Also, the pre-determined group assignment, $g = (s \bmod k) + 1$, is used as a default. The number of groups, k , is varied from 2 to 50. For each of N and k , 10 different topologies are generated using a uniform distribution. We also changed the network size while maintaining the same node density. Finally, all the simulation results are derived by averaging 10 simulation runs.

Figures 4.2 and 4.3 show the CMAC evaluation cost of the two heuristics. When $k = 2$, the average CMAC evaluation cost is around 0.5, meaning that only 1 transmission is



(a) OPT takes more iterations than MIN to construct ATs (b) OPT sends more messages than MIN to construct ATs

Figure 4.4: These graphs show the cost of constructing ATs with MIN and OPT heuristics while varying k and node density.

required, because at least one of a node's neighbors will likely belong to a different group than its own in a dense network. As k increases up to a certain point, the average cost decreases since all or most of the groups are likely to be found within a single or a very small number of hops. However, the average cost slowly increases as k increases under the MIN heuristic (Figure 4.2), while it remains stable under the OPT heuristic (Figure 4.3), where the average CMAC evaluation cost varies from 0.174 to 0.555 when $k = 50$. From these observations, we can conclude that the OPT heuristic requires fewer transmissions, i.e., less energy consumption for an CMAC evaluation, than the MIN heuristic. Also, the increase in energy consumption gets smaller as k increases. Thus, the OPT heuristic is preferred. Also, a denser network is observed to incur a lower cost in both heuristics because a node will have more neighbors, i.e., a smaller number of hops will be required to reach a certain group in a denser network.

The costs of constructing ATs with the two heuristics are shown in Figure 4.4. Figure 4.4(a) shows the number of iterations to construct ATs. With both heuristics, a sparser network takes longer to build ATs than a denser network, as it will take more hops to reach all the groups in a sparser network. With the MIN heuristic, it takes 14.3 iterations when $N = 250$ and $k = 50$, and 6.7 iterations when $N = 1000$ and $k = 50$. On the other hand,

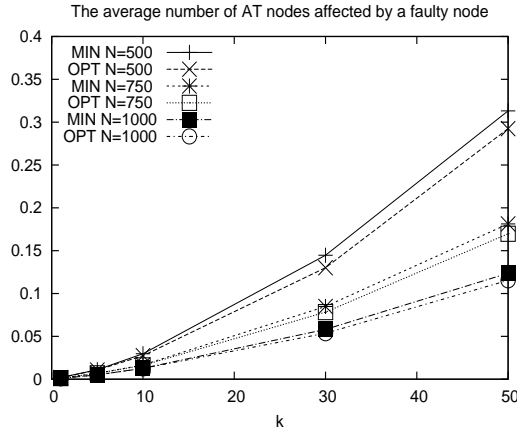


Figure 4.5: When removing a faulty node, the average number of affected nodes per AT increases as k increases for both heuristics.

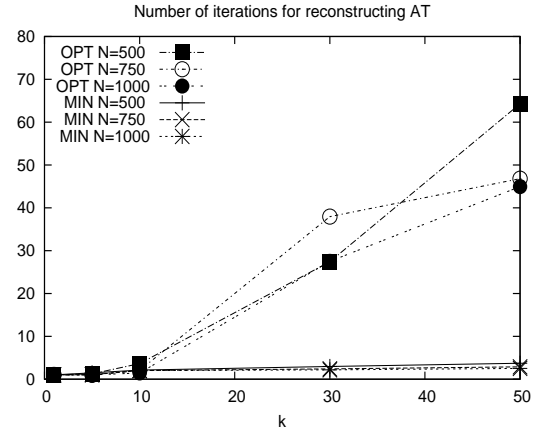


Figure 4.6: When reconstructing ATs, the number of iterations remain at a small number in MIN, while it increases as k increases in OPT.

the OPT heuristic requires 82.4 iterations when $N = 250$ and $k = 50$, and 57.9 iterations when $N = 1000$ and $k = 50$. Since the OPT heuristic can add at most one node into its transmission set (T), it requires much more time to build an AT.

Figure 4.4(b) shows the average number of route request/reply messages. As expected, the required number of messages decreases as N increases. When comparing the two heuristics, we observe that the MIN heuristic exchanges fewer messages than the OPT heuristic in a sparser network. On the other hand, the OPT heuristic exchanges fewer messages in a denser network than the MIN heuristic.

Figures 4.5 and 4.6 plot the performance evaluation results when a node is removed from the network. Figure 4.5 shows the average number of nodes removed for each AT upon occurrence of a problem node. There was only a small difference between the two heuristics. However, the number of affected AT nodes increases as the network gets sparser or k increases. In a sparser network, there are unlikely to be many alternative routes from a node to other nodes, i.e., a node is likely to be on more routes. Thus, one problem node can affect more nodes. When k increases, the number of alternative nodes of a certain group decreases. Figure 4.6 shows the number of iterations to finish the reconstruction

of ATs. MIN is found to take much fewer iterations than OPT. This means that it will take much longer to construct ATs with the OPT heuristic when a node becomes faulty or compromised.

We also evaluated the performance of ARCMA for different network sizes while maintaining the same node density. However, it is found that the network size does not affect the performance of ARCMA for the same node density, and thus, we did not repeat the result here.

4.9 Conclusion

In this chapter, we proposed a novel security mechanism for DCS, called ARCMA, focusing on resilience against node-capture attacks. Under such attacks, securing DCS is very difficult since attackers have access to all the valid keying materials extracted from the compromised nodes. In ARCMA, sensor nodes collaboratively authenticate event-report, event-query and query-response messages which typically travel multiple hops. Each sensor node belongs to one of k groups, and builds and maintains an AT with k nodes, each from a distinct group. With the help from the nodes in its AT, a sensor node can evaluate CMACs to authenticate messages.

When an event is identified by a set of cooperating sensor nodes, they generate an event-report with CMAC, which will then be forwarded to, and verified by, storage nodes. Before a mobile user issues a query, he needs to collect k tokens by contacting k sensor nodes, one from each distinct group. When a query is issued along with these tokens, it is authenticated as was done for an event-report message, and then forwarded to storage nodes. Finally, the storage node verifies and processes the valid message. Likewise, a response to the query can be authenticated.

ARCMA is shown to be $(k - 1)$ -collusion resistant, i.e., the same level of security is preserved as long as no more than $(k - 1)$ nodes are captured. We also presented and evaluated two heuristics (MIN and OPT) to build ATs. MIN builds ATs using the nearest

nodes from a specific group. This heuristic is constructed within fewer iterations both when ATs are constructed from scratch and when ATs are reconstructed after revoking faulty or compromised nodes. On the other hand, OPT incurs a lower operation cost (i.e., less transmissions to send one message to all the nodes in an AT) and a slower growth in the operation cost, while it takes longer to build ATs, and the number of messages exchanged to build an AT depends on the AT.

CHAPTER V

CONCLUSION

Wireless sensor networks (WSNs) are being deployed widely for physical-environment monitoring. In a hybrid WSN, a large number of sensor nodes identify events of interest, and a relatively small number of mobile nodes carried by humans or attached to vehicles access sensor nodes to retrieve the information of identified events. Several network services have been developed to support this application scenario, including localization, time synchronization, and routing services.

This thesis proposes essential network services to better support WSN applications. Currently available network services are inefficient or insecure when supporting applications in WSNs. Therefore, we design network services complementary to the existing network services in the context of hybrid WSNs. The contributions of this thesis are summarized as follows.

First, we propose a location service, called the distributed location service protocol (DLSP), to provide sensor nodes with the location of mobile nodes to enable message delivery to mobile nodes using a geographic forward routing protocol. We provide systematic methods to elect location servers among sensor nodes responsible for storing the location information of mobile nodes, to publish location information of mobile nodes to those location servers, and to process location queries for the mobile nodes' location. We show that the proposed protocol is more efficient than others, and reliable even in the presence

of holes.

Second, we present an algorithm, TRAVERSE, which identifies the boundaries of holes in sensor networks. Holes are formed because of obstacles on the deployment area, node failures, attacks, or some other events. Holes can degrade the performance of network services on WSN. We also propose geographic forward routing with hole avoidance (GFRHA), which utilizes the hole boundary information to detour packets around holes. We demonstrate that GFRHA in conjunction with TRAVERSE significantly reduces the path length under certain shapes of holes and the locations of sources and destinations.

Finally, we designed attack-resilient collaborative message authentication (ARCMA), a mechanism for secure message delivery among sensor nodes or between a mobile node and a sensor node. In ARCMA, sensor nodes *collaboratively* evaluate a collaborative message authentication code (CMAC) to authenticate or verify messages. We provide key management mechanisms for ARCMA, and protocols to locate other sensor nodes which can collaborate to authenticate a given message. ARCMA is designed to tolerate node-capture attacks.

Future work can be pursued in the following directions.

- Performance improvement of DLSP: The performance of DLSP can be improved by caching mobiles' location at the sensor nodes, which forward location updates. However, we need to restrict the number of mobiles' locations cached in the sensor nodes since their memory is very limited. We can study the effect of cache policies on the performance of DLSP.
- Better hole summary for DHD: In GFRHA, an identified hole is summarized as a circle, and messages are routed around the circle. However, a circle may not be a tight bound for the given hole. Thus, with a tighter hole summary such as a convex hull, GFRHA may achieve more performance gain. The trade-off between the performance gain with tighter hole summaries and the cost for obtaining such summaries may be studied.

- Secure location service and hole detection: Since an entire WSN can be subverted by exploiting the weakest component, it is very important to secure each component of the network. Thus, we can improve security of DLSP and TRAVERSE to improve the security of the whole WSNs. ACRMA may be adopted to authenticate remote messages of these protocols such as location-update and query messages in DLSP and the hole summary information in DHD. In securing the protocols, node-capture attacks will be considered as main threats, as they are in ARCMA.

BIBLIOGRAPHY

BIBLIOGRAPHY

- [1] Crossbow MICAz datasheet. http://www.xbow.com/Products/Product_pdf_files/Wireless_pdf/MICAz_Datasheet.pdf.
- [2] The network simulator - ns-2. <http://www.isi.edu/nsnam/ns/>.
- [3] TinyOS. <http://www.tinyos.net>.
- [4] *Proceedings of the Fifth Annual IEEE Communications Society Conference on Sensor, Mesh and Ad Hoc Communications and Networks, SECON 2008, June 16-20, 2008, Crowne Plaza, San Francisco International Airport, California, USA, 2008.*
- [5] E. Ayday, F. Delgosha, and F. Fekri. Location-aware security services for wireless sensor networks using network coding. In *Proceedings of the 26th IEEE International Conference on Computer Communications (INFOCOM '07)*, pages 1226–1234, May 2007.
- [6] C. Blundo, A. D. Santis, A. Herzberg, S. Kutten, U. Vaccaro, and M. Yung. Perfectly-secure key distribution for dynamic conferences. In *CRYPTO '92: Proceedings of the 12th Annual International Cryptology Conference on Advances in Cryptology*, pages 471–486, 1993.
- [7] P. Bose, P. Morin, I. Stojmenović, and J. Urrutia. Routing with guaranteed delivery in ad hoc wireless networks. *Wirel. Netw.*, 7(6):609–616, 2001.

- [8] N. Bulusu, J. Heidemann, D. Estrin, and T. Tran. Self-configuring localization systems: Design and experimental evaluation. *Trans. on Embedded Computing Sys.*, 3(1):24–60, 2004.
- [9] T. Camp, J. Boleng, and V. Davies. A survey of mobility models for ad hoc network research. *Wireless Communication and Mobile Computing (WCMC): Special issue on Mobile Ad Hoc Networking*, 2002.
- [10] Z. Chen, M. gyu Cho, and K. G. Shin. Design of location service for a hybrid network of mobile actors and static sensors. In *the 27th IEEE International Real-Time Systems Symposium (RTSS '06)*, pages 202–211, Dec. 2006.
- [11] T. Dam and K. Langendoen. An adaptive energy-efficient mac protocol for wireless sensor networks. In *Proceedings of the 1st international conference on Embedded networked sensor systems (SenSys '03)*, 2003.
- [12] S. M. Das, H. Pucha, and Y. C. Hu. Performance comparison of scalable location services for geographic ad hoc routing. In *Proceedings of the 24th Annual Joint Conference of the IEEE Computer and Communications Societies (INFOCOM '05)*, pages 217–228, 2005.
- [13] W. Du, J. Deng, Y. Han, S. Chen, and P. Varshney. A key management scheme for wireless sensor networks using deployment knowledge. In *Proceedings of the 23rd Annual Joint Conference of the IEEE Computer and Communications Societies (INFOCOM '04)*, volume 1, pages –597, 2004.
- [14] W. Du, J. Deng, Y. S. Han, and P. K. Varshney. A pairwise key pre-distribution scheme for wireless sensor networks. In *Proceedings of the 10th ACM conference on Computer and communications security (CCS '03)*, pages 42–51, 2003.
- [15] A. El-Hoiydi and J. Decotignie. WiseMAC, an ultra low power mac protocol for the

- WiseNET wireless sensor network. In *IEEE International Symposium on Computers and Communications*, 2004.
- [16] J. Elson, L. Girod, and D. Estrin. Fine-grained network time synchronization using reference broadcasts. *SIGOPS Oper. Syst. Rev.*, 36(SI):147–163, 2002.
- [17] L. Eschenauer and V. D. Gligor. A key-management scheme for distributed sensor networks. In *Proceedings of the 9th ACM conference on Computer and communications security (CCS '03)*, pages 41–47, 2002.
- [18] Q. Fang, J. Gao, and L. Guibas. Locating and bypassing routing holes in sensor networks. In *INFOCOM 2004. Twenty-third Annual Joint Conference of the IEEE Computer and Communications Societies*, volume 4, pages 2458–2468vol.4, 7-11 March 2004.
- [19] R. Flury and R. Wattenhofer. MLS: an efficient location service for mobile ad hoc networks. In *Proceedings of the 7th ACM international symposium on Mobile ad hoc networking and computing (MobiHoc '06)*, pages 226–237, 2006.
- [20] R. Fonseca, S. Ratnasamy, J. Zhao, C. Ee, D. Culler, S. Shenker, and I. Stoica. Beacon vector routing: Scalable point-to-point routing in wireless sensor networks. In *Proceedings of NSDI 2005*, pages 329–342, 2005.
- [21] S. Funke. Topological hole detection in wireless sensor networks and its applications. In *DIALM-POMC '05: Proceedings of the 2005 joint workshop on Foundations of mobile computing*, pages 44–53, 2005.
- [22] S. Ganeriwal, R. Kumar, and M. B. Srivastava. Timing-sync protocol for sensor networks. In *Proceedings of the 1st international conference on Embedded networked sensor systems (SenSys '03)*, pages 138–149, 2003.

- [23] S. Ganeriwal and M. B. Srivastava. Reputation-based framework for high integrity sensor networks. In *Proceedings of the 2nd ACM workshop on Security of ad hoc and sensor networks (SASN '04)*, pages 66–77, 2004.
- [24] D. Ganesan, D. Estrin, and J. Heidemann. Dimensions: why do we need a new data handling architecture for sensor networks? *SIGCOMM Comput. Commun. Rev.*, 33(1):143–148, 2003.
- [25] A. Ghose, J. Grossklags, and J. Chuang. Resilient data-centric storage in wireless ad-hoc sensor networks. In *MDM '03: Proceedings of the 4th International Conference on Mobile Data Management*, pages 45–62, 2003.
- [26] T. Goff, N. B. Abu-Ghazaleh, D. S. Phatak, and R. Kahvecioglu. Preemptive routing in ad hoc networks. In *Mobile Computing and Networking*, pages 43–52, 2001.
- [27] B. Greenstein, D. Estrin, R. Govindan, S. Ratnasamy, and S. Shenker. DIFS: a distributed index for features in sensor networks. In *Sensor Network Protocols and Applications, 2003. Proceedings of the First IEEE. 2003 IEEE International Workshop on*, pages 163–173, 2003.
- [28] M. Grossglauser and M. Vetterli. Locating nodes with ease: last encounter routing in ad hoc networks through mobility diffusion. In *Proceedings of the 22nd Annual Joint Conference of the IEEE Computer and Communications Societies (INFOCOM'03)*, volume 3, pages 1954–1964 vol.3, March-3 April 2003.
- [29] R. B. Hayward, J. P. Spinrad, and R. Sritharan. Improved algorithms for weakly chordal graphs. *ACM Trans. Algorithms*, 3(2):14, 2007.
- [30] T. He, C. Huang, B. M. Blum, J. A. Stankovic, and T. Abdelzaher. Range-free localization schemes for large scale sensor networks. In *Proceedings of the 9th annual international conference on Mobile computing and networking (MobiCom '03)*, pages 81–95, 2003.

- [31] L. Hu and D. Evans. Localization for mobile sensor networks. In *Proceedings of the 10th annual international conference on Mobile computing and networking (MobiCom '04)*, pages 45–57, 2004.
- [32] Q. Huang, J. Cukier, H. Kobayashi, B. Liu, and J. Zhang. Fast authenticated key establishment protocols for self-organizing sensor networks. In *Proceedings of the 2nd ACM international workshop on Wireless sensor networks and applications (WSNA '03)*, pages 141–150, 2003.
- [33] B. Karp and H. T. Kung. GPSR: greedy perimeter stateless routing for wireless networks. In *Proceedings of the 6th annual international conference on Mobile computing and networking (MobiCom '00)*, pages 243–254, 2000.
- [34] W. Kieß, H. Füßler, J. Widmer, and M. Mauve. Hierarchical location service for mobile ad-hoc networks. *SIGMOBILE Mob. Comput. Commun. Rev.*, 8(4):47–58, 2004.
- [35] H. Kim and J. C. Hou. Improving protocol capacity with model-based frame scheduling in ieee 802.11-operated wlans. In *Proceedings of the 9th annual international conference on Mobile computing and networking (MobiCom '03)*, pages 190–204, 2003.
- [36] S. Kumar, T. H. Lai, and J. Balogh. On k-coverage in a mostly sleeping sensor network. In *Proceedings of the 10th annual international conference on Mobile computing and networking (MobiCom '04)*, pages 144–158, 2004.
- [37] S. M. LaValle. *Planning Algorithms*. Cambridge University Press, Cambridge, U.K., 2006. Available at <http://planning.cs.uiuc.edu/>.
- [38] L. Lazos and R. Poovendran. SeRLoc: secure range-independent localization for wireless sensor networks. In *Proceedings of the 2004 ACM workshop on Wireless security (WiSe '04)*, pages 21–30, 2004.

- [39] S. Lee, B. Bhattacharjee, and S. Banerjee. Efficient geographic routing in multihop wireless networks. In *Proceedings of the 6th ACM international symposium on Mobile ad hoc networking and computing (MobiHoc '05)*, pages 230–241, 2005.
- [40] J. Li, J. Jannotti, D. S. J. D. Couto, D. R. Karger, and R. Morris. A scalable location service for geographic ad hoc routing. In *Proceedings of the 6th annual international conference on Mobile computing and networking (MobiCom '00)*, pages 120–130, 2000.
- [41] M. Li and Y. Liu. Rendered path: range-free localization in anisotropic sensor networks with holes. In *Proceedings of the 13th annual international conference on Mobile computing and networking (MobiCom '07)*, pages 51–62, 2007.
- [42] X. Li, Y. J. Kim, R. Govindan, and W. Hong. Multi-dimensional range queries in sensor networks. In *Proceedings of the 1st international conference on Embedded networked sensor systems (SenSys '03)*, pages 63–75, 2003.
- [43] Y. Li, W. Ye, and J. Heidemann. Energy and latency control in low duty cycle MAC protocols. In *Proceedings of the IEEE Wireless Communications and Networking Conference*, March 2005.
- [44] D. Liu and P. Ning. Establishing pairwise keys in distributed sensor networks. In *Proceedings of the 10th ACM conference on Computer and communications security (CCS '03)*, pages 52–61, 2003.
- [45] A. Mainwaring, J. Polastre, R. Szewczyk, D. Culler, and J. Anderson. Wireless sensor networks for habitat monitoring. In *Proceedings of the 1st ACM international workshop on Wireless sensor networks and applications (WSNA '02)*, 2002.
- [46] D. Malan, M. Welsh, and M. Smith. A public-key infrastructure for key distribution in TinyOS based on elliptic curve cryptography. In *Proceedings of the 1st Annual*

- IEEE Communications Society Conference on Sensor and Ad Hoc Communications and Networks (SECON '04)*, pages 71–80, 2004.
- [47] M. Maróti, P. Völgyesi, S. Dóra, B. Kusý, A. Nádas, A. Lédeczi, G. Balogh, and K. Molnár. Radio interferometric geolocation. In *SenSys '05: Proceedings of the 3rd international conference on Embedded networked sensor systems*, pages 1–12, 2005.
- [48] D. Moore, J. Leonard, D. Rus, and S. Teller. Robust distributed network localization with noisy range measurements. In *SenSys '04: Proceedings of the 2nd international conference on Embedded networked sensor systems*, pages 50–61, 2004.
- [49] T. Muetze, P. Stuedi, F. Kuhn, and G. Alonso. Understanding radio irregularity in wireless networks. In *SECON* [4], pages 82–90.
- [50] S. D. Nikolopoulos and L. Palios. Hole and antihole detection in graphs. In *SODA '04: Proceedings of the fifteenth annual ACM-SIAM symposium on Discrete algorithms*, pages 850–859, 2004.
- [51] S. Olariu, M. Eltoweissy, and M. Younis. ANSWER: autonomous wireless sensor network. In *Proceedings of the 1st ACM international workshop on Quality of service & security in wireless and mobile networks (Q2SWinet '05)*, 2005.
- [52] J. Ortiz, C. R. Baker, D. Moon, R. Fonseca, and I. Stoica. Beacon location service: a location service for point-to-point routing in wireless sensor networks. In *Proceedings of the 4th International Symposium on Information Processing in Sensor Networks (IPSN 2007)*, pages 166–175, 2007.
- [53] B. Parno, M. Luk, E. Gaustad, and A. Perrig. Secure sensor network routing: A clean-slate approach. In *CoNEXT'06: Proceedings of the 2006 ACM conference on Emerging network experiment and technology*, 2006.

- [54] J. Polastre, J. Hill, and D. Culler. Versatile low power media access for wireless sensor networks. In *Proceedings of the 2nd international conference on Embedded networked sensor systems (SenSys '04)*, 2004.
- [55] B. Przydatek, D. Song, and A. Perrig. SIA: secure information aggregation in sensor networks. In *Proceedings of the 1st international conference on Embedded networked sensor systems (SenSys '03)*, pages 255–265, 2003.
- [56] S. Ratnasamy, B. Karp, L. Yin, F. Yu, D. Estrin, R. Govindan, and S. Shenker. GHT: a geographic hash table for data-centric storage. In *Proceedings of the 1st ACM international workshop on Wireless sensor networks and applications (WSNA '02)*, pages 78–87, 2002.
- [57] K. Ren, W. Lou, and Y. Zhang. Leds: Providing location-aware end-to-end data security in wireless sensor networks. In *Proceedings of the 25th IEEE International Conference on Computer Communications (INFOCOM '06)*, pages 1–12, April 2006.
- [58] N. Sadagopan, F. Bai, B. Krishnamachari, and A. Helmy. PATHS: analysis of PATH duration statistics and their impact on reactive manet routing protocols. In *Proceedings of the 4th ACM international symposium on Mobile ad hoc networking and computing (MobiHoc '03)*, pages 245–256, 2003.
- [59] A. Savvides, C.-C. Han, and M. B. Strivastava. Dynamic fine-grained localization in ad-hoc networks of sensors. In *Proceedings of the 7th annual international conference on Mobile computing and networking (MobiCom '01)*, pages 166–179, 2001.
- [60] M. Shao, S. Zhu, W. Zhang, and G. Cao. pdcs: Security and privacy support for data-centric sensor networks. In *INFOCOM 2007. 26th IEEE International Conference on Computer Communications. IEEE*, pages 1298–1306, May 2007.
- [61] S. Singh and C. S. Raghavendra. PAMAS – power aware multi-access protocol with

- signalling for ad hoc networks. *SIGCOMM Comput. Commun. Rev.*, 28(3):5–26, 1998.
- [62] I. Stojmenovic. A routing strategy and quorum based location update scheme for ad hoc wireless networks. Technical report, University of Ottawa, 1999.
- [63] W. Su and I. F. Akyildiz. Time-diffusion synchronization protocol for wireless sensor networks. *IEEE/ACM Trans. Netw.*, 13(2):384–397, 2005.
- [64] K. Sun, P. Ning, and C. Wang. TinySeRSync: secure and resilient time synchronization in wireless sensor networks. In *Proceedings of the 13th ACM conference on Computer and communications security (CCS '06)*, pages 264–277, 2006.
- [65] P. F. Tsuchiya. The landmark hierarchy: A new hierarchy for routing in very large networks. In *Proceedings of SIGCOMM'88*, Aug. 1988.
- [66] A. C. Viana, M. D. de Amorim, S. Fdida, Y. Viniotis, and J. F. de Rezende. Easily-managed and topology-independent location service for self-organizing networks. In *Proceedings of the 6th ACM international symposium on Mobile ad hoc networking and computing (MobiHoc '05)*, pages 193–204, 2005.
- [67] D. Wagner. Resilient aggregation in sensor networks. In *Proceedings of the 2nd ACM workshop on Security of ad hoc and sensor networks (SASN '04)*, pages 78–87, 2004.
- [68] R. Watro, D. Kong, S. fen Cuti, C. Gardiner, C. Lynn, and P. Kruus. TinyPK: securing sensor networks with public key technology. In *Proceedings of the 2nd ACM workshop on Security of ad hoc and sensor networks (SASN '04)*, pages 59–64, 2004.
- [69] Č. Westpha. Little tom thumb went straight home: Asymptotic behavior of a routing protocol in ad-hoc networks with a mobile access point. In *Proceedings of the 26th IEEE International Conference on Computer Communications (INFOCOM '07)*, pages 1847–1856, May 2007.

- [70] Y. Xue, B. Li, and K. Nahrstedt. A scalable location management scheme in mobile ad-hoc networks. In *Proceedings of IEEE Conference on Local Computer Networks*, pages 102–111, Nov 2001.
- [71] H. Yang, F. Ye, Y. Yuan, S. Lu, and W. Arbaugh. Toward resilient security in wireless sensor networks. In *Proceedings of the 6th ACM international symposium on Mobile ad hoc networking and computing (MobiHoc '05)*, pages 34–45, 2005.
- [72] F. Ye, H. Luo, J. Cheng, S. Lu, and L. Zhang. A two-tier data dissemination model for large-scale wireless sensor networks. In *Proceedings of the 8th annual international conference on Mobile computing and networking (MobiCom '02)*, pages 148–159, 2002.
- [73] F. Ye, H. Luo, S. Lu, and L. Zhang. Statistical en-route filtering of injected false data in sensor networks. In *Proceedings of the 23rd Annual Joint Conference of the IEEE Computer and Communications Societies (INFOCOM '04)*, volume 4, pages 2446–2457 vol.4, 2004.
- [74] F. Ye, H. Luo, S. Lu, and L. Zhang. Statistical en-route filtering of injected false data in sensor networks. *IEEE Journal on Selected Areas in Communications*, 23(4):839–850, 2005.
- [75] W. Ye and J. Heidemann. Ultra-low duty cycle mac with scheduled channel polling. Technical Report ISI-TR-2005-604b, USC/Information Sciences Institute, July 2005.
- [76] W. Ye, J. Heidemann, and D. Estrin. An energy-efficient mac protocol for wireless sensor networks. In *Proceedings of the 21st Annual Joint Conference of the IEEE Computer and Communications Societies (INFOCOM'02)*, volume 3, pages 1567–1576, 23-27 June 2002.
- [77] J. Yick, B. Mukherjee, and D. Ghosal. Wireless sensor network survey. *Computer Networks*, 52(12):2292–2330, Aug. 2008.

- [78] J. Yoon, M. Liu, and B. Noble. Sound mobility models. In *Proceedings of the 9th annual international conference on Mobile computing and networking (MobiCom '03)*, Sept. 2003.
- [79] W. Zhang, H. Song, S. Zhu, and G. Cao. Least privilege and privilege deprivation: towards tolerating mobile sink compromises in wireless sensor networks. In *Proceedings of the 6th ACM international symposium on Mobile ad hoc networking and computing (MobiHoc '05)*, pages 378–389, 2005.
- [80] Y. Zhang, W. Liu, W. Lou, and Y. Fang. Location-based compromise-tolerant security mechanisms for wireless sensor networks. *IEEE Journal on Selected Areas in Communications*, 24(2):247–260, Feb. 2006.
- [81] Q. Zheng, X. Hong, and S. Ray. Recent advances in mobility modeling for mobile ad hoc network research. In *ACM-SE 42: Proceedings of the 42nd annual Southeast regional conference*, pages 70–75, 2004.
- [82] G. Zhou, T. He, S. Krishnamurthy, and J. A. Stankovic. Impact of radio irregularity on wireless sensor networks. In *MobiSys '04: Proceedings of the 2nd international conference on Mobile systems, applications, and services*, pages 125–138, 2004.
- [83] S. Zhu, S. Setia, S. Jajodia, and P. Ning. An interleaved hop-by-hop authentication scheme for filtering of injected false data in sensor networks. In *Proceedings of the 2004 Symposium on Security and Privacy*, pages 259–271, 2004.